

**A Measurement Technique Guide on the Application of
Tracer-Gas Techniques for Measuring
Airflow in HVAC Systems**

by

K.W. Cheong and S.B. Riffat

Building Technology Group

School of Architecture

University of Nottingham

**A Measurement Technique Guide on the Application of
Tracer-Gas Techniques for Measuring
Airflow in HVAC Systems**

by

K.W. Cheong and S.B. Riffat

Building Technology Group

School of Architecture

University of Nottingham

CONTENTS

| | Page |
|---|-------------|
| Abstract | i |
| List of Figures | ii |
| List of Tables | vi |
| List of Symbols | viii |
| | |
| CHAPTER 1 - INTRODUCTION | 1 |
| | |
| CHAPTER 2 - REVIEW OF AIR FLOW INSTRUMENTATIONS AND TECHNIQUES | 3 |
| | |
| 2.1 EXISTING TECHNIQUES AND INSTRUMENTATION | 3 |
| 2.1.1 Pressure-differential technique | 3 |
| 2.1.1.1 Orifice plate | 4 |
| 2.1.1.2 Pitot-static tube | 5 |
| 2.1.2 Methods based on the rates of cooling hot bodies | 7 |
| 2.1.2.1 Hot-wire anemometer | 8 |
| 2.1.3 Other airflow measuring device | 10 |
| 2.2 AIR FLOW MEASUREMENT USING TRACER-GAS TECHNIQUES | 11 |
| 2.2.1 Tracer-gas measurement techniques | 12 |
| 2.2.1.1 Constant-injection technique | 14 |
| 2.2.1.2 Pulse-injection technique | 18 |
| 2.2.1.3 Concentration-decay technique | 23 |
| 2.2.1.4 Constant-concentration technique | 24 |
| 2.2.2 Tracer-gas requirements | 24 |
| 2.2.3 Accuracy of tracer-gas techniques | 27 |
| 2.2.3.1 Development of tracer-gas injection | 28 |
| 2.2.3.2 Development of tracer-gas sampling | 33 |

| | | |
|--|--|-----------|
| 2.3 | MEASUREMENT ERRORS | 35 |
| 2.3.1 | Pitot-tube and hot-wire anemometer | 35 |
| 2.3.2 | Tracer-gas techniques | 35 |
| 2.4 | CORRECTION FOR TRACER-GAS INJECTION RATE | 36 |
| 2.5 | CORRECTION FOR DENSITY OF AIR IN DUCT | 37 |
| CHAPTER 3 - MEASUREMENT OF AIR FLOW IN A DUCT USING TRACER-GAS TECHNIQUES | | 38 |
| 3.1 | EXPERIMENTAL WORK | 38 |
| 3.1.1 | Airflow rate measurements in ducts using constant-injection and pulse-injection technique | 39 |
| 3.1.2 | Airflow rate measurements in ducts using pitot-tube and hot-wire anemometer | 41 |
| 3.2 | RESULTS AND DISCUSSION | 43 |
| 3.3 | MEASUREMENT OF AIRFLOW THROUGH A POROUS MEDIUM | 57 |
| 3.3.1 | Materials and methods | 58 |
| 3.3.2 | Results and discussion | 60 |
| CHAPTER 4 - TESTS ON A SMALL-SCALE HVAC SYSTEM | | 63 |
| 4.1 | EXPERIMENTAL PROCEDURE | 63 |
| 4.2 | RESULTS AND DISCUSSION | 64 |
| 4.3 | BALANCING OF HVAC SYSTEMS USING TRACER-GAS TECHNIQUES | 67 |
| 4.4 | PRINCIPLE OF BALANCING HVAC SYSTEMS | 68 |
| 4.4.1 | CIBSE method | 68 |
| 4.4.2 | Tracer-gas method | 72 |
| 4.5 | DESCRIPTION OF TRACER-GAS EQUIPMENT | 74 |
| 4.6 | RESULTS AND DISCUSSION | 76 |

| | |
|--|-----------|
| CHAPTER 5 - PERFLUOROCARBON TRACER (PFT) FOR MEASUREMENT OF AIRFLOW IN DUCTS | 80 |
| 5.1 DEVELOPMENT OF A NEW CONSTANT-INJECTION TECHNIQUE FOR MEASURING AIRFLOW IN DUCT USING PERFLUOROCARBON TRACER | 80 |
| 5.1.1 How is the liquified PFT being released in a gaseous state? | 81 |
| 5.1.1.1 Diffusion tube theory | 81 |
| 5.1.1.2 Sizing the diffusion tube | 82 |
| 5.1.2 Initial development of a controlled tracer-gas injection technique | 83 |
| 5.1.2.1 Demonstration of this prototype tracer-injection system | 84 |
| 5.1.3 Redesign of the prototype tracer-gas injection unit | 86 |
| 5.1.3.1 Detailed description of the heating block | 87 |
| 5.2 DEVELOPMENT OF THE PROTOTYPE SAMPLING SYSTEM | 89 |
| 5.2.1 The prototype sampling system design | 91 |
| 5.2.1.1 Choice of components | 91 |
| 5.2.2 Building the sampling system | 97 |
| 5.2.3 Detailed construction of the case for the sampling system | 98 |
| 5.3 GENERAL INSTRUCTIONS FOR THE SAMPLING SYSTEM | 98 |
| 5.4 SAMPLE ANALYSIS | 102 |
| 5.4.1 The thermal desorption unit | 103 |
| 5.4.1.1 Description and functions | 103 |
| 5.4.1.2 System use | 105 |
| 5.4.1.3 Analysis of results from the multi-gas monitor | 107 |
| 5.4.1.3.1 Calibration method | 107 |
| 5.4.2 Packing and conditioning the adsorber tubes | 110 |
| 5.4.2.1 The adsorber tube | 110 |
| 5.4.2.2 Packing the tube | 110 |
| 5.4.2.3 Conditioning the packed adsorbent tube | 112 |
| 5.4.3 Choice of perfluorocarbon tracers | 112 |

| | | |
|-------|--|------------|
| 5.4.4 | Choice of adsorbent | 112 |
| 5.4.5 | Optimum sampling volumes | 115 |
| - | 5.4.5.1 Determine the optimum sampling volumes | 117 |
| 5.5 | ADVANTAGES AND DISADVANTAGES OF THE NEW PFT SYSTEM | 118 |
| 5.6 | LABORATORY TESTS OF THE NEW PFT TECHNIQUE FOR MEASURING AIRFLOW IN DUCTS | 119 |
| 5.6.1 | Experimental work | 119 |
| 5.6.2 | Results and discussion | 122 |
| | CHAPTER 6 - FIELD TESTING | 125 |
| 6.1 | DESCRIPTION OF MEASUREMENTS | 125 |
| 6.1.1 | Measurement of airflow in air handling unit and exhaust system | 125 |
| 6.1.2 | Results and discussion | 129 |
| | CHAPTER 7 - DETERMINATION OF THE AIR-TIGHTNESS OF DUCT SYSTEM USING TRACER-GAS TECHNIQUES | 130 |
| 7.1 | REVIEW OF TECHNIQUES | 130 |
| 7.1.1 | Concentration-decay technique | 130 |
| 7.1.2 | Constant-injection technique | 131 |
| 7.2 | METHODOLOGY | 131 |
| 7.2.1 | Stationary technique | 132 |
| 7.2.2 | Mobile technique | 132 |
| 7.3 | RESULTS AND DISCUSSION | 134 |
| 7.3.1 | Stationary technique | 134 |
| 7.3.2 | Mobile technique | 136 |
| | REFERENCES | r1 |

ABSTRACT

This handbook describes the use of tracer-gas techniques for measurement of airflow in ducts. Initial measurements were carried out in the laboratory to examine the accuracy of these techniques. The mixing of tracer gases (eg, sulphur hexafluoride, SF₆) in ducts of various shapes and sizes was examined using different types of tracer injector. Airflow estimated using tracer-gas techniques (eg, constant-injection, pulse-injection) was compared with measurements made with traditional instrumentation such as pitot-tubes and hot-wire anemometers. Work also involved the development of tracer-gas equipment for balancing airflow in HVAC systems. This equipment was used to balance airflow in a small-scale HVAC system.

Research also involved the development of a perfluorocarbon (PFT) tracer-gas sampling system. The PFT was injected using a thermostatically-controlled injection unit and a fast-response sampling system, using stainless steel tubes packed with adsorbent, was employed to collect tracer gas samples. The samples were analysed in the laboratory using a thermal desorber and gas monitor. The PFT system was tested successfully in the laboratory. Airflow measurements were carried out in the HVAC system of an office building using tracer-gas techniques and the new PFT technique.

Tracer-gas techniques were used in other applications including measurement of airflow through a porous medium in a rectangular duct and determination of the air-tightness of ductwork.

LIST OF FIGURES

- Figure 1 Orifice plate in a duct
- Figure 2 The pitot-static tube
- Figure 3 The hot-wire anemometer
- Figure 4 Graph of $(1-e^{-lt})$ as a function of time for various values of l
- Figure 5 Schematic of constant-injection equipment
- Figure 6 Schematic of pulse-injection technique
- Figure 7 Schematic of the pulse-injection equipment
- Figure 8 Schematic of injection using a 8 mm internal bore copper tube
- Figure 9 Modified tracer-gas injector with a row of 1 mm diameter holes
- Figure 10 SF_6 and N_2 injection side by side
- Figure 11 Instrumentation for new tracer-gas injection technique
- Figure 12 Position and number of sampling probes for different shapes and sizes of ducts
- Figure 13 Different type of sampling probes
- Figure 14 Instrumentation for the constant-injection technique
- Figure 15 Instrumentation for the pulse-injection technique
- Figure 16 Insertion of a pitot-tube into the duct via a velocity tapping
- Figure 17 Variation of tracer-gas measurement with X/D_h in a 560 mm round duct, constant-injection technique
- Figure 18 Variation of tracer-gas measurement with X/D_h in a 560 mm round duct, pulse-injection technique
- Figure 19 Variation of tracer-gas measurement with X/D_h in a 300 mm x 300 mm duct, constant-injection technique
- Figure 20 Variation of tracer-gas measurement with X/D_h in a 300 mm x 300 mm duct, pulse-injection technique
- Figure 21 Variation of tracer-gas measurement with X/D_h in a 600 mm x 300 mm duct, constant-injection technique

- Figure 22 Variation of tracer-gas measurement with X/D_h in a 600 mm x 300 mm duct, pulse-injection technique
- Figure 23 Variation of tracer-gas measurement with X/D_h in a 1200 mm x 300 mm duct, constant-injection technique
- Figure 24 Variation of tracer-gas measurement with X/D_h in a 1200 mm x 300 mm duct, pulse-injection technique
- Figure 25 Comparison of tracer-gas airflow measurements with measurements made using a pitot tube, 560 mm round duct
- Figure 26 Comparison of tracer-gas airflow measurements with measurements made using a hot-wire anemometer, 560 mm round duct
- Figure 27 Comparison of tracer-gas airflow measurements with measurements made using a pitot tube, 300 mm x 300 mm duct
- Figure 28 Comparison of tracer-gas airflow measurements with measurements made using a hot-wire anemometer, 300 mm x 300 mm duct
- Figure 29 Comparison of tracer-gas airflow measurements with measurements made using a pitot tube, 600 mm x 300 mm duct
- Figure 30 Comparison of tracer-gas airflow measurements with measurements made using a hot-wire anemometer, 600 mm x 300 mm duct
- Figure 31 Comparison of tracer-gas airflow measurements with measurements made using a pitot tube, 1200 mm x 300 mm duct
- Figure 32 Comparison of tracer-gas airflow measurements with measurements made using a hot-wire anemometer, 1200 mm x 300 mm duct
- Figure 33 Schematic diagram of the duct system and instrumentation
- Figure 34 Variation of tracer-gas concentration with X_s/D_H
- Figure 35 Variation of static pressure with X_p

- Figure 36 Variation of volumetric flow rate with static pressure difference across the porous medium
- Figure 37 HVAC System for testing tracer gas techniques
- Figure 38 Comparison of tracer-gas airflow measurements with measurements made using a pitot tube, HVAC system [unit: m^3/s , {Tracer-gas results are shown in brackets}]
- Figure 39 Comparison of tracer-gas airflow measurements with measurements made using a pitot tube, HVAC system [unit: m^3/s , {Tracer-gas results are shown in brackets}]
- Figure 40 Method for measuring air velocity of a rectangular diffuser
- Figure 41 Schematic diagram of the HVAC system
- Figure 42 Injection unit
- Figure 43 Sampling unit
- Figure 44 Comparison of tracer-gas airflow measurements with measurements made using a pitot tube, HVAC system [unit: m^3/h , {Tracer-gas results are shown in brackets}], Experiment 1
- Figure 45 Comparison of tracer-gas airflow measurements with measurements made using a pitot tube, HVAC system [unit: m^3/h , {Tracer-gas results are shown in brackets}], Experiment 2
- Figure 46 Comparison of tracer-gas airflow measurements with measurements made using a pitot tube, HVAC system [unit: m^3/h , {Tracer-gas results are shown in brackets}], Experiment 3
- Figure 47 Diffusion tube
- Figure 48 Schematic of the controlled tracer-gas injection system
- Figure 49 Instrumentation for the injection of PFT into the duct
- Figure 50 PFT injection system
- Figure 51 Heating block
- Figure 52 Circuit diagram of the tracer injection system
- Figure 53 The prototype sampling system

- Figure 54 Details of the sampling unit manifold
- Figure 55 A single adsorbent tube with end cap
- Figure 56 Adsorber tube holder
- Figure 57 Schematic of connection at adsorber tube holder
- Figure 58 Details of connection
- Figure 59 High frequency sampling system's case
- Figure 60 Type SBK 1355 thermal desorber
- Figure 61 Schematic of the thermal desorber/gas analysis system
- Figure 62 First point plotted on the calibration graph
- Figure 63 The calibration graph
- Figure 64 Procedure of packing the tube
- Figure 65 Instrumentation for determining the optimum sample volumes or breakthrough volumes
- Figure 66 Instrumentation for PFT technique
- Figure 67 Connection between bag and sampling system
- Figure 68 Schematic of the air distribution system
- Figure 69 Instrumentation for airflow measurements at the air handling unit
- Figure 70 Instrumentation for determining air-tightness of duct system, stationary technique
- Figure 71 Instrumentation for determining air-tightness of duct system, mobile technique
- Figure 72 Variation of air leakage rate with airflow rate in duct system
- Figure 73 Variation of air leakage rate with pressure drop in duct system

LIST OF TABLES

| | |
|----------|---|
| Table 1 | Properties of a selection of tracer gases |
| Table 2 | Variation of airflow rate with respect to the distance from the injection points of tracer gas in a 560 mm diameter duct |
| Table 3 | Variation of airflow rate with respect to the distance from the injection points of tracer gas in a 300 mm x 300 mm duct |
| Table 4 | Variation of airflow rate with respect to the distance from the injection points of tracer gas in a 600 mm x 300 mm duct |
| Table 5 | Variation of airflow rate with respect to the distance from the injection points of tracer gas in a 1200 mm x 300 mm duct |
| Table 6 | Design flows and measured flows with all flow control open |
| Table 7 | Measurement of velocity pressure in a circular duct |
| Table 8 | Comparison of tracer-gas airflow measurements with measurements made using a pitot tube, Experiment 1 |
| Table 9 | Comparison of tracer-gas airflow measurements with measurements made using a pitot tube, Experiment 2 |
| Table 10 | Comparison of tracer-gas airflow measurements with measurements made using a pitot tube, Experiment 3 |
| Table 11 | List of perfluorocarbon tracers |
| Table 12 | List of adsorbents |
| Table 13 | Results of the optimum sampling volumes |
| Table 14 | Comparison of airflow measurements in a duct using a pitot tube and PFT technique, sampling tubes |
| Table 15 | Comparison of airflow measurements in a duct using a pitot tube and PFT technique, sampling bags |
| Table 16 | Comparison of airflow measurements in a duct using a pitot tube and tracer-gas techniques |
| Table 17 | Measurement of airflow rate in the air handling unit and exhaust duct system |
| Table 18 | Airflow rate with respect to leakage rate in 300 mm x 300 mm square duct, stationary technique |

- Table 19 Airflow rate with respect to leakage rate in a 300 mm x
300 mm square duct, mobile technique
- Table 20 Relationships of leakage rate and airflow rate in 300 mm x
300 mm square duct
- Table 21 Relationships of leakage rate and pressure drop across the
leak in 300 mm x 300 mm square duct

LIST OF SYMBOLS

| | |
|-------------|--|
| A | Cross-sectional area of duct, m^2 |
| A_x | Cross-sectional area of diffusion path, cm^2 |
| B | Barometric pressure, mbar |
| C | Concentration of tracer gas, ppm |
| C_b | Average concentration of tracer gas at the duct inlet, ppm |
| $C_{(0)}$ | Concentration of tracer gas at time $t = 0$, ppm |
| $C_{(t)}$ | Concentration of tracer gas at time t , ppm |
| $C_{d(0)}$ | Concentration of tracer gas $t = 0$ (tracer-decay technique), ppm |
| $C_{d(t)}$ | Concentration of tracer gas $t > 0$ (tracer-decay technique), ppm |
| $C_{pu(t)}$ | Concentration of tracer gas $t > 0$ (pulse-injection technique), ppm |
| D_h | Hydraulic diameter of the duct, m |
| D_0 | Diffusion coefficient at T_0 and P_0 , cm^2/s |
| D_r | Diffusion rate, ng/min |
| F | Specific airflow rate in the duct, m^3/h |
| F_d | Airflow rate using tracer-gas decay technique, m^3/s |
| F_p | Airflow rate using pitot-tube, m^3/s |
| F_t | Airflow rate using tracer-gas techniques, m^3/s |
| F_{ci} | Airflow rate using constant-injection technique, m^3/s |
| F_{pu} | Airflow rate using pulse-injection technique, m^3/s |
| F_{sb} | Airflow rate using sampling system (bag), m^3/s |
| F_{st} | Airflow rate using sampling system (tube), m^3/s |
| $G_{(t)}$ | Injection rate of a short-pulse of tracer, m^3/h |
| g | Acceleration due to gravity, m/s^2 |
| I | Air-change rate, h^{-1} |
| L | Leakage rate, m^3/s |
| L_d | Length of diffusion path, cm |
| M | Molecular weight, g |
| P | Pressure, Pa |
| P_0 | Standard atmospheric pressure (760 mm Hg) |
| P_T | Total pressure, Pa |

| | |
|--------------------|---|
| P_{atm} | Atmospheric pressure, Pa |
| p | Partial pressure, mm Hg |
| q_{corr} | Corrected injection rate of tracer gas, m ³ /s |
| q_{tr} | Tracer gas flow rate at tracer gas temperature at mass flow controller, m ³ /s |
| $q_{(t)}$ | Injection flow rate of tracer gas at time t, m ³ /h |
| Re | Reynolds number |
| T_a | Air temperature, °C |
| T_0 | Temperature at 273K |
| t | Time, s |
| V | Internal volume of duct, m ³ |
| β | Barometric pressure, Pa |
| ρ | Air density, kg/m ³ |
| ρ_{id} | Density of tracer gas at duct air temperature, kg/m ³ |
| ρ_{tm} | Density of tracer gas at mass flow controller, kg/m ³ |
| ΔP_L | Pressure drop across the leaks, Pa |
| ΔP_T | Total pressure loss, Pa |

1. INTRODUCTION

Ventilation is a fundamental consideration for the design of buildings as it has a strong influence on the internal environment and the building's energy needs. Ventilation in buildings is necessary to provide a healthy and comfortable environment for humans to live and work.

Since the oil-crisis in the early 70's, many new insulation techniques have been implemented to increase the air-tightness of buildings. Improved insulation cuts down heat losses to the outside and reduces the building's energy consumption. However, insufficient ventilation results in poor indoor air quality and under extreme conditions, can be harmful to the occupants of the building. This leads to problems associated with Sick Building Syndrome (SBS). High ventilation rates reduce the buildup of contaminants. Unfortunately, heat is also expelled with the foul air and this increases energy consumption. In addition, the performance of the heating, ventilation and air-conditioning (HVAC) system influences thermal comfort; for example, cold draughts can produce an unpleasant living or working environment for the occupants. Knowledge of optimum ventilation rates for individual buildings is essential. The minimum ventilation rate varies from building to building depending on activities, number of occupants, age and sex of occupants, contaminant sources, etc. CIBSE has therefore provided standards for ventilation engineers to assist the design of ventilation systems. Studies have shown that ventilation systems in buildings are largely responsible for Sick Building Syndrome [1-2] and so it is important to evaluate the performance of HVAC systems. The application of airflow measurements in ducts is required during the design, commissioning and maintenance of HVAC systems. It is, therefore, important to establish a method of measurement that is simple to use and provides a high degree of accuracy.

Measurements of airflow in HVAC systems are usually carried out using traditional instrumentation such as, hot-wire anemometers, vane anemometers and pitot-tubes. It is difficult to obtain accurate measurements of airflow in a ventilation system using this type of instrumentation. In practice, they require a long measuring duct for establishment of fully-developed flow profiles and this is not always possible to achieve. In many ventilation systems, the outside air intake is either not ducted at all or the exhaust air returns through the air intake. In addition, limited access to the flow passage could restrict measurements and flow velocities less than 3 m/s could lead to measurement inaccuracies. Traditional instrumentation fails to give an accurate picture of the performance of the HVAC system. Tracer-gas techniques can provide solution to these problems (see section 2.2). The versatility of tracer-gas methodology permits accurate airflow measurements to be performed in situations where traditional instrumentation cannot be employed. Traditional measurement techniques cannot determine the extent of any external or internal re-entrainment of building exhaust into building supply or the amount of natural air infiltration. Tracer-gas techniques have been used widely for ventilation measurements in buildings [3-7]. However, only a handful of researchers such as Persily and Axley [8], Riffat and Lee [9] and Sateri [10] have applied tracer-gas techniques to the measurement of airflow in HVAC systems.

The principle behind tracer gas measurements is to mark the air in the upstream of the duct with something easily identifiable, so that the concentration of the tracer can be detected. The tracer gas used in ventilation studies should possess certain properties (see section 2.2.2) and these include being colourless, odourless and existing at infinitesimally low concentration in the atmosphere.

2. REVIEW OF AIR FLOW INSTRUMENTATIONS AND TECHNIQUES

Over the years, a wide area of science and technology has stimulated the development of airflow instrumentation and measurement techniques. There is a need for instruments and techniques that can operate to an increasingly higher accuracy. There is a wide range of instrumentations used to measure airflow ranging from a simple device such as a pitot-static tube to a more complex one such as ultrasonic flowmeter.

One of the most widely used instruments employed for measurement of airflow in ducts is the pitot-static tube and is based on the principle of pressure-differential. A short description of the most popular airflow measuring techniques and instruments is provided in the next section.

2.1 Existing techniques and instrumentation

2.1.1 Pressure-differential technique

The pressure differential technique involves the insertion of some device into a fluid-carrying pipe to cause an obstruction and create a pressure difference on either side of the device. Such devices include the orifice plate, the venturi tube, the flow nozzle, the Dall flow tube and pitot-static tube. When such a restriction is placed in a pipe, the velocity of the fluid through the restriction increases and the pressure decreases. The volume flow rate is proportional to the square root of the pressure difference across the obstruction.

All applications of this technique of flow measurement assume the flow conditions upstream of the obstruction device are in steady state. This is ensured by having a certain minimum length of straight run of duct ahead

of the flow measurement point. The minimum length required for various pipe diameters are specified in the British Standards tables [11], but a useful rule of thumb widely used in the process industries is to specify a length 10 times the duct diameter.

Flow-restriction-type instruments are popular because they have no moving parts and are therefore robust, reliable and easy to maintain. However, one disadvantage of this method is that the obstruction causes a permanent loss of pressure in the flowing fluid. It is particularly important in applications of flow restriction techniques to choose an instrument which has a range appropriate to the magnitudes of flow rate being measured. This requirement arises because of the square-root relationship between the pressure difference and flow rate. This means that as the pressure difference decreases, the error in flow-rate measurement can become very large. In consequence, restriction-type flowmeters are only suitable for measuring flow rates between 30% and 100% of the instrument range.

2.1.1.1 Orifice plate

The orifice plate is a metal disk with a hole in it, as shown in Figure 1 and this is inserted into a duct carrying a flowing fluid.

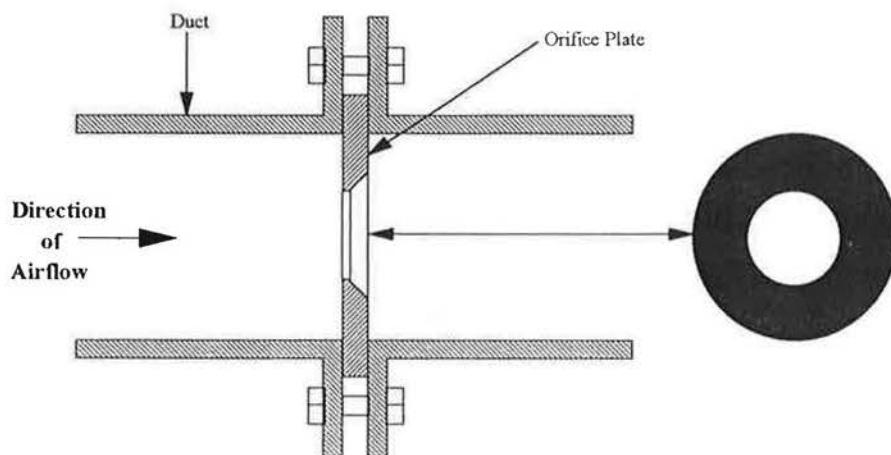


Figure 1 Orifice plate in a duct

This hole is normally concentric with the disk. The use of the orifice plate is widespread because of its simplicity, low cost and availability in a wide range of sizes. However, the best accuracy obtainable from this device is in the range of $\pm 2\%$ and the permanent pressure loss caused in the flow is very high; between 50% and 90% of the pressure difference in magnitude. Other problems with the orifice plate are a gradual change in the discharge coefficient over a period of time as the sharp edges wear away. There is a tendency for any particles in the flowing fluid to stick behind the hole and gradually build up and reduce in the diameter of the hole. The latter problem can be minimised by using an orifice with an eccentric hole. If the hole is near to the bottom of the duct, solids in the flowing fluid tend to sweep through, and build up of particles behind the plate is minimal.

2.1.1.2 Pitot-static tube

The pitot-static tube is mainly used for temporary measurements of airflow, although it is also used for permanent flow monitoring. The instrument relies on the principle that a tube is placed with its open end in a stream of fluid as shown in Figure 2.

The open end of the pitot-static tube will bring to rest that part of the fluid that impinges on it. This loss of kinetic energy will be converted to a measurable increase in pressure inside the tube. The pitot-static tube incorporates in one probe the necessary tappings to obtain readings of total, static and velocity heads when suitably connected to a manometer. The probe essentially consists of two small concentric tubes joined at the end so as to leave the central tube facing the air stream. The tube facing the air stream registers the total head in the duct, whereas the static head is obtained via the small holes into the tube annulus.

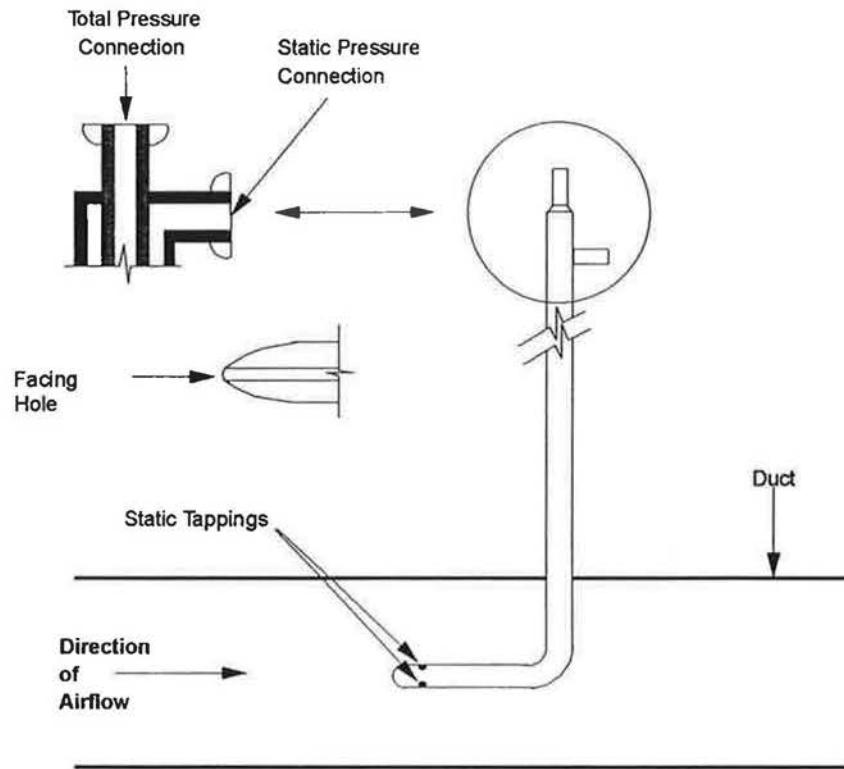


Figure 2 The pitot-static tube

Inferring the volume flow rate from the measurement of the flow velocity at one point in the fluid obviously requires the flow profile to be very uniform. If this condition is not met, multiple pitot-static tubes can be used to measure velocities across the complete cross-section of the pipe.

Pitot-static tubes have the advantage that they cause negligible pressure loss in the flow. They are also cheap, and the installation procedure consists of very simple process of pushing them down a small hole drilled in the flow-carrying pipe.

The measurement of airflow in duct gives reliable results. To ensure reasonable accuracy, measurement should be carried out at velocities greater than 3 m/s. For measurements below 3 m/s there is some degree of inaccuracy. As a good guide, the measuring range is 3 - 20 m/s. The main failing is that the measurement accuracy given is only about $\pm 5\%$ and sensitive pressure-measuring devices are needed to achieve even this limited level of accuracy, as the pressure difference created is very small. It is essential to align the head of the pitot-static tube as accurately as possible to the flow direction while measuring the velocity of the airflow in the duct. A faulty inclination may produce a faulty measurement, too high or too low.

2.1.2 Methods based on the rates of cooling hot bodies

The relationship between the rate of heat loss from a heated body and the speed of flow of a fluid in which it is immersed has been studied extensively. Attention has mainly been concentrated on the use of electrically heated wire as anemometers.

The law governing the convective cooling of a hot cylindrical wire by a fluid stream is now well established, and the device is widely used for flow measurement when pressure tubes are inappropriate for one reason or another. The heated-body method possesses several advantages, particularly high sensitivity at low flow rates. In a hot-wire anemometer, the wire diameter must be very small (0.02 mm or less) so that it will respond quickly. Consequently, the probe is fragile and its characteristics are seriously affected by dust deposition, oil, or other surface contamination. Its principal application is the measurement of rapid fluctuations, particularly the study of turbulent flow.

There are several types of hot-wire anemometers. Most of them are based on the measurement of the rate of loss of heat. Some of these are:

- a. Hot-wire anemometers
- b. Hot-grid anemometer
- c. Sinusoidally heated hot-wire anemometer.

However, in this context, only the hot-wire anemometer is of interest.

2.1.2.1 Hot-wire anemometer

A hot-wire anemometer has a sensing element which is heated electrically and kept at a constant temperature. When the element is exposed to the airstream, either the temperature difference between the element and the airstream is measured or the electrical current which is needed to maintain a constant temperature is measured. This value is then calibrated to give the velocity of air.

A form of simple hot-wire anemometer is shown in Figure 3. The section labelled '1' is the wire forming the heated element. A length-diameter ratio of at least 200 is usually recommended in order to minimize the effects of heat conduction from the ends of the wire, which are soldered or welded to rigid prongs '2-2' held in an insulated base '3'. The leads '4-4' connect the wire to the measuring circuit.

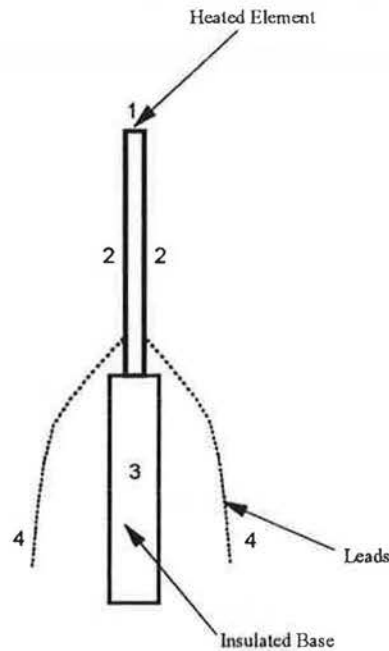


Figure 3 The hot-wire anemometer

Simmons [12] has developed a shielded hot-wire anemometer to overcome the difficulties of fragility and surface contamination (although at the expense of speed of response). This has found extensive practical application in the measurement of ventilation and other air speed measurements at normal air temperatures. It has more permanent calibration and greater mechanical strength than the unshielded hot wires. The wandering calibration of an unshielded wire is largely due to the deposition of dust and possibly also to the change of specific electrical resistance with the strain caused by the air forces acting on the wire. Simmons therefore decided to try the effect of shielding the wire by enclosing it in a fine tube. Besides protecting the wire from the air force, the shield served to increase the overall diameter of the probe without changing the wire diameter. The dust deposited produced a smaller effect.

Hot-wire anemometers can be highly sensitive and easy to use at very low air speeds. They are particularly useful for measurements of air velocity and distribution in an occupied space but can also be useful whenever low velocities are important.

This instrument requires careful calibration and, because it can be upset by dirt deposited on the sensing element, frequent calibration is essential whenever low velocity measurements are carried out.

2.1.3 Other air flow measuring device

There are many other types of airflow measuring devices on the market. The rotating vane anemometer has been extensively employed for measuring air speed, particularly low speeds where the pressures set up by the motion are so small that it is difficult to measure them accurately. The simplicity of the instrument make it exceedingly useful. The main application of the rotating vane anemometer is the measurement of airflow at grilles, hoods and other relatively large openings.

The vane anemometer is simply a windmill consisting of a number of light, flat vanes mounted on radial arms attached to a common, small steel spindle, which rotates in two low-friction bearings. Eight vanes made of thin sheets of aluminium alloy, or mica, are almost invariably used; and the forces acting on the vanes cause the spindle to rotate at a rate depending mainly on the air speed. Suitable gearing transmits the motion of the spindle to the pointer or more usually to a number of pointers moving over dials graduated in metres. Therefore, to determine the air speed it is necessary to observe with an aid of a stop-watch the number of 'metres of air', as shown by the indicating mechanism, to pass the instrument in unit time. This gives the indicated air speed; the true air speed is obtained by reference to the calibration curve for the particular anemometer in used. However, with the advancement in technology, new instruments allow the

air speed to be read directly from a digital display.

2.2 Air flow measurement using tracer-gas techniques

Tracer-gas techniques have been used extensively for ventilation measurements in buildings. The measurement of air flow in HVAC systems using tracer-gas techniques is a new application that has been established in the recent years. Tracer-gas techniques are simple and useful methods for this kind of measurement and have a number of advantages over the traditional instrumentations (i.e., pitot-static tube, rotating vane anemometer and hot-wire anemometer) as listed below:

- a. Unlike traditional instrumentation, tracer-gas techniques do not require a long measuring duct for the establishment of a fully-developed flow profile. Good tracer and air mixing at the point of sampling are all that is required for these techniques. Good tracer and air mixing can be obtained in HVAC systems as the high airflow rates produce turbulence as the air passes over a series of bends and heat exchangers.
- b. Tracer-gas techniques are not limited by the complexity of the duct configurations. Measurements of airflow rate in HVAC systems using traditional instrumentation requires averaging of the air velocities obtained from a few measurement points across the duct depending on the shape and size of the duct. However, with tracer-gas techniques, one point measurement across that section of the duct is sufficient.

- c. They can be used to measure airflow rates over a wide range of values, be it laminar or turbulent flow. However, this is not possible with the pitot-static traverse method where any air flows less than 3 m/s lead to significant inaccuracies.
- d. They can be used to measure airflow rates directly and do not require determination of the cross-sectional area of the duct. For traditional instrumentation, airflow rates are estimated by multiplying the air velocity by the cross-sectional area of the duct.
- e. They can also be used to determine the air-tightness of the ductwork.

The details of these tracer-gas techniques will be discussed in the next section.

2.2.1 Tracer-gas measurement techniques

This section examines the fundamental theory and practical aspects of each tracer-gas technique. To estimate airflow rates in a duct, the concentration of tracer gas and injection rate must be known. The mass balance relations are used to relate the measured tracer-gas concentrations to the airflow rates. A generalised tracer mass balance equation can be written as:

| | | | | |
|---|---|--|---|---|
| Rate of change in concentration of tracer in duct | = | Amount of tracer introducing into the duct | - | Amount of tracer leaving the duct |
|---|---|--|---|---|

$$V \frac{dC(t)}{dt} = Q(t) + F(t) * C_e - F(t) * C(t) \quad (1)$$

where,

- V = Duct volume, m^3
- $F_{(t)}$ = Airflow rate through the duct, m^3/h
- C_e = External concentration of tracer gas, ppm
- $C_{(t)}$ = Internal concentration of tracer gas at time t , ppm
- $q_{(t)}$ = Injection rate of tracer gas into the duct, m^3/h

The classification of tracer-gas techniques is based on the injection strategy and the form of the mass balance equation. There are four types of tracer-gas measurement techniques, namely,

- a. Constant Injection
- b. Pulse Injection
- c. Concentration Decay
- d. Constant Concentration

They are classified according to the injection method and form of the mass balance equations.

Each tracer-gas technique possesses specific advantages and disadvantages: some are better for short term measurements while others are better for long term measurements; some are more applicable for measurement of airflow rate in buildings and HVAC systems while others are limited to measurement of airflow in buildings; some techniques are less sensitive to mixing problems than others and some techniques are simpler and less expensive than others. Each technique will be described in detail below:

2.2.1.1 Constant-injection technique

Theory

In this technique, the tracer-injection term of the mass balance equation is set at a fixed value. In practice, this condition is achieved by regulating the gas cylinder to inject tracer gas at a uniform rate. Assuming that the external tracer-gas concentration is zero, and that the air and tracer are perfectly mixed within the duct, the mass balance equation is given by:

$$V \frac{dC_{(t)}}{dt} = -F_{(t)} C_{(t)} + Q_{(t)} \quad (2)$$

By solving equation (2) in terms of concentration of tracer gas in the duct, it becomes:

$$C_{(t)} = \frac{Q}{F} + [C_{(0)} - \frac{Q}{F}] e^{-\frac{F_{(t)}}{V} t} \quad (3)$$

The duct air-exchange rate I is given by:

$$I_{(t)} = \frac{F_{(t)}}{V} \quad (4)$$

Assuming that both the injection of tracer gas into the duct and the air exchange rate remain constant during the measurement, and there is no tracer present at the start of the measurement, equation (3) becomes:

$$C_{(t)} = \frac{Q}{F} [1 - e^{-It}] \quad (5)$$

If the change of tracer-gas concentration is small, the system is closed to equilibrium. After a sufficiently long period of time, the transient term in equation (5) (see Figure 4) would die out and the flow rate through the duct would simply be given by:

$$F = \frac{Q}{C_{(t)}} \quad (6)$$

Hence, by setting the tracer-gas injection rate (q) to an appropriate value and monitoring the concentration (C) in the duct, the value of the specific airflow rate (F) can be determined.

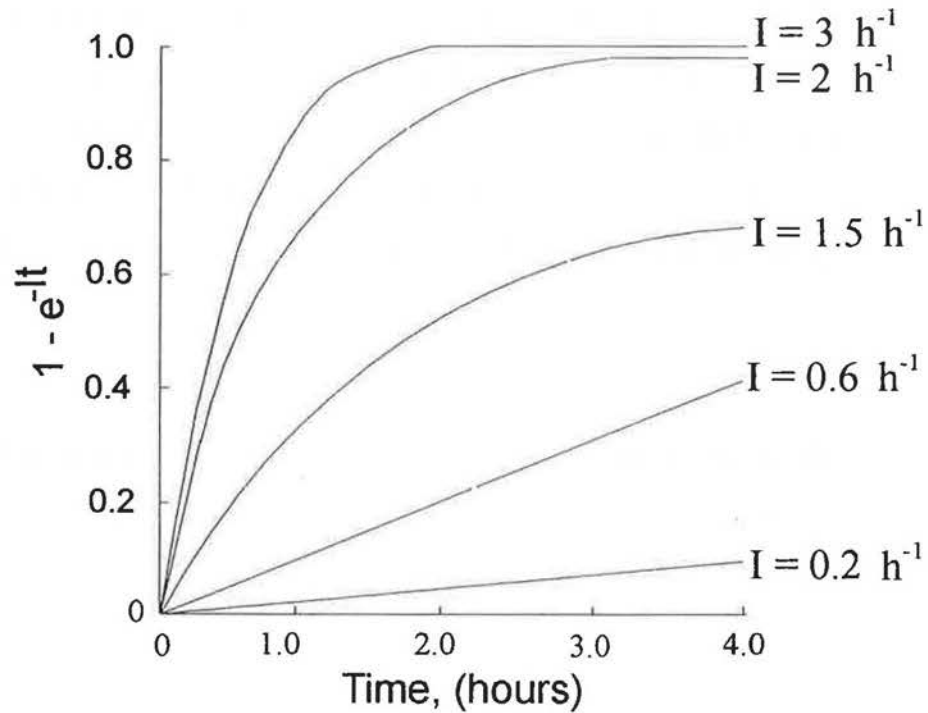


Figure 4 Graph of $(1 - e^{-It})$ as a function of time for various values of I

Practical Aspect

The constant-injection technique is based on the injection at constant rate of tracer gas into the airstream of the duct. This technique can be classified under two categories:

- a. Analysis of tracer conducted on site.
- b. Analysis of tracer conducted off site.

On-site analysis

For on-site analysis, all the equipment required to carry out the airflow measurement in the HVAC system is brought into the building. Tracer gas is continuously injected upstream of the duct section under test while the concentration of tracer is measured at a point downstream of that section. Tracer-gas concentration cannot commence immediately after injection of tracer; time must be allowed for an approximate state of equilibrium to be reached. As the transient effect has become minimal, the airflow rate is inversely proportional to the tracer-gas concentration monitored in the duct. Therefore, the higher the tracer-gas concentration, the lower the airflow rate.

The injection of a known quantity of tracer gas is controlled by a mass flow controller connected to a digital readout unit. The flow rate through the mass flow controller is determined by the settings on the digital readout unit. This unit will actuate the opening of the mass flow controller's valve by varying the power supply. The sampling and analysis of the tracer gas is carried out continuously using the gas analyser. A schematic of the constant-injection equipment is shown in Figure 5.

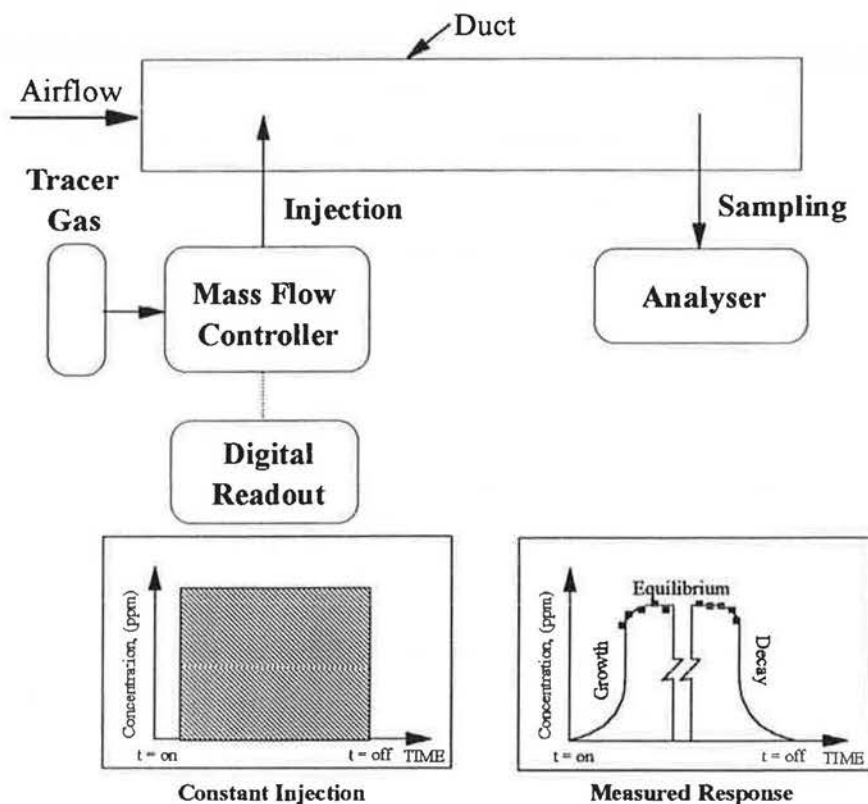


Figure 5 Schematic of constant-injection equipment

This technique requires a continuous injection of tracer gas and therefore can be excessive costly in regard to tracer-gas consumption. However, this can be minimised by careful choice of the tracer gas; the required level of tracer concentration and the detectability limit (e.g., parts per billion or parts per trillion) of the analyser.

Off-site analysis

In this case, only the injection and sampling systems are left on site. All expensive and highly technical, analytical and calculational equipment can be left off-site and analysis of all gas samples is carried out in the laboratory. The only significant disadvantage of this technique is the information collected is not available in real-time.

The injection technique is the same as for the on-site analysis' technique. However, air samples are collected in an air sampling device (e.g., sample bags/tubes) using a sampling system (see Figure 85).

Alternatively, to avoid using an expensive tracer-gas release technique, the active perfluorocarbon tracer technique could be employed. Perfluorocarbon tracer gas is released into a duct by heating liquidified perfluorocarbon tracer in a bottle using a thermal bath. Samples are collected in sampling tubes via a sampling system. This technique can be conducted by non-technical personnel and mailed back to the laboratory when the test is complete. Further details of this technique are presented in Chapter 5.

2.2.1.2 Pulse-injection technique

Theory

Considering air flows in a duct section (see Figure 6) at a time-varying mass flow rate $F_{(t)}$. A short-duration pulse of tracer gas is injected into the inlet of the duct at a rate of $G_{(t)}$ and the time variation of the tracer-gas concentration is measured at the exit $C_{(t)}$. The amount of tracer-gas injected is small, therefore it does not contribute significantly to the mass flowrate of air in the duct and the exit mass flowrate of air will equal $F_{(t)}$.

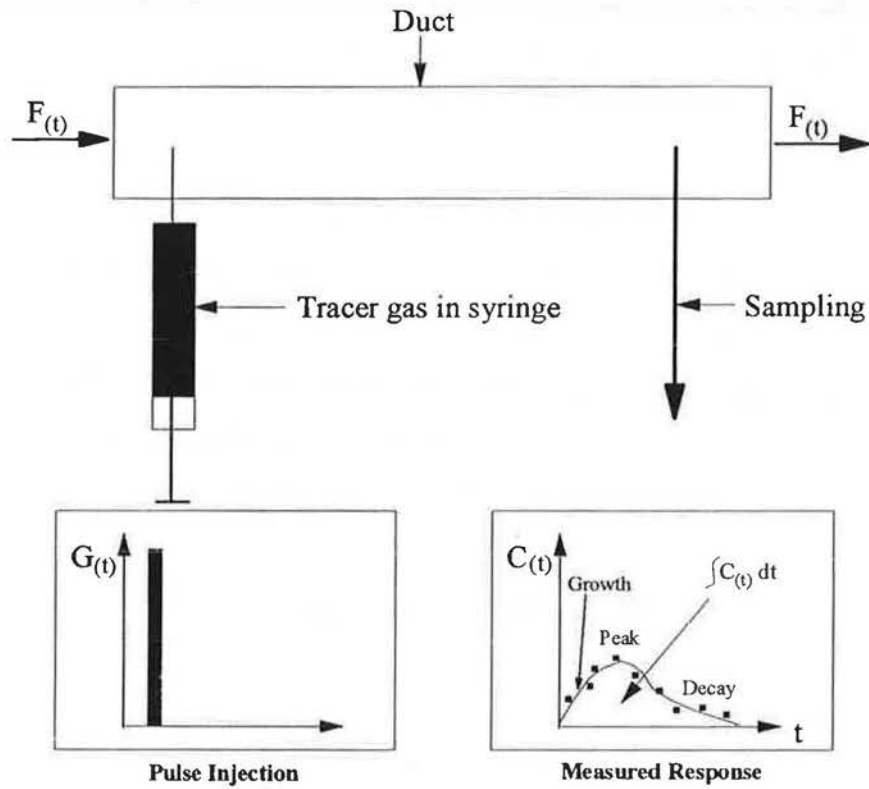


Figure 6 Schematic of pulse-injection technique

If we assume that the tracer gas is well mixed across the section of the duct, then the exit volume flow rate will be a product of the flow rate and the exit concentration, $F(t)C(t)$. If the tracer gas is assumed to be completely purged from the duct after a time interval (t_1 to t_2) then the volume of tracer gas leaving the duct must be equal to the amount injected. Applying the integral volume balance of tracer gas, we have:

$$\int_{t_1}^{t_2} F(t) C(t) dt = \int_{t_1}^{t_2} G(t) dt \quad (\text{for } F(t) \geq 0) \quad (7)$$

The integral mean value theorem can be applied to the left of equation (7), as the concentration variation does not involve a sign change, and simplified to obtain the governing equation of duct pulse tracer-gas technique:

$$F_{(\alpha)} = \left[\int_{t_1}^{t_2} C_{(t)} dt \right]^{-1} \int_{t_1}^{t_2} G_{(t)} dt \quad (\text{for } t_1 \leq \alpha \leq t_2) \quad (8)$$

The above expression, states that the volume flow rate of air that occurs at sometime, α , during time interval (t_2, t_1) is the ratio of the volume of tracer gas injected to the integral of the concentration response downstream from the injection point. If the volume flow rate in the duct remains constant, then the determination will yield a constant value. However, if the volume flow rate changes very little during the interval, then $F_{(\alpha)}$ will be a good estimate of the average flow rate during that interval.

Practical Aspect

This technique is based on the injection of a short-duration pulse of tracer gas into the duct and measurement of the variation of tracer-gas concentration with time at a point downstream of the injection point. It does not matter whether the analysis is carried out on-site or off-site, the equipment that is required to carry out the measurement is very simple. Figure 7 shows a schematic of the pulse-injection equipment.

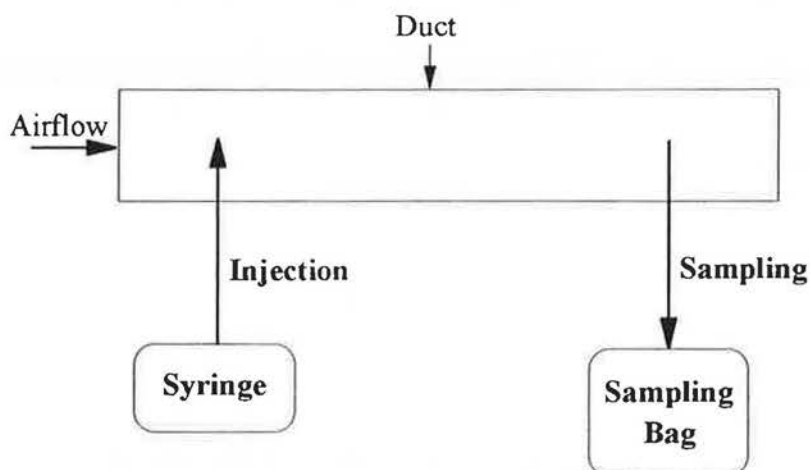


Figure 7 Schematic of the pulse-injection equipment

The short-pulses of tracer-gas injection are performed by using a syringe. This syringe is calibrated so that the volume of tracer-gas injected is known. Samples are collected in bags via a pump or using a sampling system. These samples are then analysed either on-site or off-site.

Several important points must be considered when applying this technique to measure airflow in HVAC systems. The equation governing this technique reveals the importance of knowing the actual volume of tracer gas being injected into the duct and obtaining an accurate determination of the concentration integral. These two factors will affect the accuracy of the pulse-injection technique for determining the airflow rate in the HVAC systems.

It is not essential to know the actual injection profile. It is more important to know the actual volume of tracer-gas injected into the duct. The volume of tracer gas can be measured either before or during the injection. However, one must ensure that all the tracer gas in the syringe is injected into the duct. The determination of the integral of the concentration at the downstream point of the duct is equally important. It relies not only on the accuracy of the measurement of the concentration of tracer gas, but also on

the method of collecting the integral's samples. The integral must be based on the cross-sectional average concentration (i.e., the concentration at the point of measurement must be varying along the duct but not across the duct's cross-section). Multi-point injection across the duct will help to achieve a uniform concentration at the point of sampling.

The concentration integral is very difficult to determine from the numerical integration of real-time concentration measurement because of the concentration in the duct will decay very quickly once tracer is injected. Unless the measuring equipment has a high frequency and covers a wide range of measurable concentrations, it is easier to determine the concentration integral by measurement of the average tracer-gas concentration at the measurement point. Air samples from the duct can be collected in appropriate sampling bags for the average tracer-gas concentration to be determined. The collection of air samples begins well before the pulse-injection and continues until the tracer is completely purged from the duct. The concentration integral is the average concentration of the air sample in the bag multiplied by the length of time over which it is collected.

When applying this technique to measure airflow in specific HVAC systems, there will be some initial uncertainty concerning the correct amount of tracer gas to be injected and the length of time over which air samples should be collected. The primary requirement is that the average concentration in the air sample bag is within range of high measurement accuracy of the gas analyser. In order to satisfy this requirement, one has to choose an appropriate combination of the injected volume and concentration averaging time. In general, to obtain the right combination some 'trial and error' may be required. Since each set of measurements requires only a few minutes, it is not too difficult to find the appropriate values for these quantities. As several measurements can be made in a short time, estimate of the repeatability of the results can easily be obtained.

This technique does have some limitations. The accuracy of the technique deteriorates when high airflow rates are to be obtained in a short length of duct because samples cannot be collected sufficiently quickly. As the volume flow rate in the duct is very high, large amount of tracer must be injected into the duct so that the tracer concentration in the air sample collected is within detectability limit of the gas analyser. However, this is not practical when the volume flow rate is so high that an enormous quantity of tracer-gas needs will have to be injected.

2.2.1.3 Concentration-decay technique

This technique involves an initial injection of tracer gas into the duct. The gas is allowed to mix with the internal air while the duct fan is switched off. The fan is then switched on and the decay of concentration of tracer gas is monitored over a given time interval. Equation (9) below is derived from the generalised tracer mass balance equation (See Equation (1)).

$$C_{(t)} = C_{(0)} e^{-It} \quad (9)$$

If the logarithm of the tracer-gas concentration is plotted against elapsed time, the slope of the line is equal to I . The volumetric flow rate F can be determined by multiplying the air change rate, I by the internal volume of the duct, V .

This technique can provide accurate measurement of ventilation rate in buildings very well because the air change rate is low and good mixing of tracer and air can be achieved by using table fan. It is difficult to achieve uniform tracer concentration throughout the whole length of the duct and the airchange rate in a duct is so high that the decay in the concentration of tracer is almost instantaneous. In addition, it is not possible to estimate the effective volume of the duct system accurately. These factors discourage the use of concentration-decay techniques for measuring air flow in HVAC systems.

2.2.1.4 Constant-concentration technique

This technique involves controlling the tracer-gas injection rate to maintain at a constant concentration throughout the section of the duct. The expression shown in equation (10) is derived from the general mass balance equation:

$$F = \frac{Q(t)}{C} \quad (10)$$

This equation is the same as the one used for the constant-injection technique. The only difference is the variation in tracer-gas injection rate. The airflow rate in the duct is proportional to the tracer-gas injection rate required to maintain the concentration level.

Equipment with a sophisticated control mechanism is required to provide feedback between the concentration level and the injection rate of tracer gas. This technique also requires technically trained personnel to operate the system and carried out. All these factors increase the overall cost of using this technique. Although this technique is automated, time is required for the equipment to arrive at the correct injection rate to maintain the concentration level. The concentration in the duct may oscillate about its mean value in an asymmetric manner. More sensitive equipment would reduce the time of oscillation, but this would of course be more expensive.

2.2.2 Tracer-gas requirements

The type of gas to be used as tracer for ventilation studies is important as it can affect the accuracy of tracer-gas measurements. An ideal tracer gas must possess the following properties:

- + Safety : the presence of tracer should not pose a hazard to people, materials or activities in and around the test area. The tracer should therefore be odourless, non-irritant, non-toxic, non-flammable and non-explosive.
- + Non-reactivity : the tracer-gas must not react chemically (e.g. react with duct surfaces, room air or decompose during measurements) or physically (e.g. absorbed by the air-filters in the ducts) with any part of the system under study.
- + Insensibility : the presence of the tracer should not affect the processes that are being studied. Thus, an ideal tracer gas should not affect the air flow or air density of the system.
- + Distinctive : an ideal tracer should not normally be present in the building nor as a normal constituent of air. However, a tracer with a non-zero background may be used provided the background is stable and additional tracer concentration is significantly larger than the steady background.
- + Measurability : the concentration of the tracer must be quantifiable through some established experimental technique which prevents interference with air. It must be easily and economically measured with high reliability by some sort of instrumentation.
- + Availability : the tracer must be commercially obtainable.
- + Others : easily stored, transported and dispersed as an atmospheric gas; tracer-gas concentration must be measurable to a good order of accuracy even when highly diluted. It should have similar density, specific heat and diffusion properties to air.

From the theoretical point of view, the ideal tracer gas must possess the above criteria. However, one must not forget practical considerations such as cost of the tracer.

No tracer gas fulfils all the requirements, but several gases are used successfully as tracers. These include nitrous oxide, carbon dioxide and sulphur hexafluoride. Table 1 gives a broad outline of the properties of some of the most commonly used tracer-gases.

| Tracer | Formula | Density Compared to air | Concentration Safety Limit, (ppm) | Remarks |
|-------------------------------|------------------|-------------------------|-----------------------------------|--|
| Nitrous oxide | N ₂ O | 1.53 | 25 | Anaesthetic gas. Widely used as a tracer. |
| Carbon dioxide | CO ₂ | 1.53 | 5000 | High unstable background aggravated by the building occupants and non-electric heating systems. |
| Sulphur hexafluoride | SF ₆ | 5.11 | 1000 | Detection-affected by other halogenated compounds in air. Decomposes to toxic compounds at 550°C. Widely used as a tracer. |
| Perfluorocarbon tracers (PFT) | - | - | - | Low background concentration. Non-toxic and cheap to use. Widely used as a tracer in long-term monitoring for multizone and interzone flow measurements. |

Table 1 Properties of a selection of tracer gases

Perfluorocarbon tracers are also very popular [13-16], especially for the measurement of airflow in large buildings because they are relatively inexpensive to employ. Only small quantities of these electronegative tracer gases is required because these levels are well above the background concentrations. Furthermore, these tracers can be detected as low as parts per million or less. These gases are relatively easy to handle and the concentrations used for tracer gas studies are much lower than the accepted OSHA standard environmental levels.

2.2.3 Accuracy of tracer-gas techniques

The measurement of airflow in HVAC systems using tracer-gas techniques is based on the measurement of tracer concentration at a given point in the duct. There must be sufficient distance between the point of tracer injection and the region where samples are taken for the total variation in concentration of the tracer over the cross-section of the duct to be less than some predetermined value. The accuracy of these techniques depends largely on the homogeneity of this tracer-air mixture sample [17]. In order to ensure that an uniform tracer-air mixture is achieved, a sufficiently long distance between the injection and sampling points is required. The minimum distance between the point of tracer-gas injection to the point downstream whereby the tracer-air mixture is uniform across the duct cross-section is called the mixing length. Knowledge of this mixing length is crucial.

When measuring ventilation rate in buildings, the uniformity of the tracer-air mixing is improved by using oscillating fans or injecting tracer gas at several points in the room and taking samples and averaging the averaging concentration values. However, this may not be practical when mixing of the tracer with air is poor in particular sections of the HVAC system. In certain parts of a HVAC system, natural mixing is provided by the fan and obstructions from the filters, heat-exchangers coils, bends and contraction or

expansion transition connections. The flow in the duct of a HVAC system is usually turbulent and therefore assists tracer-air mixing. A short mixing length is required in situations where measurements are carried out in a short duct. Better tracer-gas mixing in ducts can be achieved by improving the method of tracer-gas injection and sampling.

2.2.3.1 Development of tracer-gas injection

In practice, the mixing length can be reduced by using different methods of injection and types of injectors, for example, annular injection, injector with multiple orifices and high-speed jets [18]. The next section will describe the development of different types of injector and techniques of injection.

a. Types of injectors

Early development was focused solely on the injector. They were made from 8 mm internal copper tubes. The injectors were positioned in such a way that the gas was injected into the centre of the duct from four sides (see Figure 8).

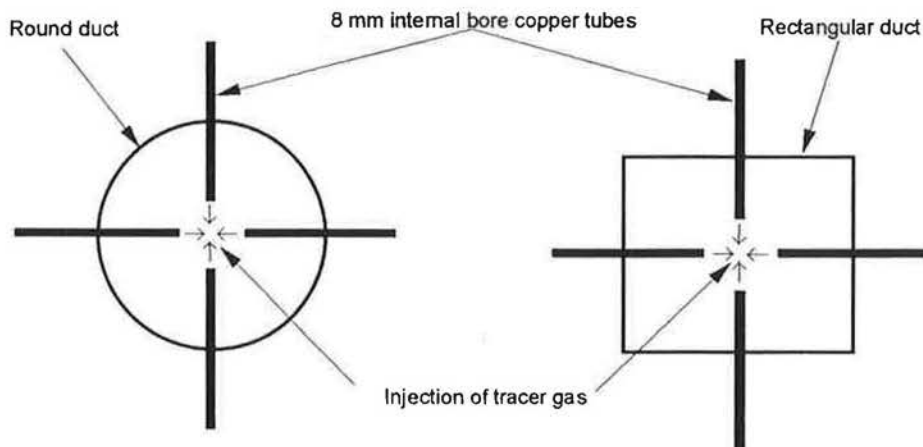


Figure 8 Schematic of injection using 8 mm internal bore copper tube

The tracer-air mixing using these 8 mm tracer-gas injector was studied. Tracer gas was injected at a constant rate into the duct through these tubes and samples were taken using a single tube. The sample tube was traversed across the cross-section area of the duct at various distances from the injection point. Any variation of tracer concentration across the duct indicates poor tracer-air mixing. In addition to the injection of tracer, smoke visualization tests were conducted by injecting smoke through these tubes to visualize the mixing pattern in the duct. The results show that these 8 mm tracer injectors provide a very poor tracer-air mixture even at a large distance from the injection points. In the next test, the 8 mm internal bore copper tubes were replaced by smaller tubes with an internal bore of 4 mm. The smoke visualisation test and monitoring of the variation of tracer concentration across the duct section at various distances from the injection point showed that the tracer-air mixing was still poor. The smoke visualisation test showed that once the smoke leaves the injector at the centre of the duct, it tends to distribute itself towards the sides of the duct.

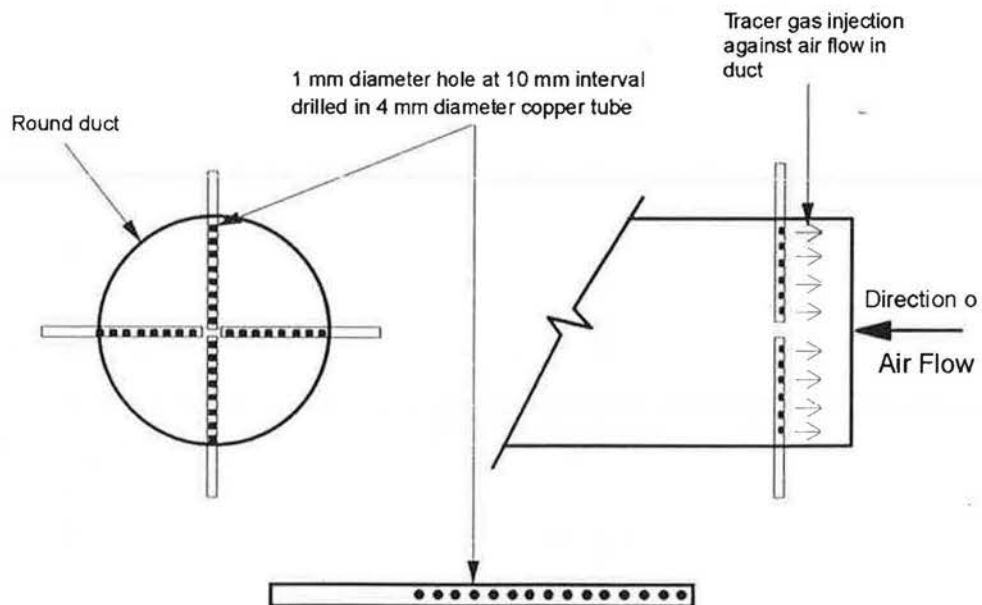


Figure 9 Modified tracer-gas injector with a row of 1 mm diameter holes

In order to overcome this problem, the 4 mm tracer injectors were modified by drilling a series of 1 mm diameter holes along the tube at an interval of 10 mm (see Figure 9).

The results obtained from the smoke and tracer-air profile tests were promising. The mixing length was found to be about $10D_h$ for rectangular ducts with aspect ratios of 1:1, 2:1, 4:1 and a 560 mm diameter round duct over a wide range of flow rates.

b. Method of injection

The method of injection is equally as important as the type of injector if a short length of tracer-air mixing is to be achieved. A high-speed jet with multiple-points for injection of tracer-gas was implemented. The high-speed jet can be provided by a nitrogen cylinder. The premixing of the nitrogen and tracer gas could be achieved using a manifold or the T-connectors.

One disadvantage of these above methods of injection is the high percentage measurement error. The N_2 coming into the manifold or T-connector is at a much higher flow rate than the SF_6 flow rate. This will create a pressure on the incoming SF_6 and stop it entering the manifold or T-connector. So, SF_6 injection rate registered on the mass flow controller is not the true SF_6 injection rate.

In order to overcome this problem, a new set up has been established (see Figure 10). The SF_6 injection point is placed next to the N_2 injection points. This high speed jet of N_2 will disturb the flow of SF_6 coming out of the injection tubes and therefore encourage better tracer-air mixing.

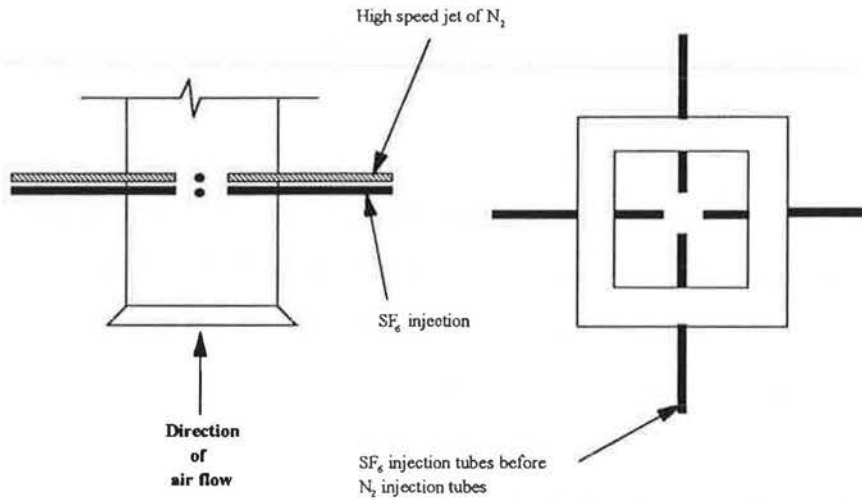


Figure 10 SF₆ and N₂ injection points side by side

The results obtained using the above technique showed a large variation in the tracer-gas concentration across the duct.

To improve tracer-gas mixing, attempts were made to inject N₂ and SF₆ using two concentric tubes. The N₂ was supplied in the inner tube while the SF₆ was supplied through the other tube.

This method of injection produce a tracer-air mixing no better than the previous technique. Finally, a new tracer-gas injection technique was developed. Figure 11 shows the instrumentation required for this new injection technique to obtain a much shorter mixing length. Tracer-gas is injected into the duct using an air-tight diaphragm pump. Pre-mixing between the air and the tracer is carried out in the pump as it goes into the duct, so that air and tracer will be well mixed.

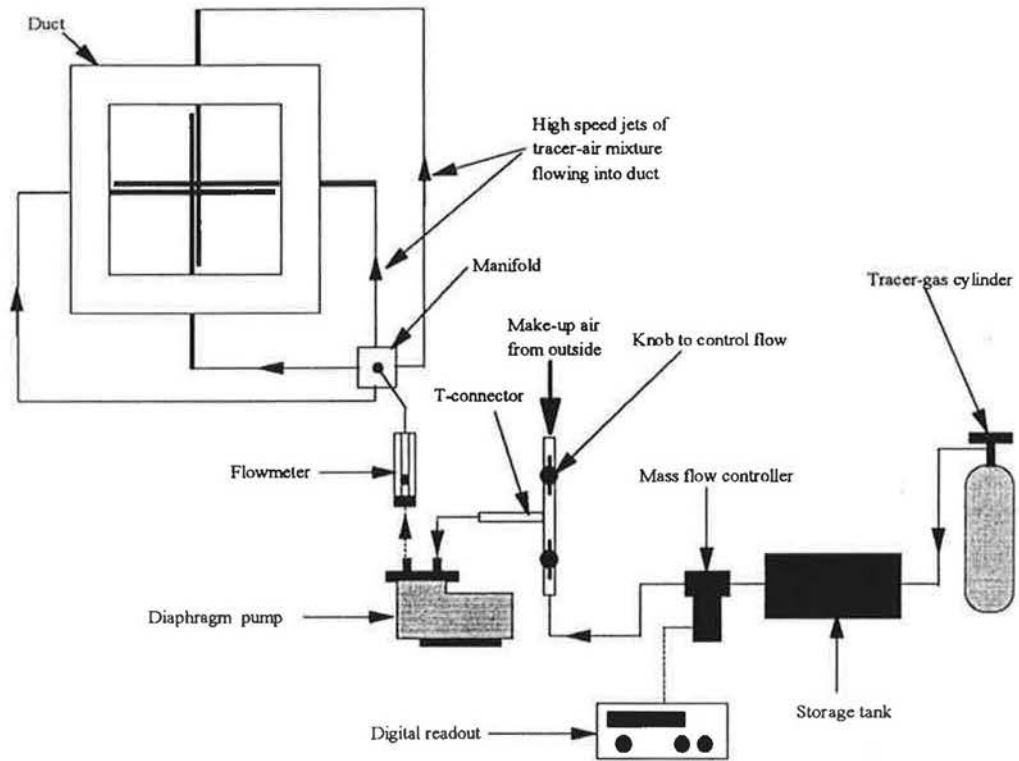


Figure 11 Instrumentation for new tracer-gas injection technique

In addition, the diameter and position of the injector is very important. The tracer-gas injector is made from P.T.F.E. (polytetrafluorethylene) and has an internal diameter of 1.5 mm to produce a high-speed jet of tracer-air mixture into the duct. A shorter mixing length is achieved by putting the outlet of the injector closer to the sides of the duct wall (the high-speed jet of tracer-air mixture from the injector hits the duct wall and is deflected off it before mixing with the oncoming air from the inlet of the duct). A flow meter is connected between the manifold and the pump so that the additional airflow rate generated by the pump going into duct can be noted. Knowledge of this additional airflow rate is important as the true airflow rate in the duct is the difference between this airflow rate and the airflow rate determined using the tracer-gas technique.

A uniform tracer-air mixture was obtained at a mixing length of 7 hydraulic diameters over a range of air velocity. However, at higher airflow rates in the duct, a high injection rate into the duct is required to obtain a short mixing length.

2.2.3.2 Development of tracer-gas sampling

An apparent reduction in mixing length can be obtained if samples are recovered simultaneously from a number of positions across the duct and are mixed prior to measurement. The design of the sampling probes is vital [19]. In the early tests, 3/8" ID sampling probes were inserted into the duct with the holes at right angles to the direction of the airflow (see Figure 12). This did help to improve the mixing length and these sampling probes were then bent to form 90° angle similar to a pitot-tube (see Figure 12). Now, the hole of the sampling probe faces the direction of the airflow in the duct. There was a slight improvement in the mixing length. This shows that mixing length is affected by the orientation of the sampling position with respect to the direction of airflow in the duct. However, this method of sampling only collects samples at a single point in the duct. This was further improved by drilling a row of 2 mm diameter holes in the straight length of a 3/8" ID copper tube (see Figure 12). The sampling probes were inserted into the duct with the holes facing the direction of the airflow. This type of sampling probes ensured that the samples were collected over the whole cross-section of the duct and the mixing length was reduced greatly.

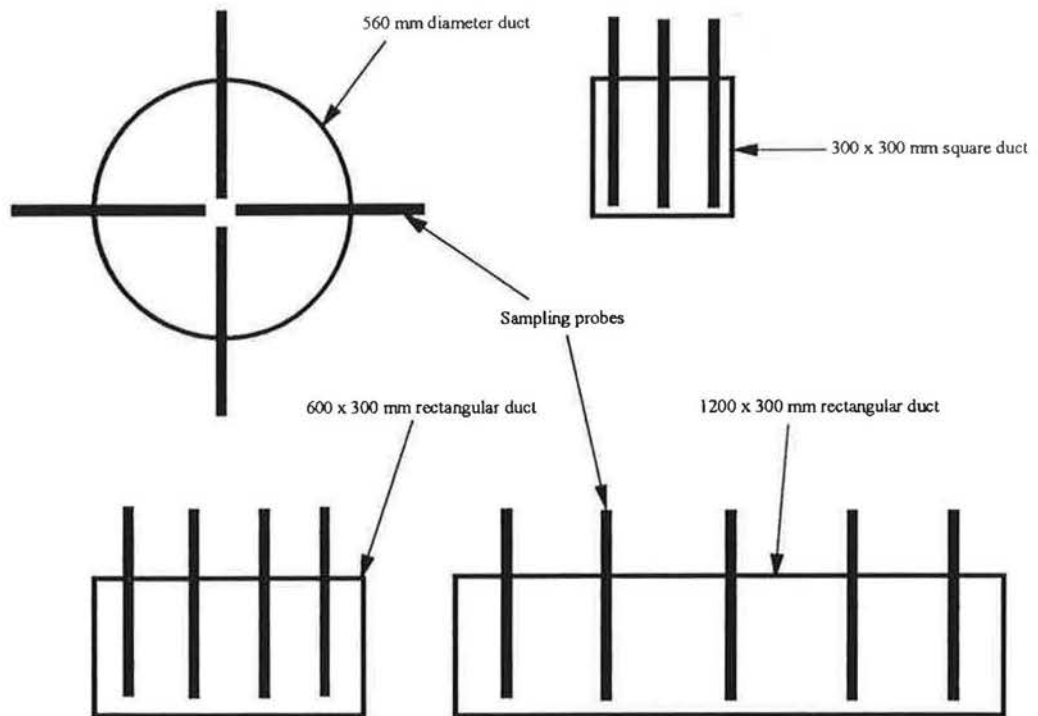


Figure 12 Position and number of sampling probes for different shapes and sizes of ducts

The number of sampling probes depends on the shape and size of the ducts. Figure 13 illustrates the number of sampling probes required for different shapes and sizes of ducts.

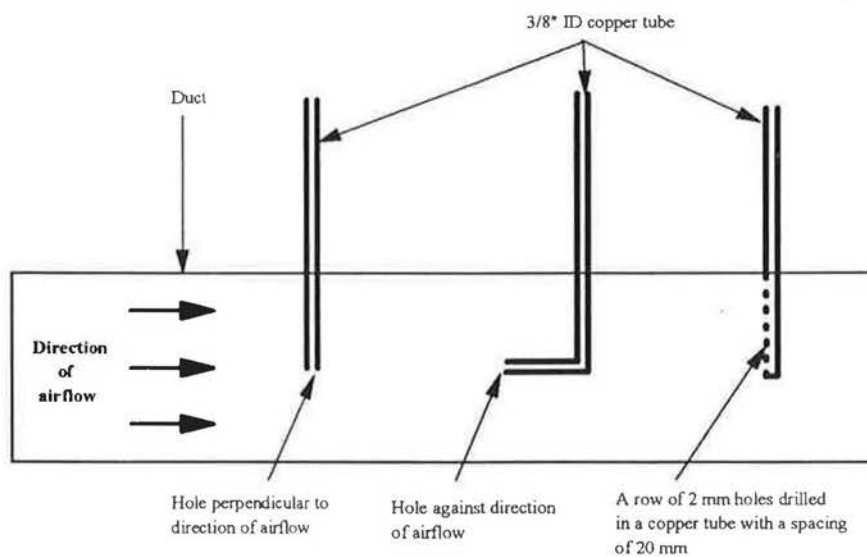


Figure 13 Different type of sampling probes

2.3 Measurement errors

2.3.1 Pitot-tube and hot-wire anemometer

Information on the measurement errors of airflow measurement techniques and instrumentation is vital. A brief description of the derivation of measurement errors for the pitot-tube and hot-wire anemometer is presented in this section.

The probable measurement error, $|m|$, shall be calculated in accordance with the following [20]:

$$|m| = \sqrt{m_1^2 + m_2^2 + m_3^2} \quad (11)$$

where,

- $m_1 =$ error of measuring instrument, %
- $m_2 =$ error of measuring method, %, (because of the nonagreement with the calibration values). Included in this type of error are also deviations from the calibration curve for mass-produced measuring devices, dampers or air terminal devices with built-in measurement outlets (i.e. pressure nozzles)
- $m_3 =$ reading error, %

2.3.2 Tracer-gas techniques

Measurement errors for the tracer-gas techniques were evaluated in a similar way to that used for the pitot-tube and hot-wire anemometer. Errors were applied to the determination of the flow rate or volume of tracer gas injected into the duct and in part to determination of its concentration. If the flow rate of the tracer gas was evaluated with the measurement errors, $|m_f|%$ and the concentration of this gas sample was determined with the measurement error, $|m_k|%$, the probable measurement error, $|m_q|$ becomes:

$$\dot{m}_G = \sqrt{(\dot{m}_F)^2 + (\dot{m}_K)^2} \quad (12)$$

If a homogenous mixture of the tracer gas is obtained, the method error is usually negligible and solely due to leakage from the duct between the tracer gas injection and the sampling cross-section.

2.4 Correction for tracer-gas injection rate

This correction factor applies to the constant-injection tracer-gas technique. The mass flow controller must be calibrated for the actual tracer gas. It is not possible to use a single factor for conversion of the mass flow controller's calibration curve from air to tracer gas.

The injection rate of the tracer gas, q , is converted to apply at the prevailing temperature in the ventilation duct. Therefore, the temperature of the tracer gas must be measured when passing through the mass flow controller. The corrected flow rate is obtained from :

$$Q_{corr} = Q_{tr} \frac{\rho_{tm}}{\rho_{td}} \quad (13)$$

where,

q_{tr} = tracer gas flow rate at tracer gas temperature at mass flow controller, m^3/min

ρ_{tm} = density of tracer gas at mass flow controller, kg/m^3

ρ_{td} = density of tracer gas at duct air temperature, kg/m^3

The airflow rate, F , in the duct is obtained as:

$$F = \frac{Q_{CORR}}{C} \quad (14)$$

where,

C = gas concentration at steady-state in the cross-section used for sampling, ppm

2.5 Correction for density of air in duct

Correction has to be made to obtain the actual airflow rate in the duct. The density of air is indirectly affected by the pressure and temperature. This is shown by the following expression:

$$\rho = 1.293 \times \frac{B}{1013} \times \frac{273}{273 + T_a} \quad (15)$$

where,

ρ = density of air, kg/m^3
 B = barometric pressure, mbar
 T_a = air temperature, $^{\circ}\text{C}$

3. MEASUREMENT OF AIR FLOW IN A DUCT USING TRACER-GAS TECHNIQUES

This chapter describes the application of constant-injection and pulse-injection tracer-gas techniques for measuring airflow in HVAC systems. Preliminary work on the use of tracer-gas techniques for measuring airflow in ducts has been carried out by Riffat and Lee [9], and Riffat [21]. Results indicated that tracer-gas techniques were in close agreement with the pitot-static traverse method. However, more rigorous tests are necessary to check the feasibility of these techniques on a wider scale. In this study, laboratory tests involving the use of these tracer-gas techniques to measure airflow rates in ducts of different configurations have been carried out. Results were compared with the measurements made using traditional instrumentation such as pitot-static tube and hot-wire anemometer.

The ducts used in the laboratory tests were cylindrical and rectangular with a range of lengths and aspect ratios. Four ducts with the following dimensions were used for the tests:

- a. 0.56 m diameter round duct.
- b. 0.3 m x 0.3 m square duct.
- c. 0.6 m x 0.3 m rectangular duct.
- d. 1.2 m x 0.3 m rectangular duct.

3.1 Experimental work

The airflow rates in cylindrical and rectangular ducts with different aspect ratios were measured using the constant-injection and pulse-injection tracer-gas techniques [22]. The pitot-static traverse technique and hot-wire anemometer were also used to measure airflow rates in these ducts. In addition, tracer-gas concentration and air velocity were measured at various distances from the duct wall and inlet.

The joints of these duct systems were carefully sealed to avoid the loss of tracer gas. The tightness of these duct systems were checked by sealing the both ends of the duct, injecting tracer gas and monitoring the concentration decay for several hours. The test showed that all the duct system were leaktight before airflow measurements were carried out.

3.1.1 Airflow rate measurements in ducts using constant-injection and pulse-injection technique

Figure 14 shows the instrumentation used for airflow measurement in a typical duct using the constant-injection technique. The downstream end of the duct was connected to an axial fan by means of a diffuser. The flow rate through the duct was varied using a speed controller made by ABB Stromberg Drives, Finland. The fan was driven by a 4 kW AC motor with a maximum speed of 2880 rpm. The fan was manufactured by Elta Fans Ltd., Surrey, UK. The fan exhausted air/tracer to the outside and no recirculation of tracer was permitted.

The constant-injection technique consists of injection of tracer gas and sampling and analysis of the gas sample in the duct downstream of the injection points. Injection consisted of supplying SF₆ into the duct inlet at a constant rate via a number of injection probes (see Figure 9). The position and number of injection probes varies with the shape and size of the duct. These injection probes were connected to the manifold using flexible tubing. Constant rate of SF₆ injection was achieved using a mass flow controller, type F-201-EA, made by Bronkhorst Hi-Tech B.V., Ruurlo, Holland. It had a maximum flow capability of 3.9 L/min and a measurement accuracy of ±1%. The flow rate was controlled using a variable power supply, and the tracer-gas injection was displayed on a digital unit, type E-5523-FA, made by Bronkhorst Hi-Tech B.V. The storage tank between the SF₆ gas cylinder and the mass flow controller was used to stabilise the flow of SF₆ into the mass flow controller.

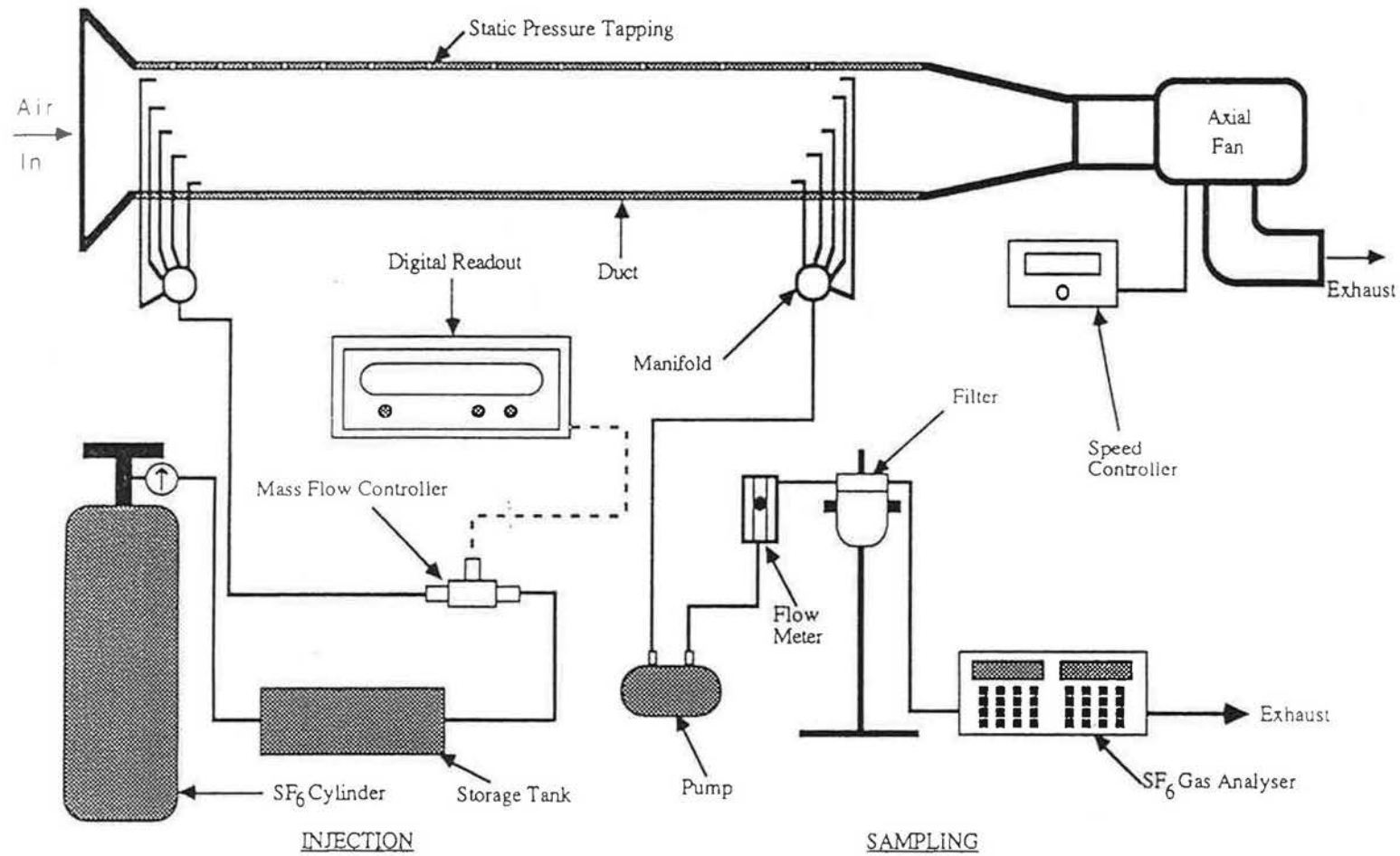


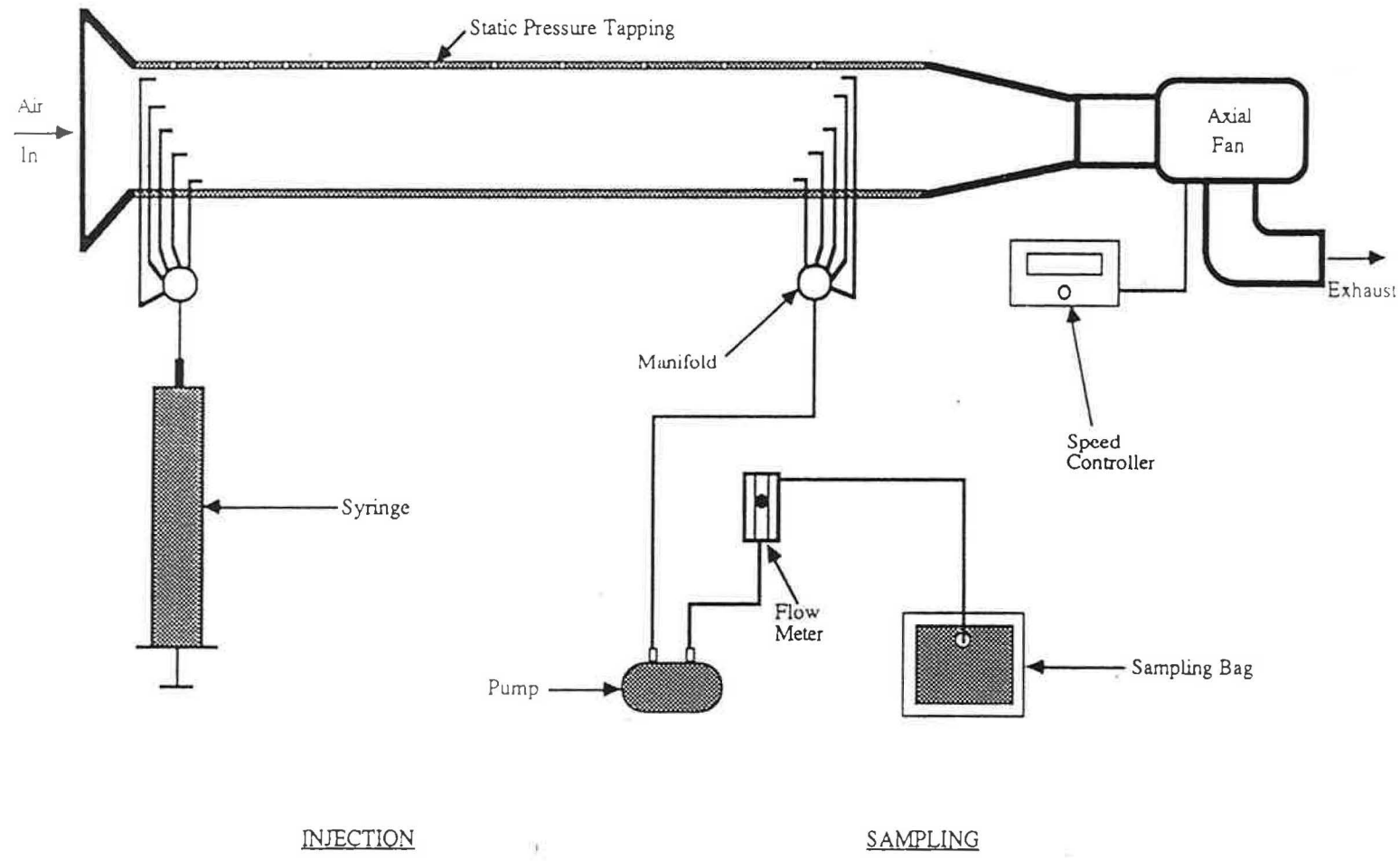
Figure 14 Instrumentation for the constant-injection technique

Sampling was achieved by insertion of sampling probes (see Figure 13) into the duct downstream of the injection points. These probes were connected to the manifold using flexible tubing and the concentration of tracer gas was measured using an infra-red gas analyser, type BINOS 1000, made by Rosemount GmbH & Co (RAE), Hanau, Germany. The accuracy of the analyser was estimated to be within $\pm 2\%$. The flowmeter limited flow rate into the analyser to a maximum of 2.5 L/min. The filter removed any particles present in the air sample taken from the duct via the sampling probes to protect the analyser from damage.

The pulse-injection technique also consists of two parts. SF_6 tracer gas was injected at the inlet of the duct using a 1.5 L capacity syringe (see Figure 15). Multi-point injection (see Figure 9) was necessary for the approximation of a uniform concentration across the cross-section of the duct at the measurement point. It was necessary to measure the concentration of tracer gas at the downstream point to determine the integral of the concentration. This was achieved by filling an air sample bag by means of a small pump via a flowmeter. Sampling was begun once the pulse was injected, and continued until the pulse was completely purged from the duct. Analysis of these samples were carried out using the BINOS 1000 infra-red gas analyser. The probable measurement error of the constant-injection and pulse-injection techniques was found to be $\pm 5.48\%$ and $\pm 6.17\%$, respectively.

3.1.2 Airflow rate measurements in ducts using pitot-tube and hot-wire anemometer

Figure 16 shows the insertion of a pitot-tube into the duct via a velocity tapping. The pitot-tube could be traversed across the cross-section of the duct to measure the velocity at various distances from the duct wall. The number of readings and position of each reading were governed by the shape and size of the duct. The velocity pressure from the pitot-tube was



INJECTION

SAMPLING

Figure 15 Instrumentation for the pulse-injection technique

measured using an EMD 2500 micromanometer, made by Airflow Development Limited, UK. The probable measurement error was found to be $\pm 7.35\%$.

The velocity in the duct was also measured by using a hot-wire anemometer, type TA2, made by Airflow Development Limited, UK. The number and positions of measurements was the same as for the pitot-static traverse technique. This technique had a probable measurement error of $\pm 5.39\%$.

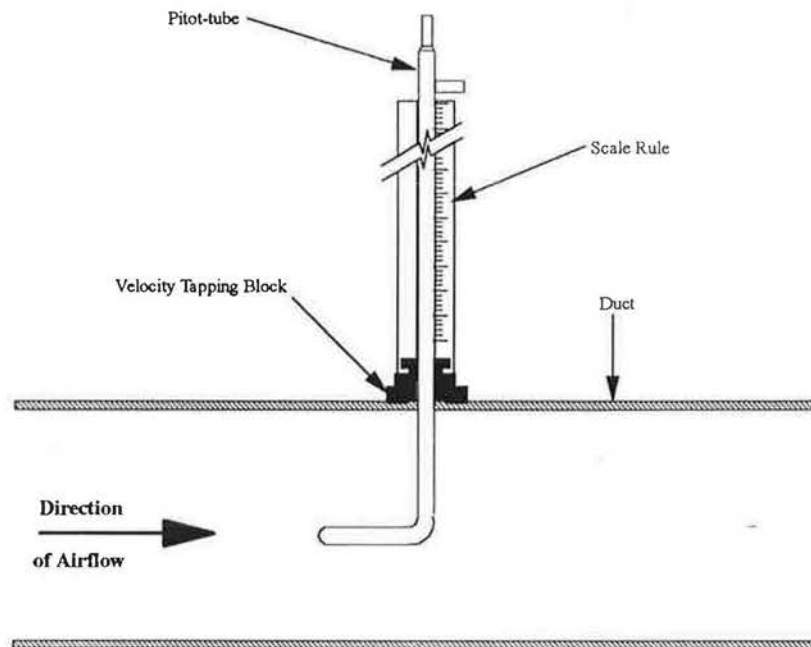


Figure 16 Insertion of a pitot-tube into a duct via the velocity tapping block

3.2 Results and Discussion

Measurement of airflow rate in these ducts was carried out by means of the constant-injection and pulse-injection techniques as well as using a pitot-tube and hot-wire anemometer. SF_6 was injected into ducts with dimensions of 560 mm, 300 mm x 300 mm, 600 mm x 300 mm and 1200 mm x 300

mm at $X/D_h = 0.357, 0.667, 0.5$ and 0.417 , respectively, and the concentration of tracer gas was monitored at various positions downstream.

Figures 17 and 18 show the variation of tracer-gas concentration with X/D_h in a 560 mm diameter duct for Reynolds numbers in the range 7.6×10^4 to 39.3×10^4 using constant and pulse-injection techniques, respectively. The concentration of tracer gas was found to be higher closed to the injection points, and decreased as X/D_h increased. The tracer-gas concentration remained constant when X/D_h was greater than 15 (for constant-injection) and 8 (for pulse injection technique). Table 2 shows the variation of airflow rate along the 560 mm diameter duct due to the fluctuation of concentration measured using the constant-injection tracer-gas technique.

| Airflow Rate by Pitot-tube, (m ³ /s) | Airflow Rate by Constant- Injection Technique, (m ³ /s) | | | Percentage Difference (F _{ci} - F _p)/F _p , (%) | | |
|---|---|--------------------------|---------------------------|---|--------------------------|---------------------------|
| | X/D _h 2.99 | X/D _h 7.55 | X/D _h 13.53 | X/D _h 2.99 | X/D _h 7.55 | X/D _h 13.53 |
| 0.509 | 0.586 | 0.449 | 0.510 | 15.25 | -11.79 | 0.29 |
| 0.760 | 0.929 | 0.929 | 0.868 | 22.27 | 22.27 | 14.33 |
| 1.034 | 1.754 | 1.212 | 1.149 | 69.63 | 17.21 | 11.12 |
| 1.163 | 1.754 | 1.667 | 1.626 | 50.82 | 43.34 | 21.93 |
| 1.395 | 1.631 | 1.714 | 1.262 | 16.92 | 22.91 | 9.56 |
| 1.656 | 1.910 | 2.089 | 1.714 | 15.35 | 26.17 | 3.52 |

Table 2 Variation of airflow rate with respect to the injection points of tracer gas in a 560 mm diameter duct

For airflow rates in the 560 mm diameter duct ranging from 0.51 to 1.66 m³/s, the percentage difference between the pitot-tube airflow measurements

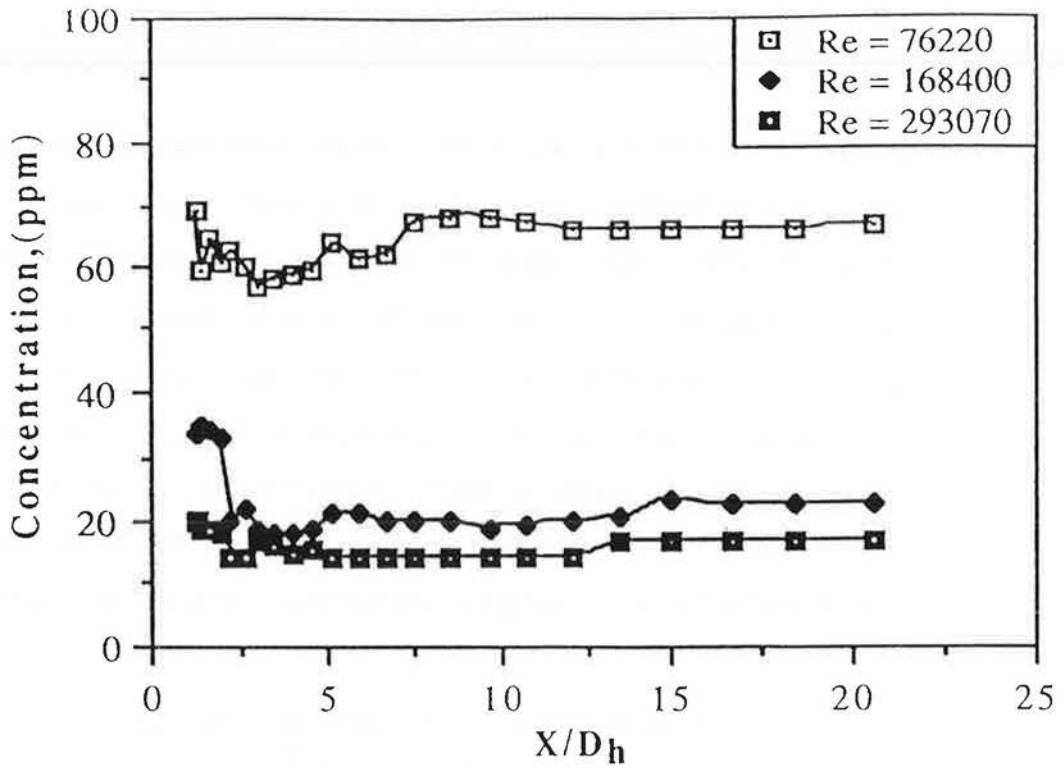


Figure 17 Variation of tracer-gas measurement with X/D_h in a 560 mm round duct, constant-injection technique

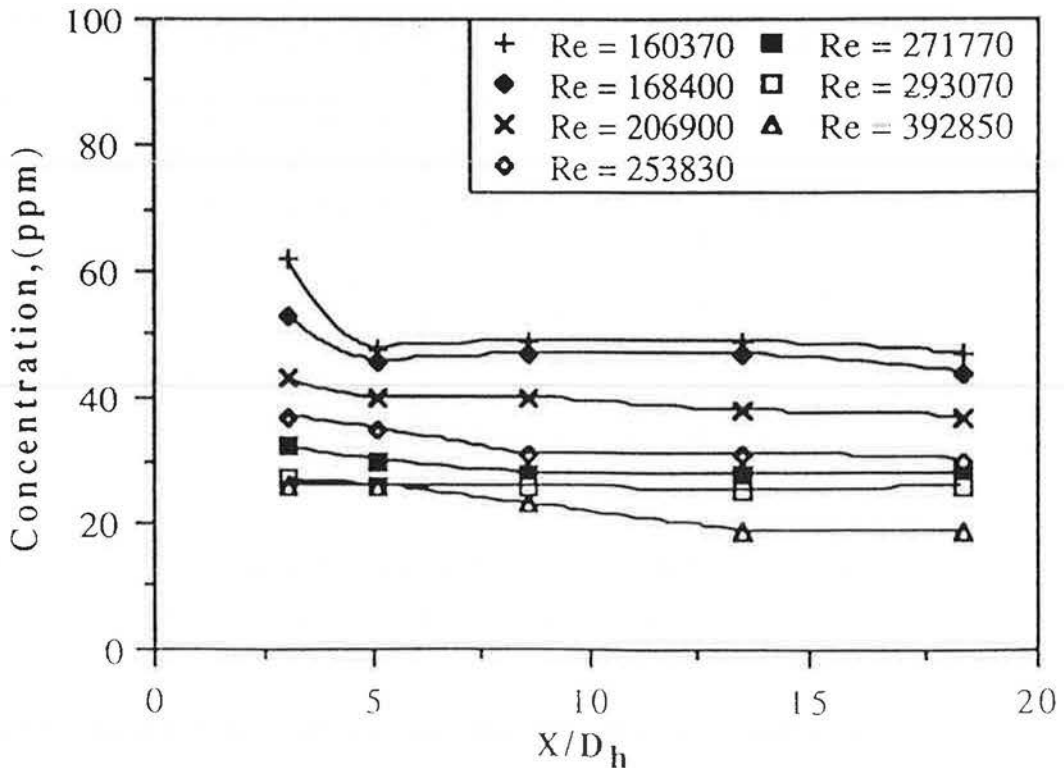


Figure 18 Variation of tracer-gas measurement with X/D_h in a 560 mm round duct, pulse-injection technique

and measurements made using the constant-injection technique for $X/D_h = 2.99, 7.55$ and 13.53 were found to be 15.25% to 69.63%, -11.79% to 43.34% and 0.29% to 21.93%, respectively. These results indicated that the airflow rates estimated using constant-injection technique were in closer agreement with the airflow rates measured using pitot-tube as the sampling points were further away from the tracer-gas injection points. Uniform tracer-air mixing at the lower section of the duct was responsible for this.

Figures 19 and 20 show variation of tracer-gas concentration with X/D_h in a 300 mm x 300 mm square duct for Reynolds numbers in the range 7.7×10^4 to 39.5×10^4 using constant and pulse-injection techniques, respectively. The concentration of tracer gas was found to be higher close to the injection points, and decreased as X/D_h increased. The tracer-gas concentration remained constant when X/D_h was greater than 10 (for constant-injection) and 23 (for pulse injection technique). Table 3 shows the variation of airflow rate along the 300 mm x 300 mm duct due to the fluctuation of concentration measured using the constant-injection tracer-gas technique.

| Airflow Rate by Pitot-tube, (m ³ /s) | Airflow Rate by Constant-Injection Technique, (m ³ /s) | | | Percentage Difference (F _{ci} - F _p)/F _p , (%) | | |
|---|---|---------------------------|---------------------------|--|---------------------------|---------------------------|
| | X/D _h 5.58 | X/D _h 14.47 | X/D _h 25.63 | X/D _h 5.58 | X/D _h 14.47 | X/D _h 25.63 |
| 0.348 | 0.303 | 0.333 | 0.333 | -12.90 | -4.21 | -4.21 |
| 0.525 | 0.470 | 0.486 | 0.486 | -10.40 | -7.41 | -7.41 |
| 0.735 | 0.641 | 0.709 | 0.709 | -12.80 | -3.51 | -3.51 |
| 0.761 | 0.572 | 0.711 | 0.711 | -28.70 | -10.40 | -10.40 |
| 0.912 | 0.758 | 0.813 | 0.813 | -16.90 | -10.90 | -10.90 |
| 1.149 | 0.868 | 1.157 | 1.157 | -24.50 | 0.73 | 0.73 |

Table 3 Variation of airflow rate with respect to the injection points of tracer gas in a 300 mm x 300 mm duct

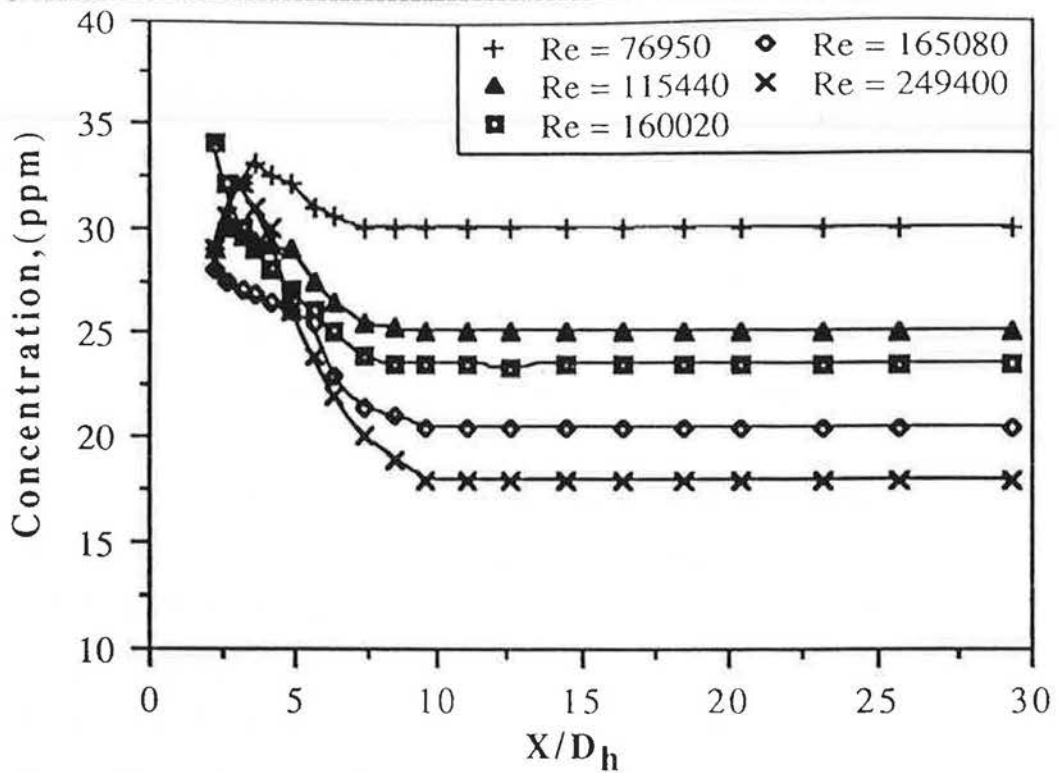


Figure 19 Variation of tracer-gas measurement with X/D_h in a 300 mm x 300 mm duct, constant-injection technique

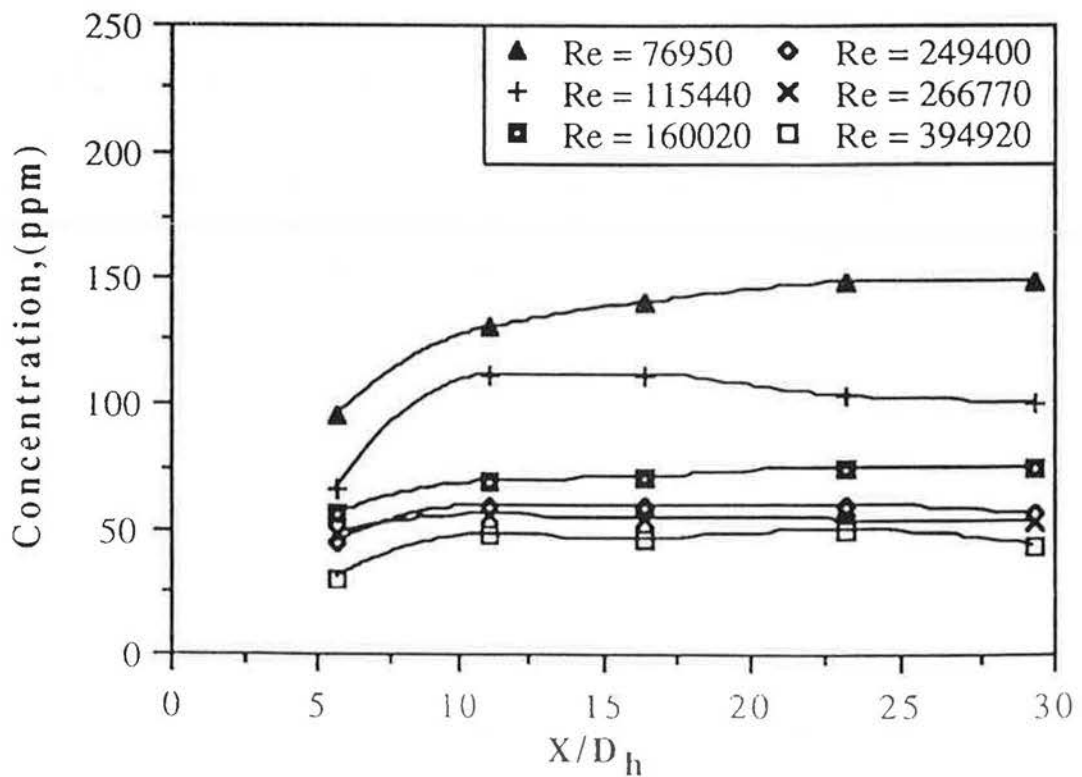


Figure 20 Variation of tracer-gas measurement with X/D_h in a 300 mm x 300 mm duct, pulse-injection technique

For airflow rates in the 300 mm x 300 mm diameter duct ranging from 0.35 to 1.15 m³/s, the percentage difference between the pitot-tube airflow measurements and measurements made using the constant-injection technique for $X/D_h = 5.58, 14.47$ and 25.63 were found to be -28.7% to -10.4%, -10.9% to 0.73% and -10.9% to 0.73%, respectively. Similar to those results obtained in the 560 mm diameter duct, the airflow rates in the 300 mm x 300 mm duct estimated using constant-injection technique were in closer agreement with those measurements obtained using the pitot-static traverse method as the sampling points of the tracer-gas techniques were further away from the tracer-gas injection points. In addition, the percentage difference in airflow rates measured between these techniques were smaller as compared to those results in the 560 mm diameter duct. This was because of a smaller cross-sectional area and shape of the duct.

Figures 21 and 22 show variation of tracer-gas concentration in 600 mm x 300 mm square duct with X/D_h for Reynolds numbers in the range 7.6×10^4 to 39.3×10^4 using constant and pulse-injection techniques, respectively. The concentration of tracer gas was found to be higher closed to the injection points, and decreased as X/D_h increased. The tracer-gas concentration remained constant when X/D_h was greater than 12 (for constant-injection) and 17 (for pulse injection technique). Table 4 shows the variation of airflow rate along the 600 mm x 300 mm duct due to the fluctuation of concentration measured using the constant-injection tracer-gas technique.

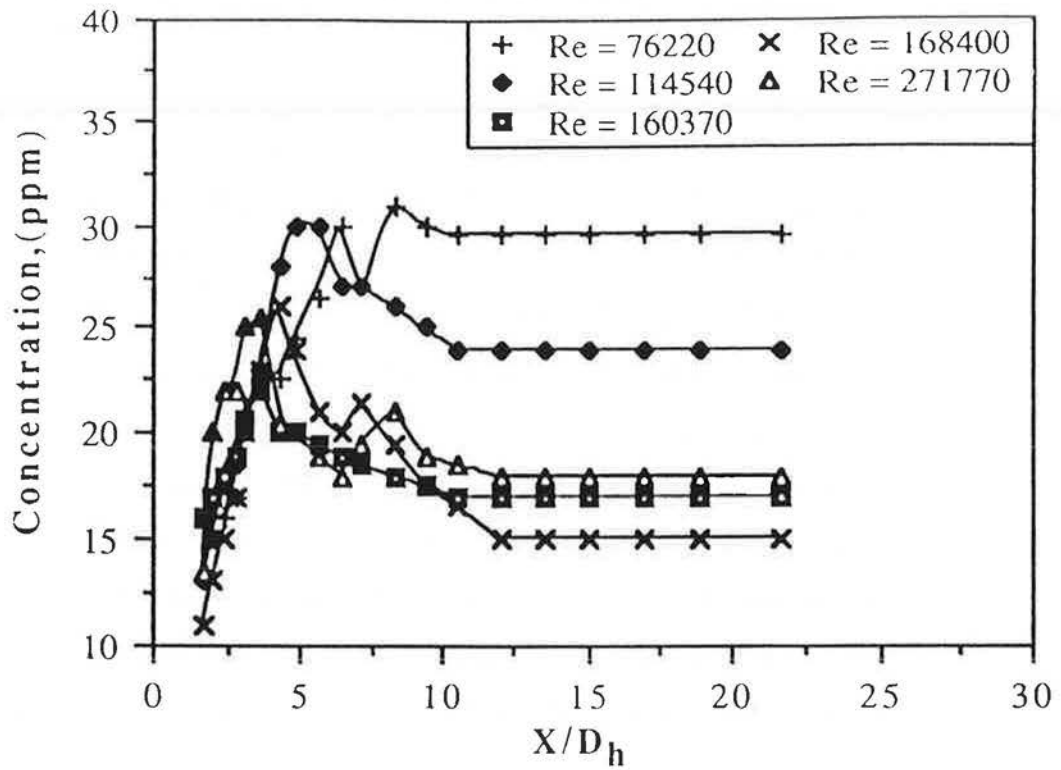


Figure 21 Variation of tracer-gas measurement with X/D_h in a 600 mm x 300 mm duct, constant-injection technique

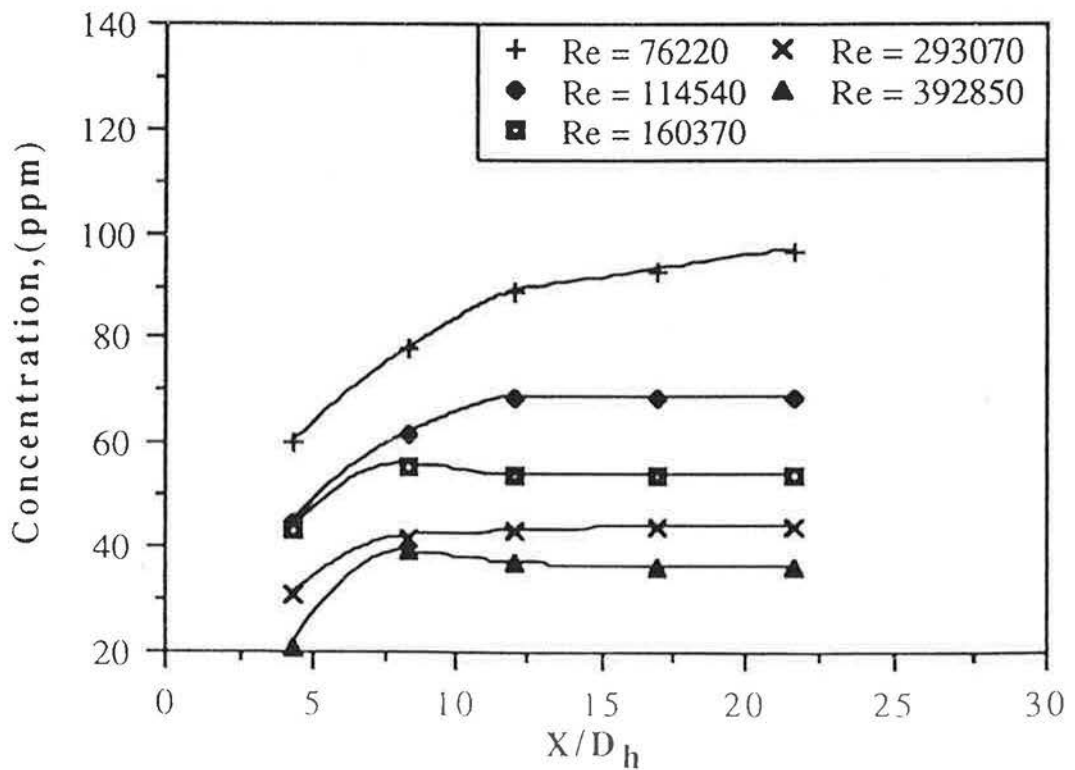


Figure 22 Variation of tracer-gas measurement with X/D_h in a 600 mm x 300 mm duct, pulse-injection technique

| Airflow Rate by Pitot-tube, (m ³ /s) | Airflow Rate by Constant- Injection Technique, (m ³ /s) | | | Percentage Difference (F _{ci} - F _p)/F _p , (%) | | |
|---|---|---------------------------|---------------------------|---|---------------------------|---------------------------|
| | X/D _h 4.19 | X/D _h 10.56 | X/D _h 18.94 | X/D _h 4.19 | X/D _h 10.56 | X/D _h 18.94 |
| 0.598 | 0.741 | 0.565 | 0.565 | 23.87 | -5.52 | -5.52 |
| 0.789 | 0.595 | 0.694 | 0.694 | -24.60 | -12.0 | -12.0 |
| 1.025 | 0.833 | 0.980 | 0.980 | -18.70 | -4.35 | -4.35 |
| 1.184 | 0.641 | 1.010 | 1.111 | -45.90 | -14.70 | -6.16 |
| 1.455 | 0.781 | 1.351 | 1.389 | -46.30 | -7.12 | -4.54 |
| 1.722 | 1.215 | 1.577 | 1.620 | -29.40 | -8.45 | -5.90 |

Table 4 Variation of airflow rate with respect to the injection points of tracer gas in a 600 mm x 300 mm duct

For airflow rates in the 600 mm x 300 mm diameter duct ranging from 0.60 to 1.72 m³/s, the percentage difference between the pitot-tube airflow measurements and measurements made using the constant-injection technique for X/D_h = 4.19, 10.56 and 18.94 were found to be -46.3% to 23.87%, -14.7% to -4.35% and -12.0% to -4.35%, respectively. Similar to those results obtained in the 560 mm diameter duct and 300 mm x 300 mm duct, the airflow rates in this duct estimated using constant-injection technique were in closer agreement with those measurements obtained using the pitot-static traverse method as the sampling points of the tracer-gas techniques were further away from the tracer-gas injection points. Table 4 shows that the percentage difference in airflow rates measured between these techniques were larger than those results obtained from the 300 mm x 300 mm duct. However, these results were still better than those from the 560 mm diameter duct. Non-uniform tracer-air mixing was experienced in a duct with larger cross-sectional area and aspect ratio.

Figures 23 and 24 show variation of tracer-gas concentration in 1200 mm x 300 mm square duct with X/D_h for Reynolds numbers in the range 7.3×10^4 to 25×10^4 using constant and pulse-injection techniques, respectively. The concentration of tracer gas was found to be higher closed to the injection points, and decreased as X/D_h increased. The tracer-gas concentration remained constant when X/D_h was greater than 14 (for constant-injection) and 14 (for pulse injection technique). Table 5 shows the variation of airflow rate along the 1200 mm x 300 mm duct due to the fluctuation of concentration measured using the constant-injection tracer-gas technique.

| Airflow Rate by Pitot-tube, (m ³ /s) | Airflow Rate by Constant- Injection Technique, (m ³ /s) | | | Percentage Difference ($F_{ci} - F_p$)/ F_p , (%) | | |
|---|---|-----------------|------------------|--|-----------------|------------------|
| | X/D_h 3.49 | X/D_h 8.83 | X/D_h 15.81 | X/D_h 3.49 | X/D_h 8.83 | X/D_h 15.81 |
| 0.828 | 0.962 | 0.714 | 0.735 | 14.47 | -15.00 | -12.50 |
| 1.251 | 0.926 | 1.042 | 1.096 | -26.00 | -16.70 | -12.40 |
| 1.773 | 1.620 | 1.667 | 1.716 | -8.61 | -6.00 | -3.23 |
| 1.956 | 2.000 | 1.667 | 1.724 | 2.25 | -14.8 | -11.90 |
| 2.361 | 1.944 | 2.160 | 2.244 | -17.60 | -8.49 | -4.97 |
| 2.841 | 2.381 | 2.564 | 2.564 | -16.20 | -9.75 | -9.75 |

Table 5 Variation of airflow rate with respect to the injection points of tracer gas in a 1200 mm x 300 mm duct

For airflow rates in the 1200 mm x 300 mm diameter duct ranging from 0.83 to 2.84 m³/s, the percentage difference between the pitot-tube airflow measurements and measurements made using the constant-injection technique for $X/D_h = 3.49, 8.83$ and 15.81 were found to be -26.0% to 14.47%, -16.7% to -6.0% and -12.5% to -3.23%, respectively. Similar to

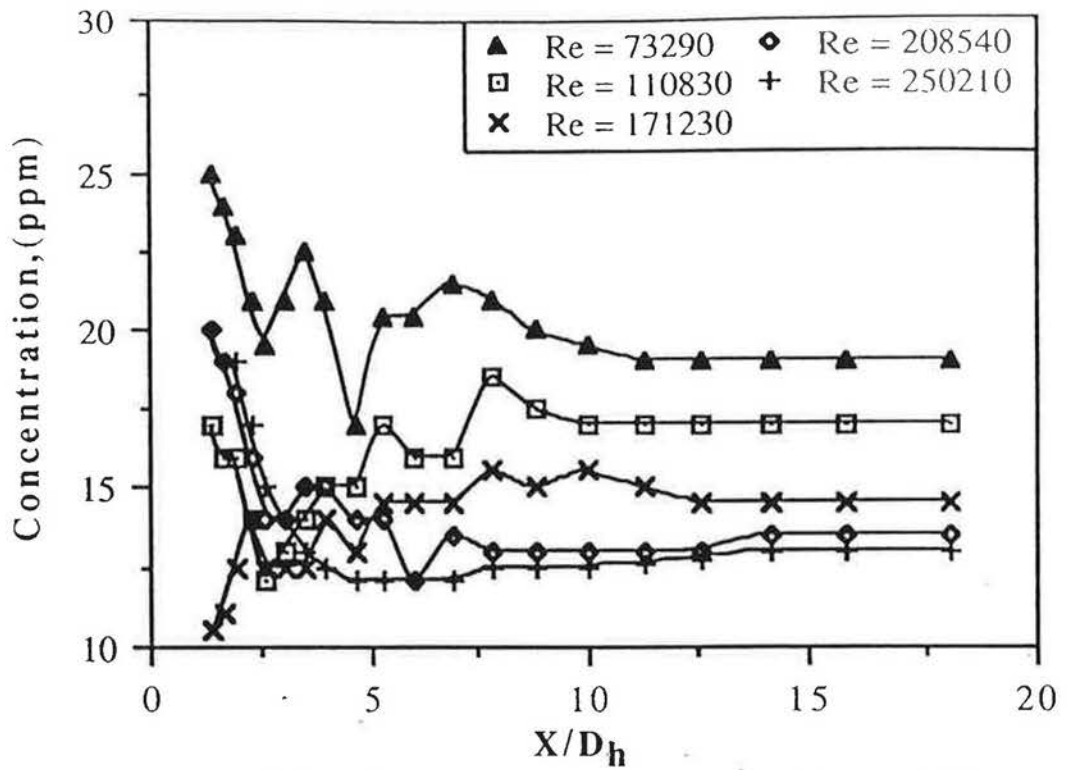


Figure 23 Variation of tracer-gas measurement with X/D_h in a 1200 mm x 300 mm duct, constant-injection technique

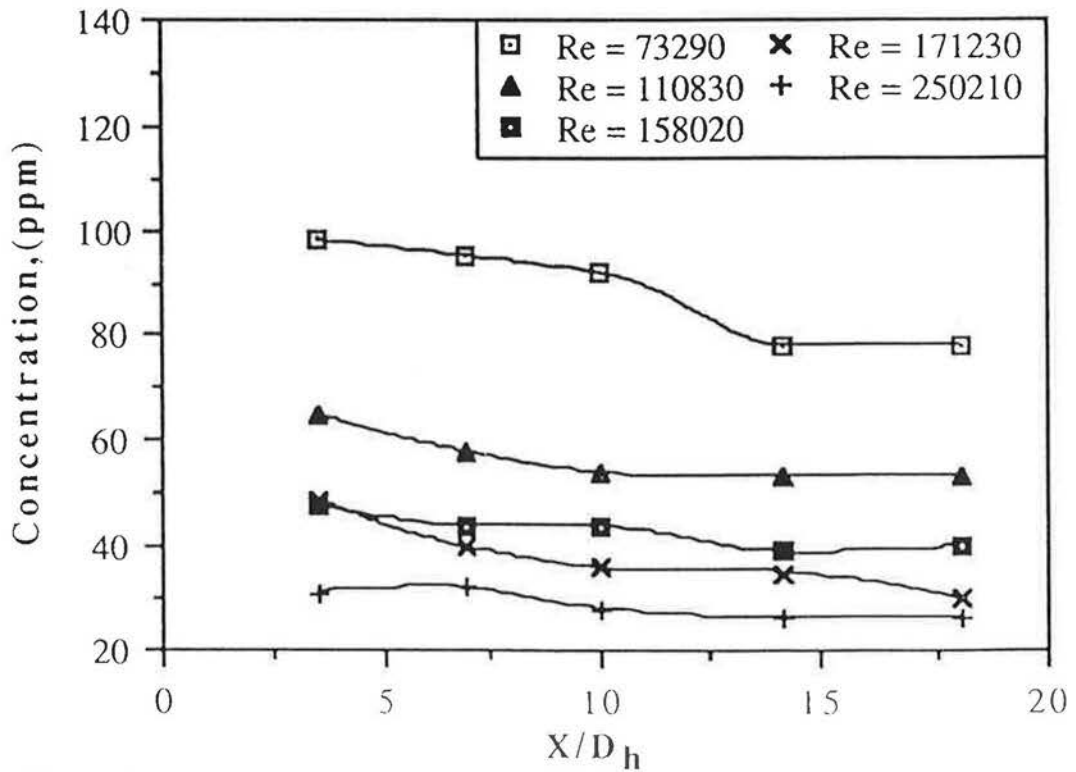


Figure 24 Variation of tracer-gas measurement with X/D_h in a 1200 mm x 300 mm duct, pulse-injection technique

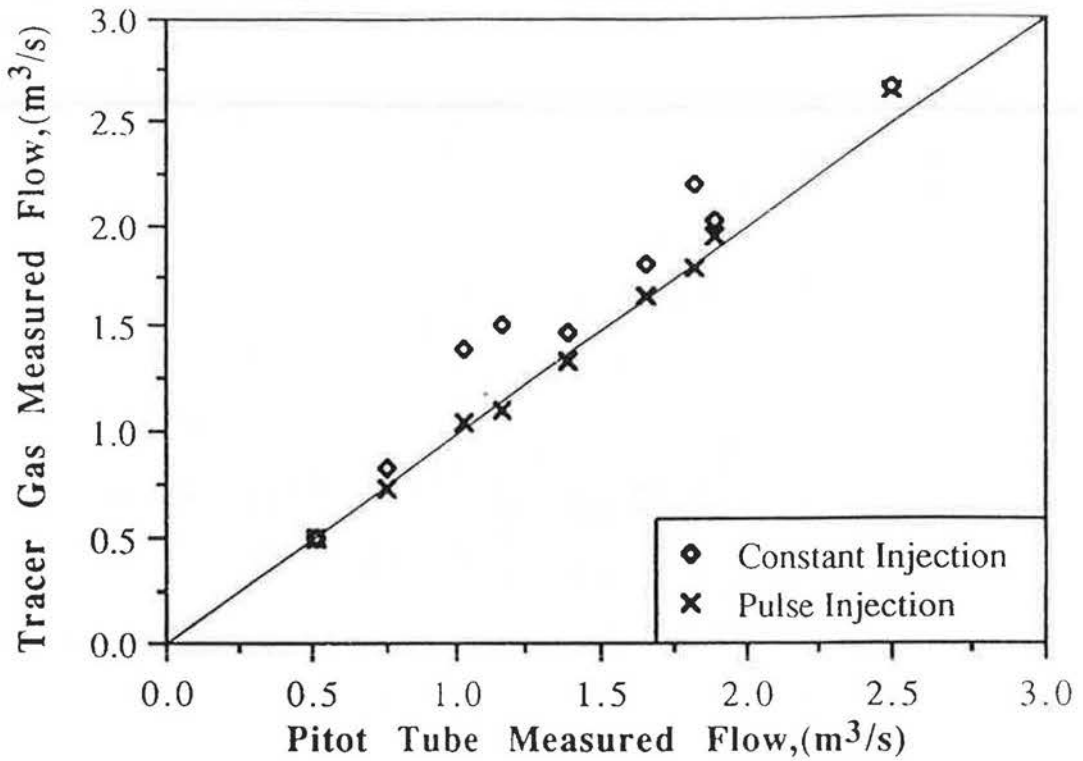


Figure 25 Comparison of tracer-gas airflow measurements with measurements made using a pitot tube, 560 mm round duct

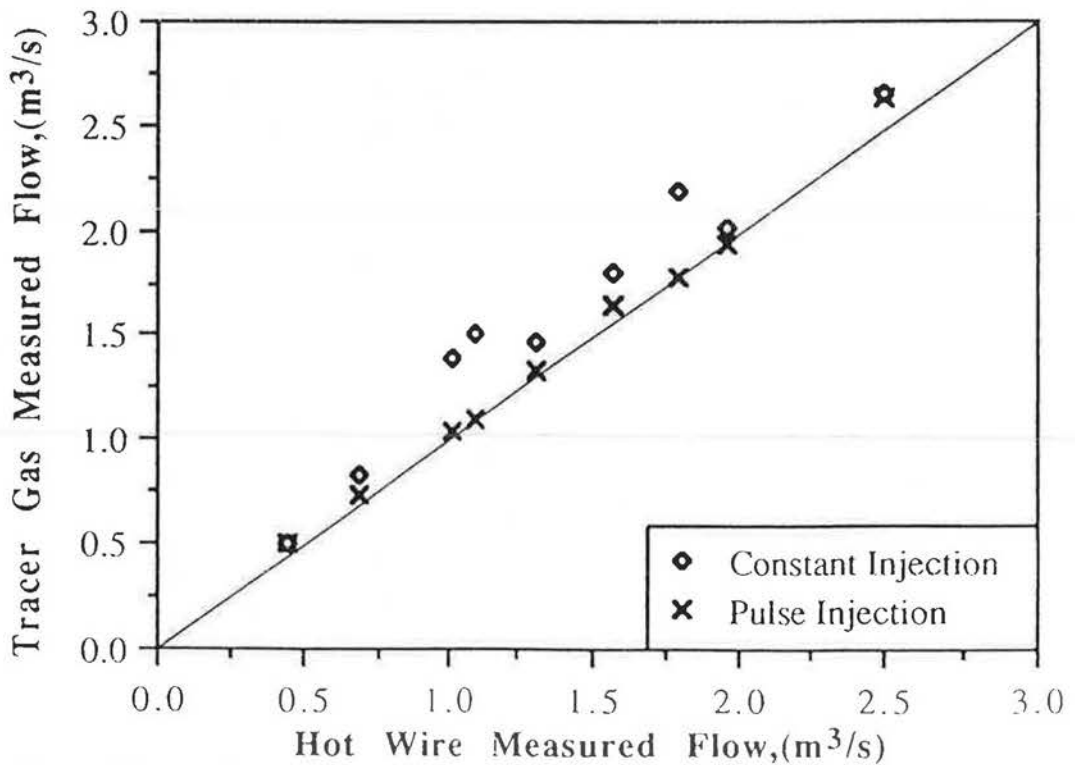


Figure 26 Comparison of tracer-gas airflow measurements with measurements made using a hot-wire anemometer, 560 mm round duct

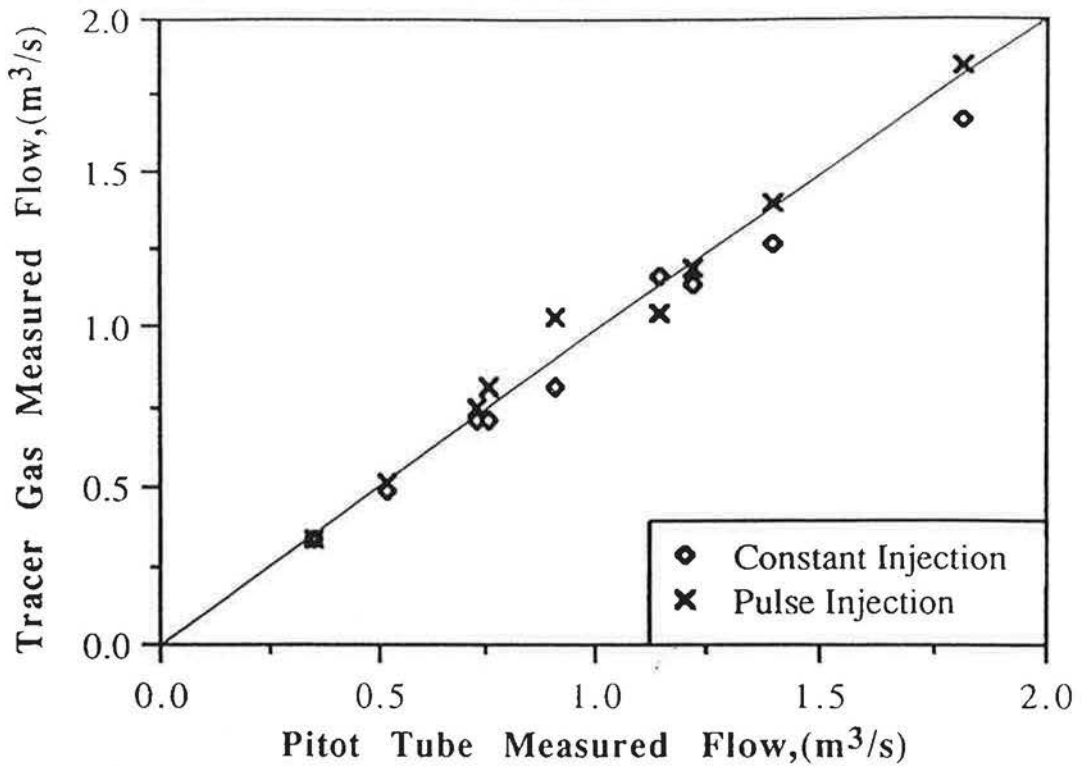


Figure 27 Comparison of tracer-gas airflow measurements with measurements made using a pitot tube, 300 mm x 300 mm duct

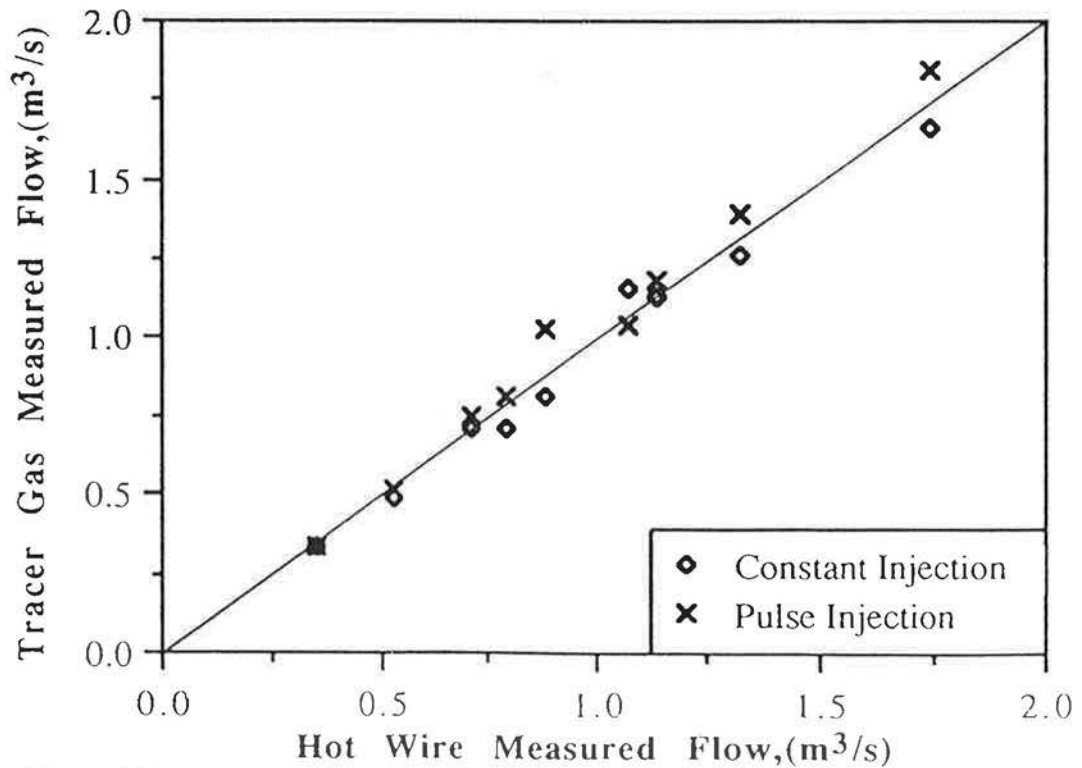


Figure 28 Comparison of tracer-gas airflow measurements with measurements made using a hot-wire anemometer, 300 mm x 300 mm duct

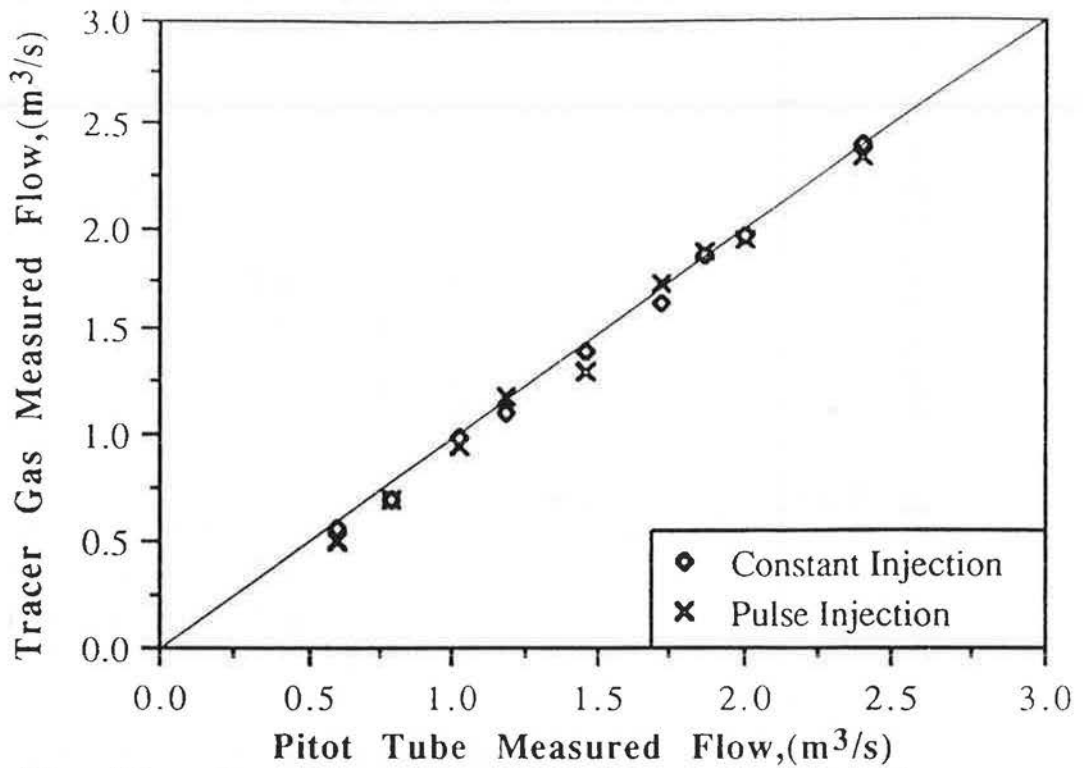


Figure 29 Comparison of tracer-gas airflow measurements with measurements made using a pitot tube, 600 mm x 300 mm duct

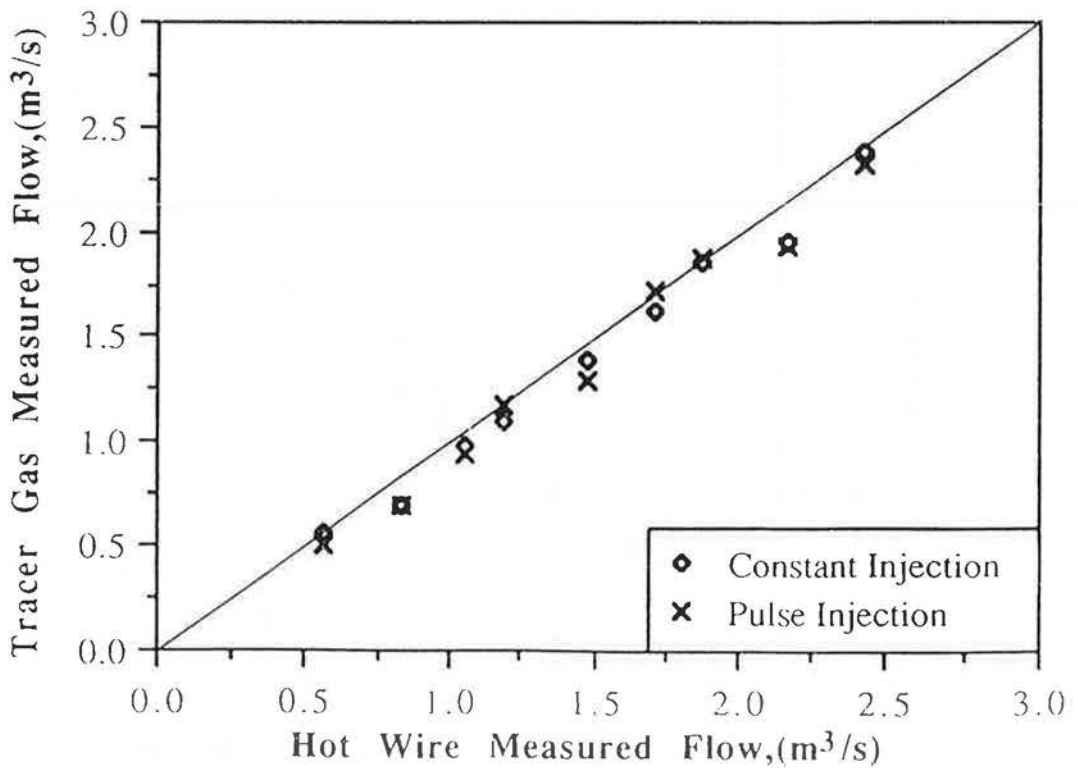


Figure 30 Comparison of tracer-gas airflow measurements with measurements made using a hot-wire anemometer, 600 mm x 300 mm duct

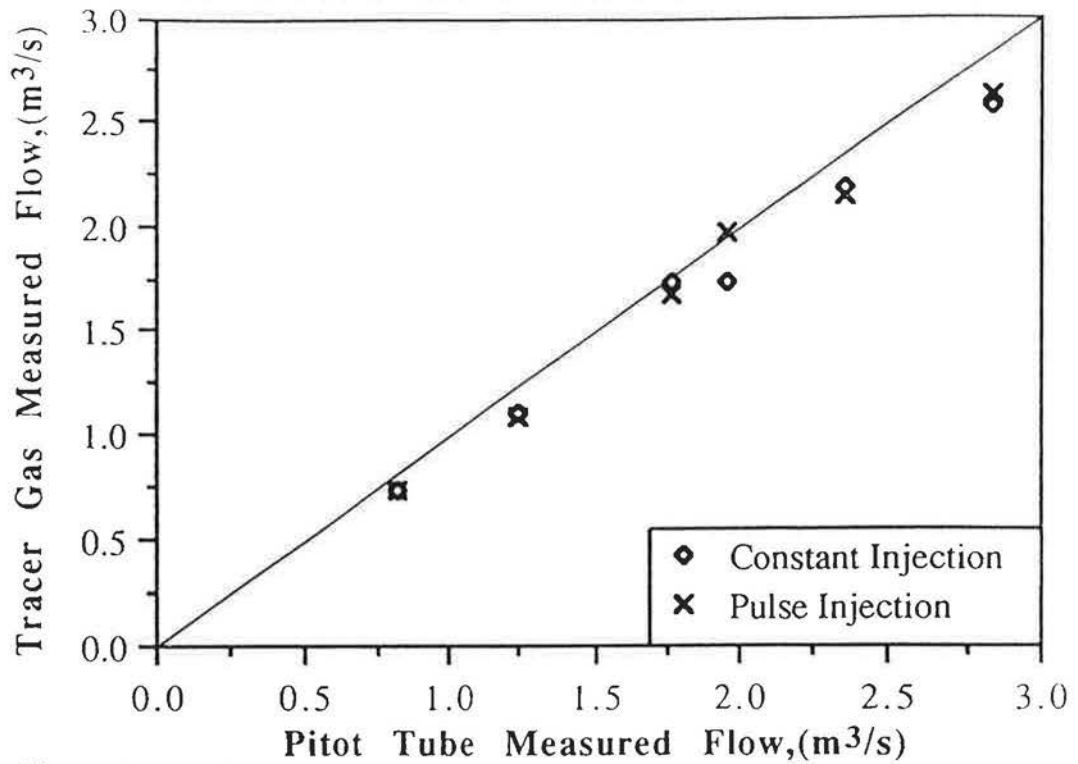


Figure 31 Comparison of tracer-gas airflow measurements with measurements made using a pitot tube, 1200 mm x 300 mm duct

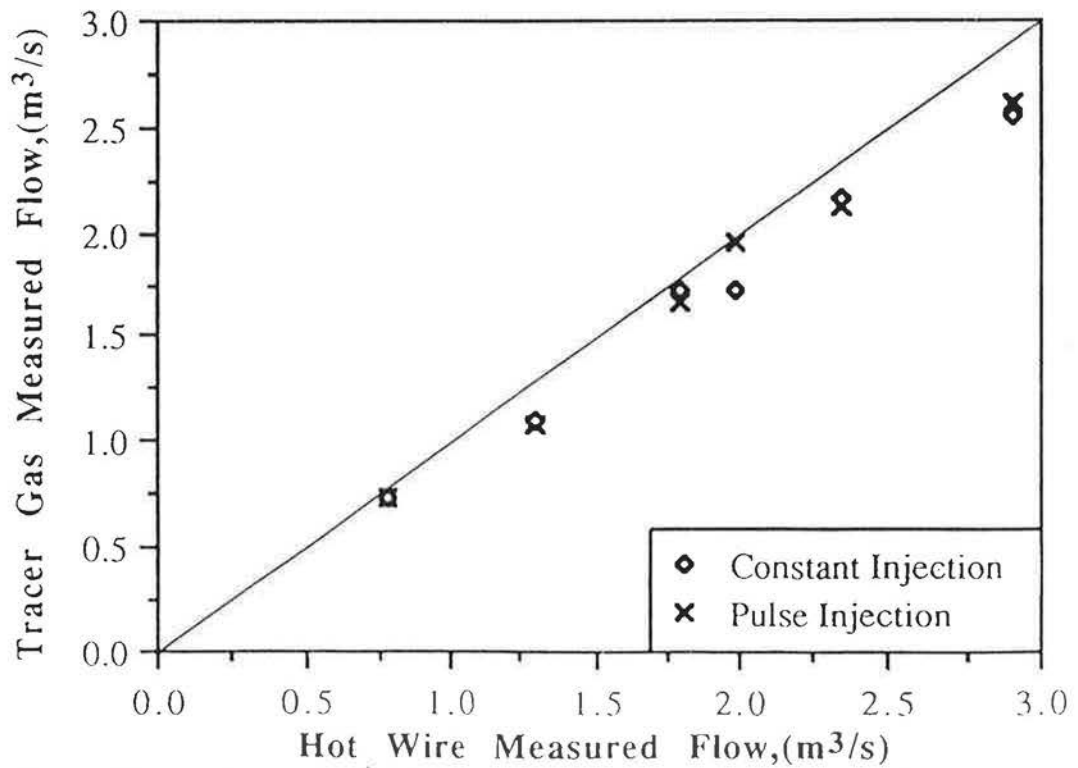


Figure 32 Comparison of tracer-gas airflow measurements with measurements made using a hot-wire anemometer, 1200 mm x 300 mm duct

the results in other ducts, the airflow rates in this duct estimated using constant-injection technique were in closer agreement with those measurements obtained using the pitot-static traverse method as the sampling points of the tracer-gas techniques were further away from the tracer-gas injection points. Table 5 shows that the percentage difference in airflow rates measured between these two techniques were larger than those results obtained from the 300 mm x 300 mm diameter duct. However, these results were still better than the 560 mm diameter duct. Poor tracer-air mixing was experienced in duct with larger cross-sectional area and aspect ratio.

Figures 25 and 26, 27 and 28, 29 and 30, and 31 and 32 compare measurements of duct airflow rate made with the tracer-gas techniques and a pitot tube and a thermal anemometer for ducts with sizes 560 mm diameter, 300 mm x 300 mm, 600 mm x 300 mm and 1200 mm x 300 mm, respectively. These graphs indicated that the flow rate obtained using the constant and pulse-injection techniques were in closed agreement with values obtained using the pitot-tube and hot-wire anemometer at various airflow rates.

3.3 Measurement of airflow through a porous medium

Tracer-gas techniques can be used in a wide range in airflow measurement's applications. One of these applications is the measurement of airflow in a duct filled with a porous medium [23].

Porous media are widely used in engineering applications such as thermal-storage devices, transportation-cooling systems and muffling devices. They are also used in mining, petroleum processes and chemical and aerospace applications. Mass and energy transplants in porous media must be well understood if these materials are to be used effectively and several studies have been carried out with this aim [24-29].

Fluids normally experience a high pressure drop as they pass through a porous medium and the resulting flow velocity is often too small to be measured accurately using traditional instrumentation such as orifice meters, pitot-tubes and hot-wire anemometers. In some cases, limited access to the flow passage or the short duct length involved prevent easy deployment of traditional instrumentation. The complex geometries of porous media and the irregular flow patterns associated with them give rise to additional difficulties.

Tracer-gas techniques such as constant injection, offer an alternative approach for the measurement of fluid (e.g. air) flow through porous media. They can be used to measure flow rates over a wide range of values (i.e. for laminar and turbulent flows) and are not limited by the complexity of the porous media or passage configuration. Moreover, tracer-gas techniques can be used to measure flow rates through porous media directly and do not require the determination of the cross-sectional area of the flow passage or the granular size of the porous medium.

This investigation examines the application of the constant-injection technique for measurement of airflow in a two-dimensional duct filled with a porous medium.

3.3.1 Materials and methods

The apparatus used for this investigation is shown in Figure 33. The rectangular duct was constructed from plywood 12 mm thick. The entrance to the duct consisted of a bell-mouth, and the duct itself was 3 m long with an internal cross-section of 250 mm x 40 mm. The downstream end was connected to the suction side of a centrifugal fan (Fischbach Ltd, Germany) by means of a diffuser, and the flow rate through the duct was varied by means of a variable speed controller. A length of 1600 mm, commencing 400 mm from the duct inlet was packed with gravel of granular size

between 5 and 10 mm.

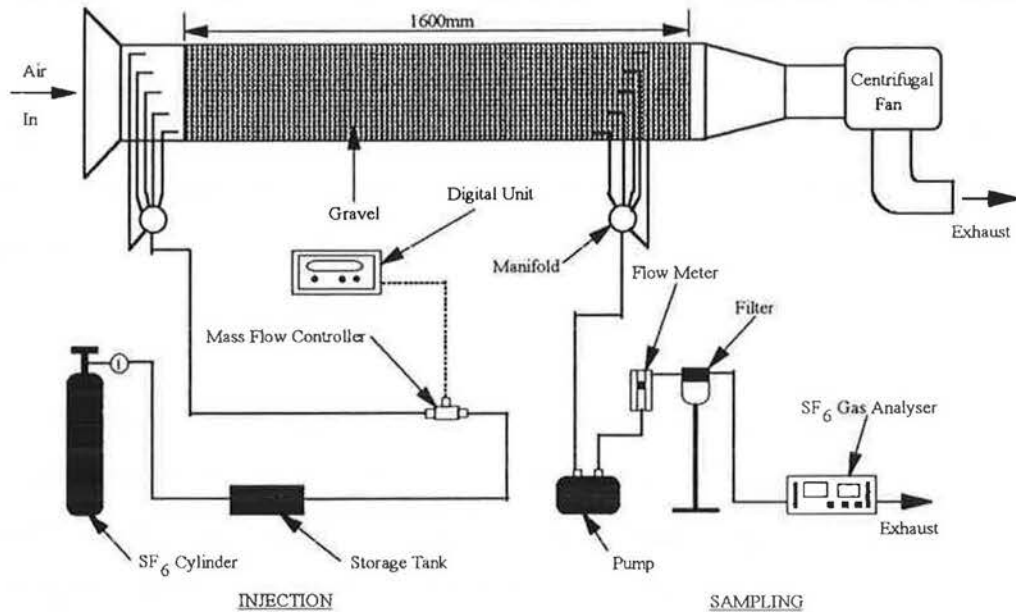


Figure 33 Schematic diagram of the duct system and instrumentation

Static pressure tapings were distributed along the duct. A single-tube inclined manometer, made by Airflow Developments Ltd, High Wycombe, UK, was used to measure the static pressure head.

The constant-injection technique was used to determine the airflow rate in the duct and SF_6 tracer gas was used as the tracer gas. The latter was injected into the duct inlet at a constant rate via several small injection tapings distributed around the perimeter of the duct. These tapings were connected to the manifold using flexible tubing. The SF_6 gas was supplied from a cylinder via a type F-100/200 mass-flow controller (Bronkhorst High-Tech BV, Ruurlo, Holland) which had a maximum capability of 3.9 L/min. The accuracy of the mass-flow controller was $\pm 1\%$. The flow rate was controlled using a variable-power supply and the rate of tracer gas introduced was displayed on a digital unit.

Tracer-gas/air samples were taken at various points along the duct as shown in Figure 33. A BINOS 1000 infra-red gas analyser manufactured by Leybold-Heraeus GmbH, Hanau, Germany was used.

3.3.2 Results and discussion

Airflow rates in the duct were measured using the constant-injection tracer-gas technique. Measurements of tracer-gas concentration and static pressure along the duct were carried out for Reynolds numbers between 1140 and 1790. SF₆ was injected at a rate of 0.25 L/min into the duct at X_s/D_h = 21.9 and the concentration of tracer gas was found to be unsteady close to the injection point but remained constant when X_s/D_h was greater than 74.5 (i.e. 0.9 m from the injection point [see Figure 34]). The flow rates were found to vary between 35 and 55 m³/h (i.e. velocities between 0.9 and 1.5 m/s). These velocities are too small to be measured accurately using traditional instrumentation. The porous medium was found to produce good mixing of the tracer gas in the duct.

Figure 35 shows the variation of the pressure difference, P_{atm} - P_s, along the duct for various Reynolds numbers. The pressure difference was found to vary nonlinearly through the porous material particularly at high Reynolds numbers. A least-squares technique was used to fit a straight line through the measurements (see Figure 36) and the flow rate was found to change in accordance with:

$$F = 4.41 (\Delta P_s)^{0.47} \quad (18)$$

Equation (18) is similar to that describing air leakage through cracks in building materials [30]. The results indicate that the flow rate is approximately proportional to the square root of the pressure drop across the porous medium.

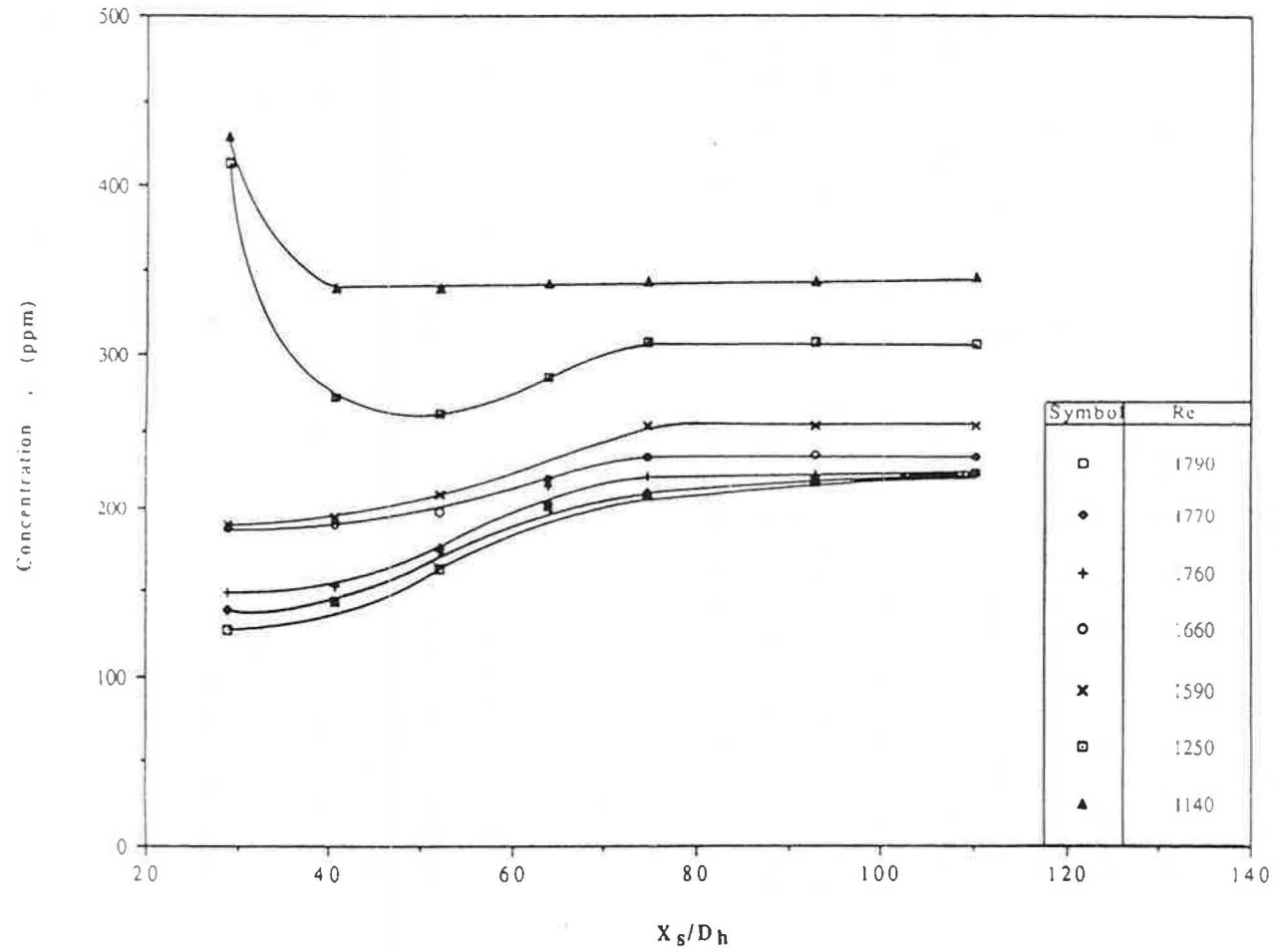


Figure 34 Variation of tracer-gas concentration with X_s/D_h

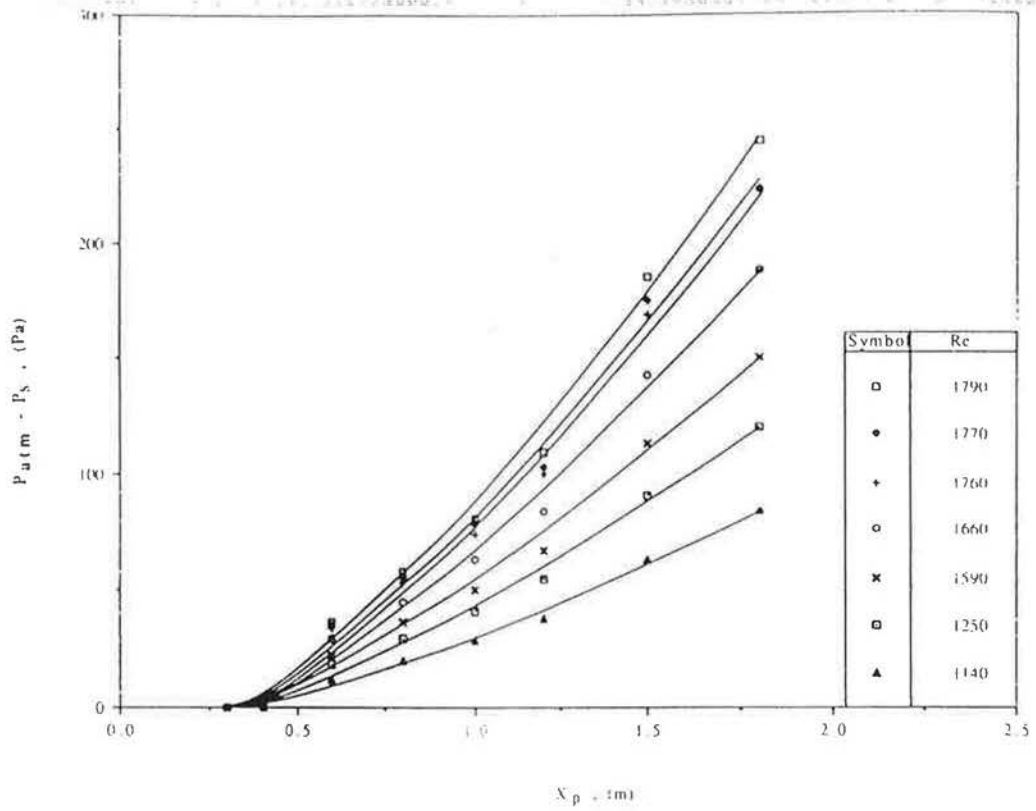


Figure 35 Variation of static pressure with X_p

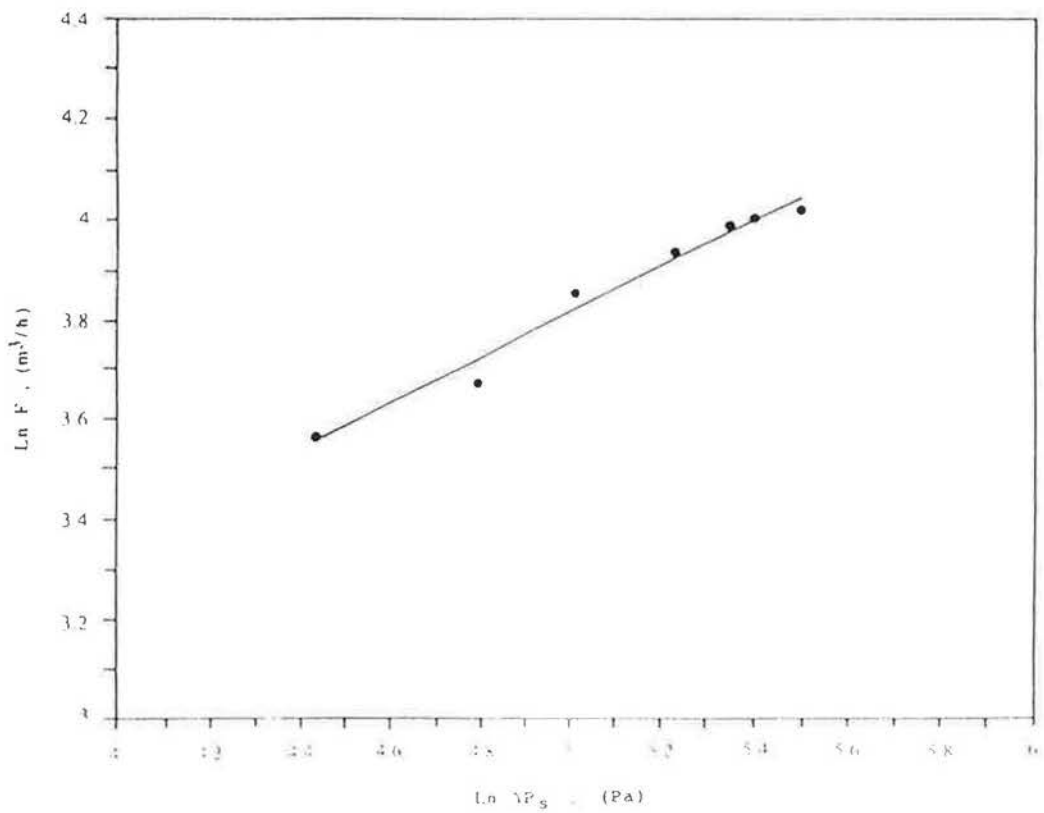


Figure 36 Variation of volumetric flow rate with static pressure difference across the porous medium

4. TESTS ON A SMALL-SCALE HVAC SYSTEM

This chapter describes the application of tracer-gas techniques for measuring airflow in a small-scale HVAC system [31]. The techniques were employed for balancing the HVAC system [32] and determining velocity-pressure (k-factors) factors of duct fittings [33].

4.1 Experimental procedure

Experimental work was carried out in a small-scale HVAC system, Figure 37. This consisted of a fan control and an instrumentation console. The fan unit had a volumetric flow rate in the range 0.1 to 0.3 m³/s, depending on the ductwork resistance and supply voltage. The console contained a variable transformer for fan speed control, together with a voltmeter and ammeter for measurement of supply voltage and current, respectively. A square-to-round fan intake transition also accepted standard 600 mm x 600 mm filters. The rectangular-to-round fan discharge transition was connected to 200 mm diameter ductwork using standard push fittings. The duct was manufactured from galvanised mildsteel. Two types of air diffusers were used and the discharge flow was controlled by means of dampers. A BINOS 1000 gas analyser, a pitot-static tube and a vane anemometer were used to estimate the flow rate through the system.

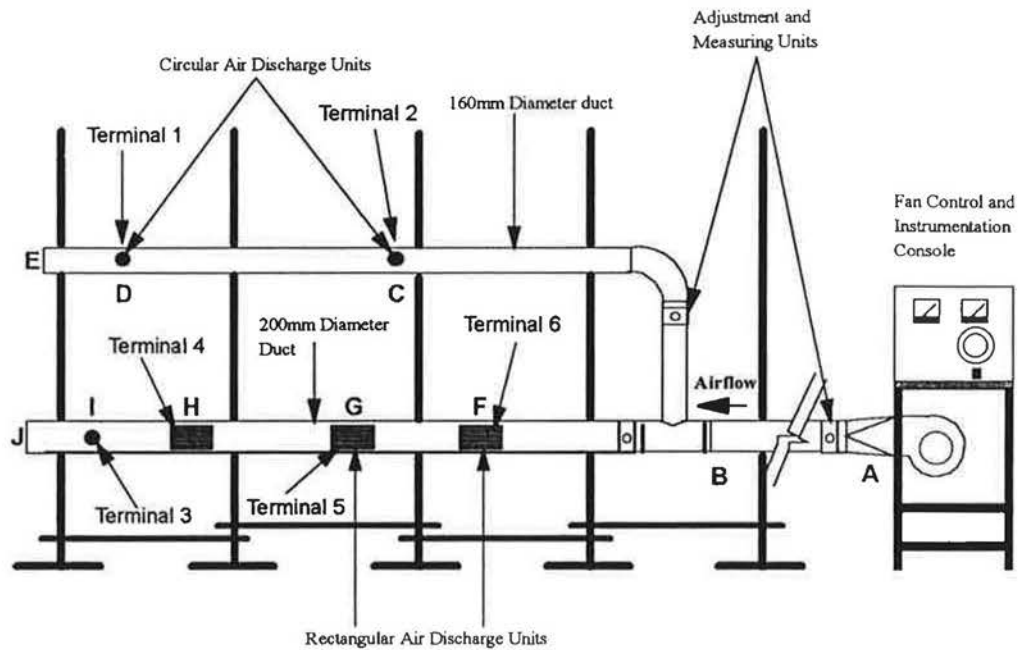


Figure 37 HVAC System for testing tracer gas techniques

4.2 Results and discussion

Airflow measurements were carried out in the HVAC system. The pulse-injection technique was used to estimate the flow rate through the main duct AB, branches BCDE and BFGHIJ and terminals 1-6. The measurement procedure involved injection of 1.5L of SF_6 at the inlet of the fan and monitoring the concentration at various points along the HVAC system using sample bags. The pumps attached to the sample bags were switched on 10 seconds before injection was begun, and switched off after purging of tracer gas has been completed. The background concentration of tracer gas was monitored continuously and included in our calculations.

To illustrate the method of calculation, the equations used to determine the airflow through branches BC and BF are shown as below:

$$F_{AB} = \left[\int_{t_1}^{t_2} C_{AB} dt \right]^{-1} \int_{t_1}^{t_2} G_{AB} dt \quad (19)$$

$$F_{BC} = \left[\int_{t_1}^{t_2} C_{BC} dt \right]^{-1} \int_{t_1}^{t_2} G_{BC} dt \quad (20)$$

$$F_{BF} = \left[\int_{t_1}^{t_2} C_{BF} dt \right]^{-1} \int_{t_1}^{t_2} G_{BF} dt \quad (21)$$

$$F_{AB} = F_{BC} + F_{BF} \quad (22)$$

$$G_{AB} = G_{BC} + G_{BF} \quad (23)$$

Equation (19-23) can be solved to determine G_{BC} , G_{BF} , F_{BC} and F_{BF} . The same method was used to estimate airflow rates through other branches and terminals.

Figure 38 and 39 show measurements of airflow made in the HVAC system using the pulse-injection technique. Airflow rates estimated from tracer-gas measurements were compared with pitot-tube measurements as shown in these figures. The differences between airflow rate estimated using tracer-gas measurements and measurements made using a pitot-tube [i.e., $100 \times (F_{pu} - F_p)/F_p$] were in the range -19.8 to 7.2%. However, it should be noted that turbulence can produce inaccuracies in pitot-tube measurements. The difficulties in measuring low velocities (i.e., below 3 m/s) using a pitot-tube can produce additional errors.

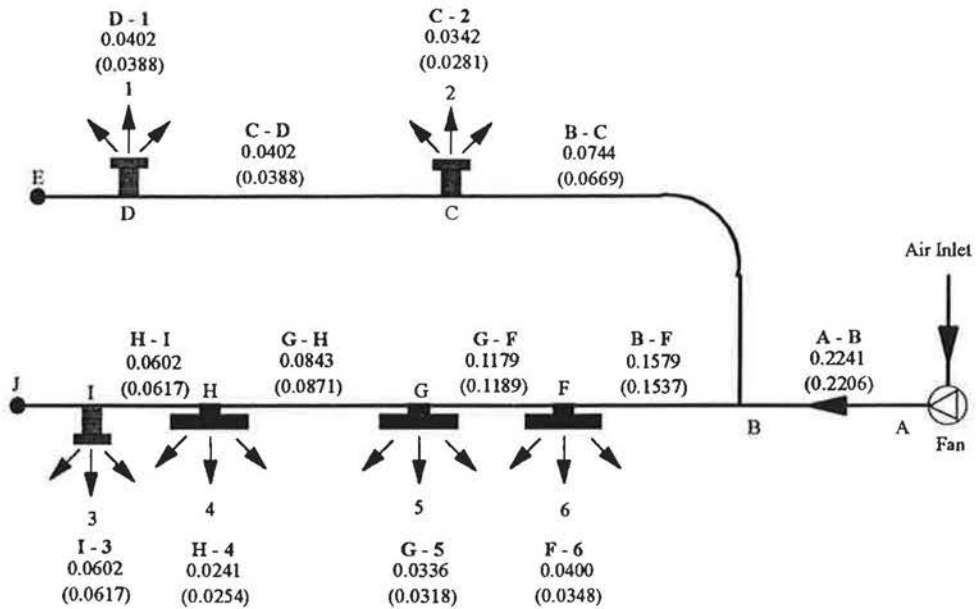


Figure 38 Comparison of tracer-gas airflow measurements with measurements made using a pitot tube, HVAC system [unit: m³/s, {Tracer-gas results are shown in brackets}]

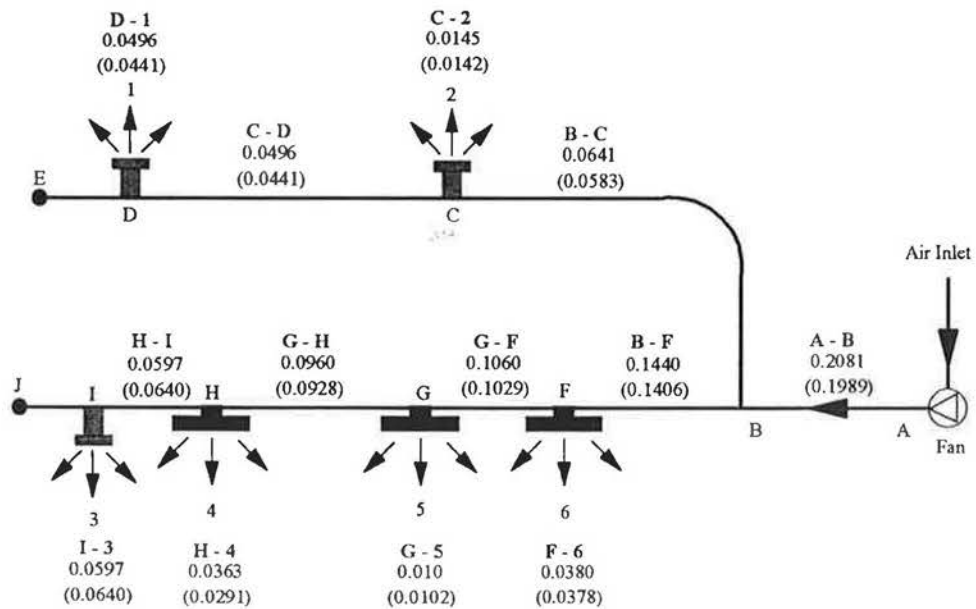


Figure 39 Comparison of tracer-gas airflow measurements with measurements made using a pitot-tube, HVAC system [unit: m³/s, {Tracer-gas results are shown in brackets}]

4.3 Balancing of HVAC systems using tracer-gas techniques

Balancing of HVAC systems is carried out once the system has been designed and installed in a building. The air distribution network must be commissioned to ensure that the HVAC system operates in conformity with the design specifications.

Regulation of airflow is normally carried out in accordance with the method set out by the CIBSE Code "The Commissioning of Air Distribution Systems, High and Low Velocity" [34]. The procedure consists of working back towards the fan from the remote branches setting the correct "proportional" airflow at each junction of the HVAC system without regard to absolute values of airflow. Once the HVAC system has been balanced so that all parts of the system are carrying the same "proportion" of their design airflow, the fan speed or main damper may be adjusted so that the main feed duct carries 100% of its design flow.

HVAC systems are usually balanced using traditional instrumentation such as a pitot tubes and vane anemometers; the measurement method depends on the size and shape of the duct and the type of terminal used. Regulation of airflow in this way is tedious and time consuming and in some cases is inaccurate.

This work describes the balancing of HVAC systems using a new equipment which allows the constant-injection tracer-gas technique to be employed. This has a number of advantages over the existing balancing method including:

- i. It is simple to use and allows HVAC systems to be balanced in a short period.

- ii. It can be used to measure airflow rates in HVAC systems directly and does not require determination of the cross-sectional areas of ducts or velocity profiles.
- iii. It can be used to provide accurate measurement of airflow over a wide range of air velocities.
- iv. It can be used to measure airflow rates in ducts of different sizes, shapes and lengths and does not require a long measuring duct for the establishment of fully-developed flow.

4.4 Principle of balancing HVAC systems

This section examines the CIBSE and tracer-gas methods for balancing airflows in an HVAC system. A simple example is used to demonstrate the two methods.

4.4.1 CIBSE method

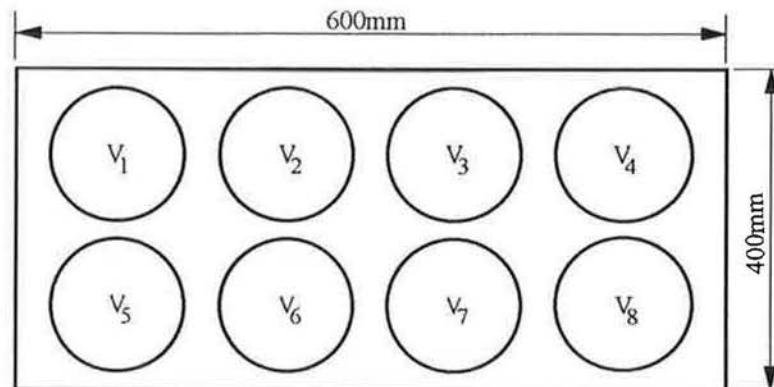
A schematic diagram of an HVAC system is shown in Figure 41. Assume that the design airflow rates are those given in Table 6.

| Branch | B - F | | B - D | |
|-----------------------------------|-------|-----|-------|-----|
| | 1 | 2 | 3 | 4 |
| Measured Flow (m ³ /h) | 100 | 120 | 200 | 300 |
| Design Flow (m ³ /h) | 100 | 100 | 150 | 200 |
| % of Design Flow | 110 | 120 | 133 | 150 |
| % of Design Flow (branch) | 115 | | 143 | |

Table 6 Design flows and measured flows with all flow control open

The procedure for balancing the system is as follows:

- i. Open all diffusers and branch dampers fully, together with the main damper adjacent to the fan.
- ii. Measure the airflow from the discharge units (or diffusers) using a hand-held vane anemometer. Figure 40 shows the methods for measuring the air velocity of a rectangular diffuser.
- iii. Assume that the measured airflow rates with all dampers open are those given in Table 6.
- iv. Branch B-C-D has the highest percentage of design flow and according to the CIBSE method this should be adjusted first.
- v. Having decided that branch B-C-D has the highest percentage of design flow, the least favoured discharge unit on the line is determined.
- vi. From Table 6, diffuser 3 is the least favoured (i.e., it is at the furthest point from the fan and is passing the lowest percentage of the design airflow). If the end unit had not been the least favoured it should be closed until it is the least favoured.
- vii. Adjustment can now begin as follows:



$$\text{Average Velocity} = \frac{V_1 + V_2 + V_3 + \dots + V_8}{8}$$

Figure 40 Method for measuring air velocity of a rectangular diffuser

Branch B-C-D

- a. Adjust diffuser 4 until its percentage of the design flow matches that of diffuser 3. This involves measuring the flow from diffuser 4 and checking the flow of diffuser 3. If the diffusers do not give an acceptable balance, diffuser 4 must be readjusted and checked again against 3. The balancing procedure is given in the following example:

Measure flow from diffuser 4.

| | | | |
|-------------------------------------|---|-----------------------|---------|
| e.g., Airflow of diffuser 4 | = | 300 m ³ /h | % = 150 |
| Adjust diffuser 4 gives flow | = | 270 m ³ /h | % = 135 |
| Checking diffuser 3 gives flow rate | = | 205 m ³ /h | % = 136 |

This is an acceptable balance and diffusers 3 and 4 are said to be balanced at 135% of the design airflow.

We assume that two attempts are sufficient to achieve the same percentage of the design flow. In practice several attempts are necessary to obtain the same percentage of the design airflow.

Branch B - E - F

- b. Measure airflow rate of diffusers 1 and 2

| | | | |
|----------------------------------|---|-----------------------|---------|
| e.g., Airflow rate of diffuser 1 | = | 110 m ³ /h | % = 110 |
| e.g., Airflow rate of diffuser 2 | = | 120 m ³ /h | % = 120 |

This is not an acceptable balance. Readjust 2.

| | | | |
|---|---|-----------------------|---------|
| e.g., Airflow rate of diffuser 2 | = | 113 m ³ /h | % = 113 |
| Check against 1, airflow rate of diffuser | = | 112 m ³ /h | % = 112 |

This is an acceptable balance since diffuser 1 and 2 are each discharging 112% of their design flow.

After adjusting all diffusers, the next step is to adjust the branches B-C and B-E. First check the percentage of the total design airflow that branches B-C and B-E are carrying using a pitot tube.

e.g., Branch B-C airflow rate = 475 m³/h % = 136

e.g., Branch B-E airflow rate = 225 m³/h % = 113

As branch B-C is carrying the highest percentage of the airflow, this is adjusted first. The regulation of airflow in the branch should be used as a reference. In this case diffusers 2 and 4 can be used.

Measure airflow of diffusers 2 and 4.

e.g., Airflow rate of diffuser 2 = 113 m³/h % = 113

e.g., Airflow rate of diffuser 4 = 270 m³/h % = 135

Readjust the damper on branch B-C and measure the flow rates of diffusers 2 and 4.

e.g., Airflow rate of diffuser 2 = 115 m³/h % = 115

e.g., Airflow rate of diffuser 4 = 226 m³/h % = 113

This is an acceptable balance and both branches B-C and B-E are carrying the same percentage of design flow.

The next step is to regulate the total airflow in the main duct A-B to 100% of the design value. The pitot-static traverse method should be used employing the CIBSE recommended measurement positions, Table 7. The damper on the main duct or fan speed should be adjusted to achieve the correct airflow in the system. The system is now balanced and operating at the "design" airflow rates.

| Duct Size, mm (diameter) | No. of points at each traverse | No. of traverse | Location of test point from duct wall as % of duct dia. | | | | | |
|--|---|-----------------------|--|----|----|----|----|----|
| | | | 1 | 2 | 3 | 4 | 5 | 6 |
| 150 | 2 | 1 | 12 | 88 | - | - | - | - |
| 150 - 240 | 2 | 2 | 12 | 88 | - | - | - | - |
| 250 - 435 | 4 | 2 | 4 | 29 | 71 | 96 | - | - |
| 450 and over | 6 | 2 | 3 | 14 | 32 | 68 | 86 | 97 |
| For disturbed flow in all sizes over 150 | 6 | 2 or 4 | 3 | 14 | 32 | 68 | 86 | 97 |

Table 7 Measurement of velocity pressure in a circular duct

It is clear that balancing even a simple HVAC system using this method is tedious and time consuming. In practice several attempts are required to obtain the same percentage of the design flow of various diffusers. The task of balancing of an HVAC system for large buildings would be lengthy and the use of vane anemometers and pitot tubes could give rise to significant errors in airflow measurements.

4.4.2 Tracer-gas method

This method is based on the application of the constant-injection technique to estimate and adjust airflow rates in HVAC system. Tracer gas is injected into a duct at a constant rate, (q), and the resulting concentration response (C) is measured. Assuming that the air and tracer gas are perfectly mixed within the duct, and the concentration of tracer gas in the outside air is zero, the following equation can be used to estimate the flow rate, (F):

$$F = \left(\frac{q}{C} \right) \times 10^6 \quad (24)$$

The procedure for balancing an HVAC system (see Figure 41) is as follows:

- i. Assume that the design airflow rates of various diffuser are those given in Table 6.
- ii. Start, for example, with branch B-C-D. Measure the airflow rate of diffuser 3 by injecting tracer gas at point 7 and monitoring the concentration at point 3. Use equation (24) to estimate the airflow rate.
- iii. Determine the percentage of the design airflow of diffuser 3 (i.e., measured flow/design flow).
- iv. Assume a target concentration of tracer gas (say 200 ppm) which is required in all ducts to achieve a balanced system. Assume that diffuser 4 is carrying the same percentage of the design flow as diffuser 3 and calculate the total flow rate in duct B-C.
- v. Use equation (24) to estimate the amount of tracer gas, q , which should be injected in duct B-C to achieve the target concentration of 200 ppm.
- vi. Inject tracer gas at point 8 and adjust damper 4 until the concentration in branch B-C equals 200 ppm. Check the concentration at point 3 and adjust damper 3 if required.
- vii. Apply procedure (i) to (iv) to the branch B-E-F. The concentration in this branch should be 200 ppm.

- viii. Adjust dampers I and II so that branches B-E and B-C carry same percentage of the design flow. Finally adjust the fan speed or damper III in the main duct so that all diffusers carry 100% of design airflow; the system is then balanced.

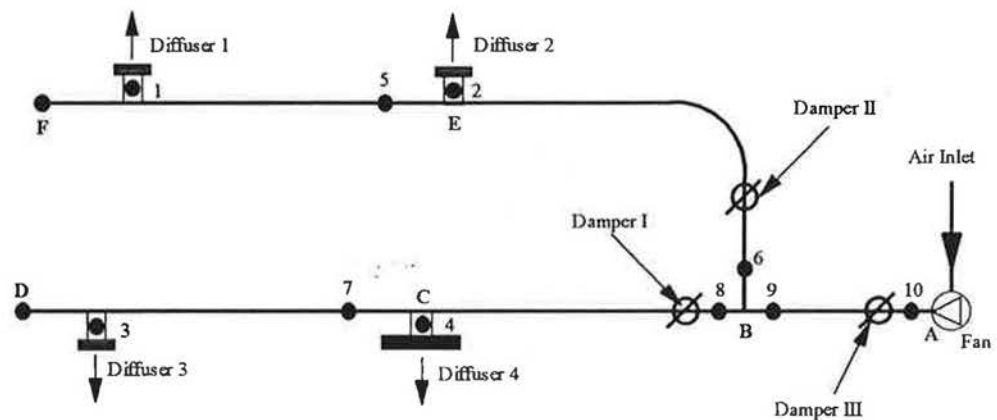


Figure 41 Schematic diagram of the HVAC system

4.5 Description of tracer-gas equipment

The HVAC system was balanced using the tracer-gas injection and sampling units shown in Figures 42 and 43. The tracer-gas injection unit incorporates solenoid valves, a manifold, a mass flow controller, a switch controller and a tracer-gas cylinder. The injection rate was controlled using a variable power supply and the rate of tracer gas injected was displayed on a digital unit.

The tracer-gas sampling system consisted of solenoid valves, a manifold, a switch controller and a gas analyser.

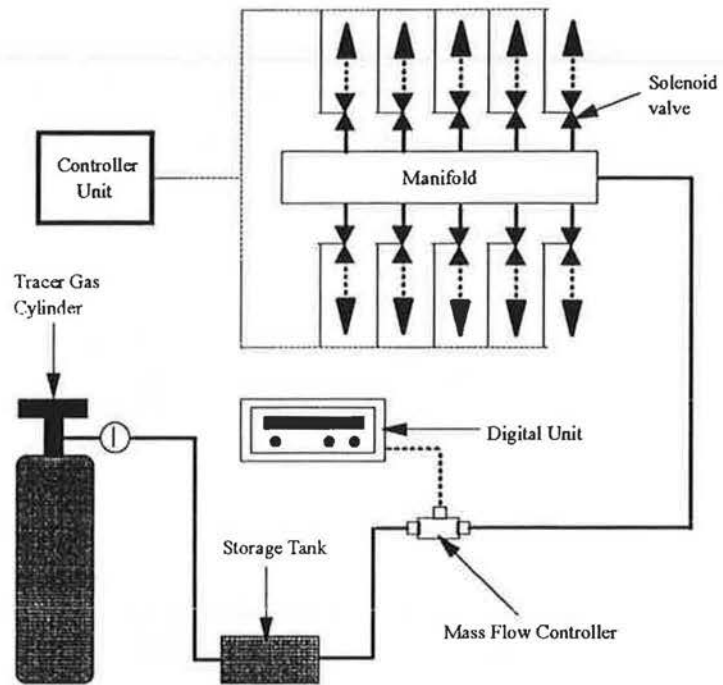


Figure 42 Injection unit

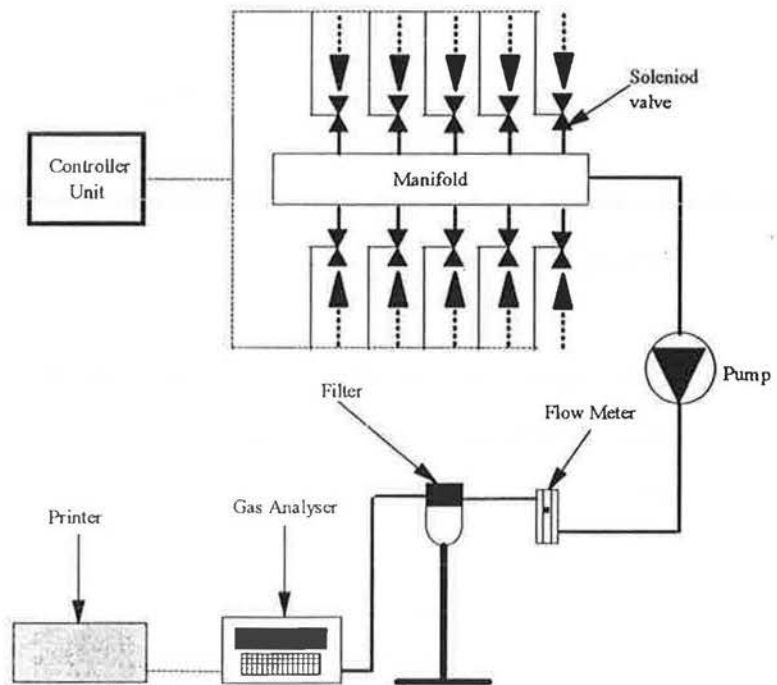


Figure 43 Sampling unit

The system could be used for sampling various tracer gases. We chose to use sulphur hexafluoride (SF_6) as it has desirable characteristics in terms of safety, detectability and cost. In addition, its suitability has been demonstrated previously by its successful use in air movement studies.

4.6 Results and discussion

A small-scale HVAC system, Figure 41, was balanced using tracer-gas equipment and a pitot tube. The constant-injection technique was used to estimate the flow rate in the main duct A-B, branches B-C-D and B-E-F and terminals 1-4. The measurement procedure involved injection of SF_6 tracer gas at points 5,6,7,8, 10 (see Figure 41) and monitoring the concentration at points 1,2,3,4 and 9, respectively. The flows in the various ducts and terminals were then balanced using the procedure described in section 4.4.2.

Figure 44, 45 and 46 show measurements of airflow for three different sets of design flow. Airflow rates estimated from tracer-gas measurements were compared with a pitot-tube measurements as shown in these figures.

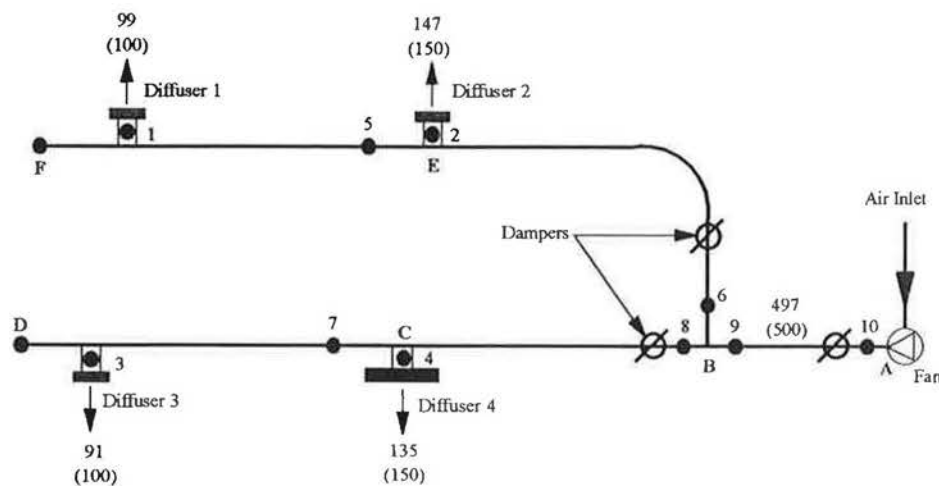


Figure 44 Comparison of tracer-gas airflow measurements with measurements made using a pitot-tube [unit: m^3/h , {Tracer-gas results are shown in brackets}], Experiment 1

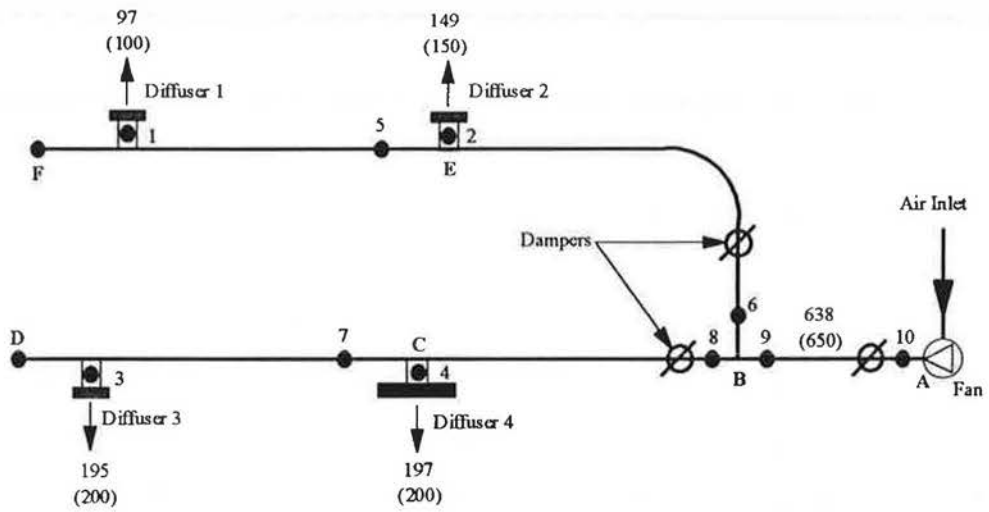


Figure 45 Comparison of tracer-gas airflow measurements with measurements made using a pitot-tube [unit: m^3/h , {Tracer-gas results are shown in brackets}], Experiment 2

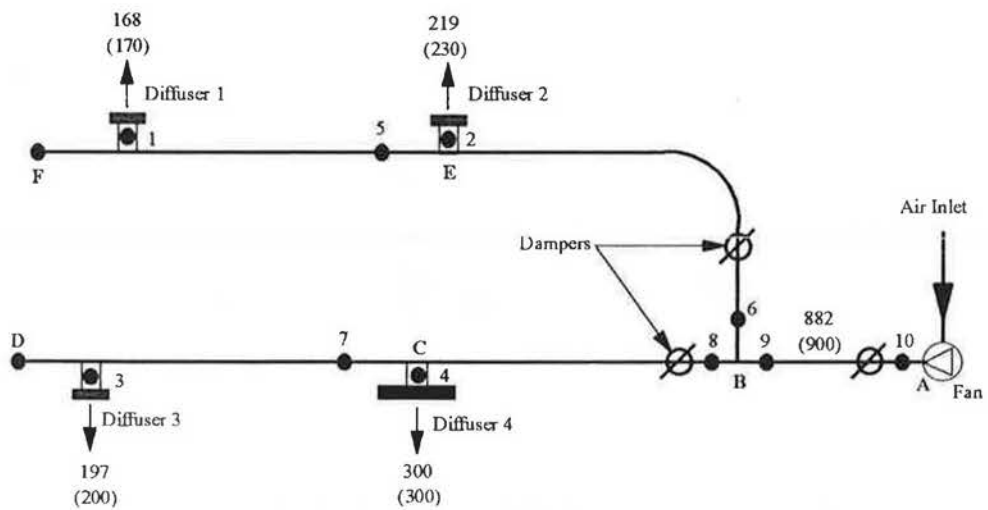


Figure 46 Comparison of tracer-gas airflow measurements with measurements made using a pitot-tube [unit: m^3/h , {Tracer-gas results are shown in brackets}], Experiment 3

The difference between airflow rate estimated using a tracer-gas technique and measurements made using a pitot-tube [$100 \times (F_{\text{tracer}} - F_{\text{pitot-tube}})/F_{\text{average}}$] was in the range 0-10% (see Tables 8,9 and 10).

| Measurement Techniques | Diffuser's Airflow Rate , (m ³ /h) | | | | Airflow Rate in A-B, (m ³ /h) |
|-------------------------|---|-----|-----|-----|--|
| | 1 | 2 | 3 | 4 | |
| Pitot Tube, F_p | 99 | 147 | 91 | 135 | 497 |
| Tracer Gas, F_t | 100 | 150 | 100 | 150 | 500 |
| $[F_t - F_p]/F_a$, (%) | 1 | 2 | 9 | 10 | 1 |

Table 8 Comparison of tracer-gas airflow measurements with measurements made using a pitot tube, Experiment 1

| Measurement Techniques | Diffuser's Airflow Rate , (m ³ /h) | | | | Airflow Rate in A-B, (m ³ /h) |
|-------------------------|---|-----|-----|-----|--|
| | 1 | 2 | 3 | 4 | |
| Pitot Tube, F_p | 97 | 149 | 195 | 197 | 638 |
| Tracer Gas, F_t | 100 | 150 | 200 | 200 | 650 |
| $[F_t - F_p]/F_a$, (%) | 3 | 1 | 3 | 2 | 2 |

Table 9 Comparison of tracer-gas airflow measurements with measurements made using a pitot tube, Experiment 2

| Measurement Techniques | Diffuser's Airflow Rate , (m ³ /h) | | | | Airflow Rate in A-B, (m ³ /h) |
|-------------------------|---|-----|-----|-----|--|
| | 1 | 2 | 3 | 4 | |
| Pitot Tube, F_p | 168 | 219 | 197 | 300 | 882 |
| Tracer Gas, F_t | 170 | 230 | 200 | 300 | 900 |
| $[F_t - F_p]/F_a$, (%) | 1 | 5 | 2 | 0 | 2 |

Table 10 Comparison of tracer-gas airflow measurements with measurements made using a pitot tube, Experiment 3

The tracer-gas method was found to be a simple and convenient way of measuring and balancing airflow in the HVAC system. The system could be balanced to a high degree of accuracy in a short period of time.

5. PERFLUOROCARBON TRACER (PFT) FOR MEASUREMENT OF AIRFLOW IN DUCTS

Application of the passive PFT technique to ventilation measurements in building is well known [35] but little work has been carried out on this techniques for measurements in ducts. Sateri [10] has examined the passive tracer-gas technique using perfluorocarbons. It involved the use of small tubes filled with PFT liquid, known as sources, placed at the inlet of the duct and tubes packed with adsorbent, known as samplers, placed downstream. The emission rate of the sources is dependent on the air temperature; the uptake rate of the samplers is significantly influenced by the air velocity and turbulence in the duct. The orientation of the sample with respect to the flow also affects the uptake rate. As a result measurement errors using the passive PFT technique are large. To overcome this problem, a new technique must be developed [36].

5.1 Development of a new constant-injection technique for measuring airflow in duct using perfluorocarbon tracer

The method of constant injection of tracer gases depends on the properties of the tracer at ambient atmospheric pressure (760 mmHg) and temperature (25°C). For example, sulphur hexafluoride, nitrous oxide and carbon dioxide are at gaseous state under these conditions. They can be easily processed and stored in cylinder. Therefore, the injection of these gases using constant-injection is simple (refer to section 2.2.1.1). However, perfluorocarbon tracers behave differently to the tracer gases described above as they are in liquid at ambient atmospheric pressure and temperature.

5.1.1 How is the liquidified PFT being released in a gaseous state?

A new method has been developed for creating standard concentration gas mixtures for calibration purpose [37] using diffusion tubes. This method has been adapted for use in producing known, controlled and constant rate of tracer gas injection.

A vessel consisting of a bulb containing the tracer liquid, attached to a capillary is placed in a thermostatically-controlled water bath. The dimensions of the vessel and the temperature of the water bath were chosen carefully to achieve the required tracer-gas injection rate.

5.1.1.1 Diffusion tube theory

A diffusion tube (see Figure 47) is a liquidified filled reservoir (≈ 3 ml) with a long fine-bore neck. The rate of liquid diffusion is dependent on several factors including the nature of the liquid, the dimensions of the capillary connected to the reservoir and the temperature. It can be measured precisely, usually by measuring the weight loss over a period of time.

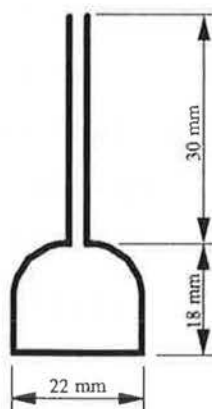


Figure 47 Diffusion tube

The basic theory of diffusion tubes is discussed by Analytical Instrument Development [37] especially as it relates to the dynamic generation of known standards. Their theoretical equation is given below to illustrate the way in which diffusion rate from a vessel with a capillary neck varies from substance to substance, with different temperatures and with different shaped capillary necks:

$$D_r = 6.169 \times 10^6 D_0 M \frac{A_x}{L_d} \left(\frac{T}{T_0} \right)^{c-1} \log \frac{P_T}{P_T - p} \quad (29)$$

where,

| | | |
|-------|---|---|
| D_r | = | Diffusion rate, (ng/min) |
| D_0 | = | Diffusion coefficient at T_0 and P_0 , (cm^2/s) |
| M | = | Molecular weight, (g) |
| P_T | = | Total pressure, (mm Hg) |
| P_0 | = | 760 mm Hg |
| A_x | = | Cross-sectional area of diffusion path, (cm^2) |
| T | = | Temperature, (K) |
| T_0 | = | 273K |
| L_d | = | Length of diffusion path, (cm) |
| p | = | Partial pressure of sample at T, (mm Hg) |
| c | = | Constant - usually 2, but may be 1.75 |

5.1.1.2 Sizing the diffusion tubes

Some simple relationships exist which are helpful when determining a suitable design tube size.

- i. The diffusion rate increases with the square of the diffusion bore.
- ii. The diffusion rate increases with decreasing path length (i.e., halving the path length doubles the resulting diffusion rate).

- iii. The diffusion rate also increases with increasing temperature. A crude rule of thumb to use here is that the diffusion rate doubles as the diffusion tube temperature is increased by 20°C.

The size of the diffusion tubes to be used in this investigation was estimated using a Table of Diffusion Tube Sizes for different substances [38]. The dimensions chosen were a reservoir volume of ≈ 3 ml, a capillary neck of 3 mm and a neck length of 30 mm.

5.1.2 Initial development of a controlled tracer-gas injection technique

Preliminary work involved placement into the duct of a diffusion bottle filled with perfluoro-n-hexane (PP1); release of the tracer gas relied on the temperature of the airflow in the duct. A series of tests were conducted and results showed that the tracer-gas release rate was too low for the detection range of the B&K analyser. The low release rates were due to the low air temperature in the duct. Furthermore, this method of injection was not reliable because the tracer-gas release rate varied with the air temperature. Development of a technique of injection which provides a stable and higher tracer-gas release rate was necessary. A controlled-temperature water-bath was introduced at this stage of development.

The controlled tracer-gas injection system that meets the above requirements consists of a number of components (see Figure 48). A diffusion tube of the required dimensions is partially filled with PP1. It is connected to one end of the stainless steel tube wind round by wire using a clear polyurethane tube. The other end of the steel tube is inserted into the duct with a diffusion cap to help to diffuse the tracer-gas injection and at the same time to provide a means of suspension for the diffusion bottle. The electrical wire that winds round the stainless steel tube is connected to a power supply to heat up this tube so that PP1's vapour from the bottle will not condense along it. A fish-tank which is almost completely filled with

water is stirred by a paddle. The 2550W water heater, type U3, manufactured by Grant Instruments, Cambridge is designed for domestic use in boiling small volumes of water very quickly and has a built-in thermostat which can control the water bath at a desired temperature. A thermometer was placed as near as possible to the diffusion bottle to check the temperature. The temperature control of this thermostat was in the range of $\pm 0.5^{\circ}\text{C}$.

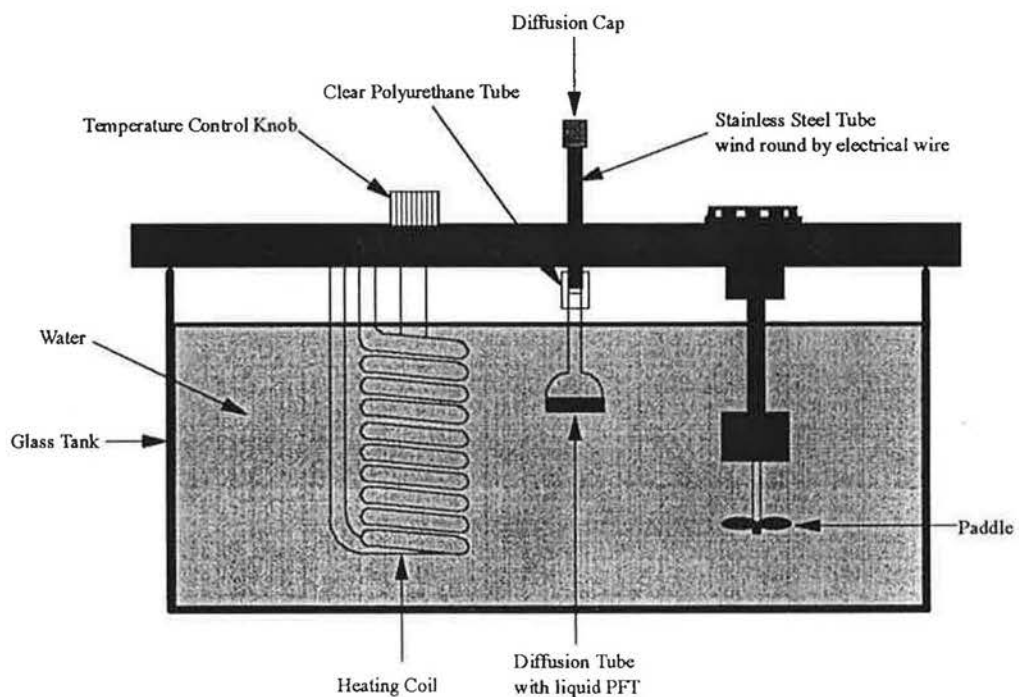


Figure 48 Schematic of the controlled tracer-gas injection system

5.1.2.1 Demonstration of this prototype tracer-injection system

A series of tests were conducted using this prototype tracer-injection system. The set-up of instrumentation for these tests is shown in Figure 49. The water bath was placed at the inlet of the duct with the neck of the diffusion bottle inserted into the duct. A diffusion cap consisting of an 'O' ring and a fine wire mesh suspended the diffusion bottle and provided the diffusion of tracer-gas into the duct. At the downstream end of the duct, a Multi-Gas Analyser, type 1302, manufactured by Bruel and Kjaer, Denmark

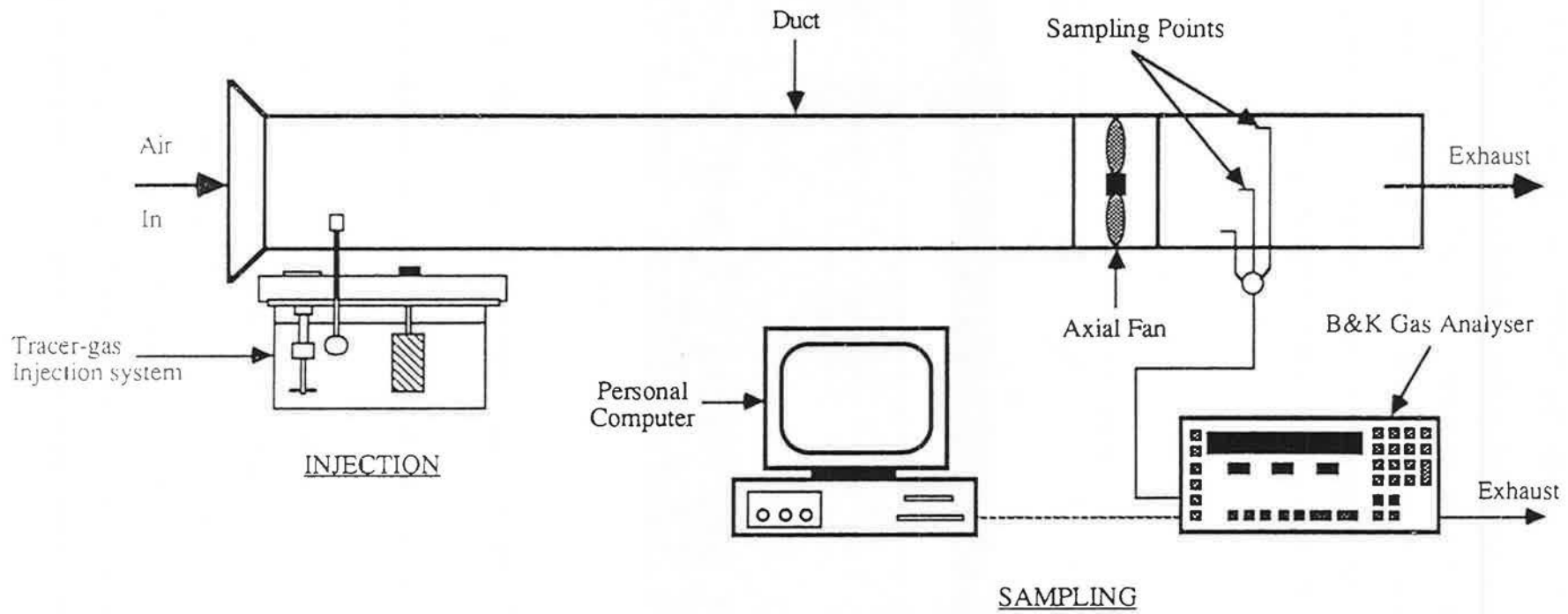


Figure 49 Instrumentation for the injection of PFT into the duct

was used to analyse the gas samples in real-time. The concentration of gas samples was monitored over the period of tracer-gas injection and this was displayed on the personal computer.

Both the temperature of the water bath and the amount of liquid tracer in the diffusion bottle played very important roles in providing a stable, constant and high injection rate of tracer gas into the duct. In the initial tests, the temperature of the water bath was set at 50°C, and the diffusion bottle was partially filled with liquidified PPI. The tracer-gas concentration monitored was very low and unsteady. This was due to insufficient heating of PPI (boiling point range of PPI is 54-60°C) and poor tracer-air mixing. This was overcome by increasing the temperature of the water bath to 60°C and placement of another fine wire mesh on the diffusion cap. The results of the tests showed that the tracer-gas concentration was much higher and steadier. A prototype of this PFT injection system was developed.

One drawback of tracer-gas injection system is that the instrumentation required to provide the tracer-gas injection is bulky. This would be impractical when injection is required in a duct suspended at a height of 3 m. The tracer-injection system needs to be simple, light and compact.

5.1.3 Redesign of the prototype tracer-gas injection system

Figure 50 shows the redesign of the prototype PFT injection system with improved features. It is small, light, compact and most important of all, it is able to be attached temporarily to the surface of the duct while injecting the tracer gas. The PFT injection system consists of a cylindrical aluminium block with a heating element inserted into the base. The block was bored to allow insertion of a small glass vessel containing the PFT liquid. Water is placed in the bore hole to ensure uniform heating throughout the glass vessel. A plastic cap is placed over the hole to prevent water from spilling over the heating block. A diffusion cap is placed at the

outlet of the vessel to allow uniform dispersion of tracer gas into the duct.

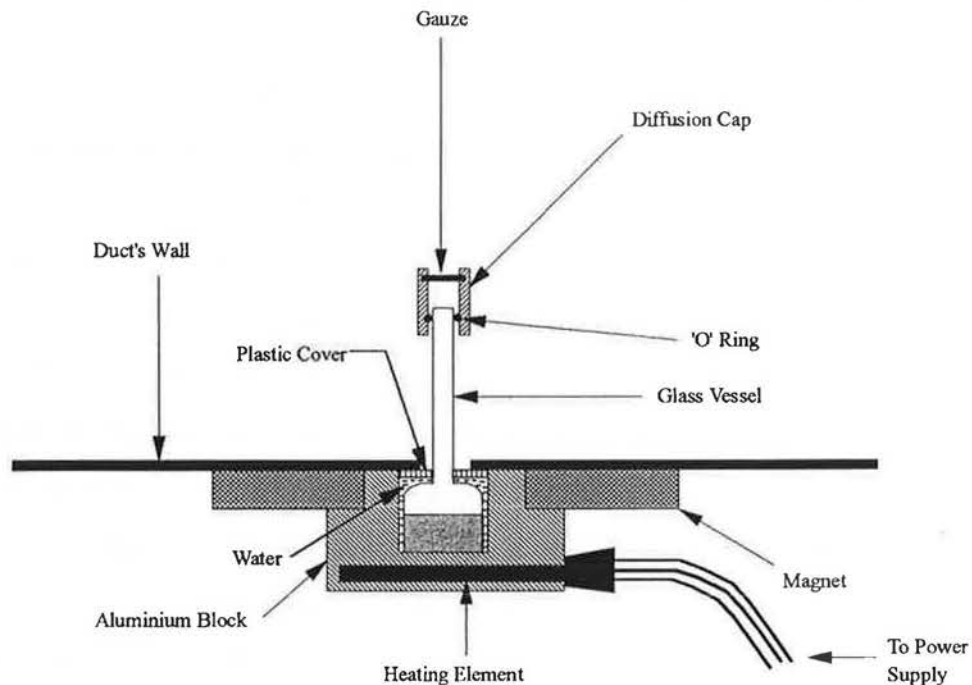


Figure 50 PFT injection system

A magnet is fixed to the heating block so that the injection system can be attached to the duct wall during airflow measurements.

5.1.3.1 Detailed description of the heating block

The heating block was made in the Department's workshop from a 64 mm diameter aluminium rod (see Figure 51) to form a step on the outside and a 22 mm diameter hole bored to a depth of 22 mm. Aluminium was chosen because it has a good heat transfer properties and is light in weight. A 8 mm hole was bored near to the base of the block to allow insertion of the heating element and another 3mm hole was drilled at right angles to the 8 mm hole for insertion of a thermistor. A 44 (ID) x 78 (OD) x 14 mm thick ring magnet was glued onto the step of the aluminium block using epoxy.

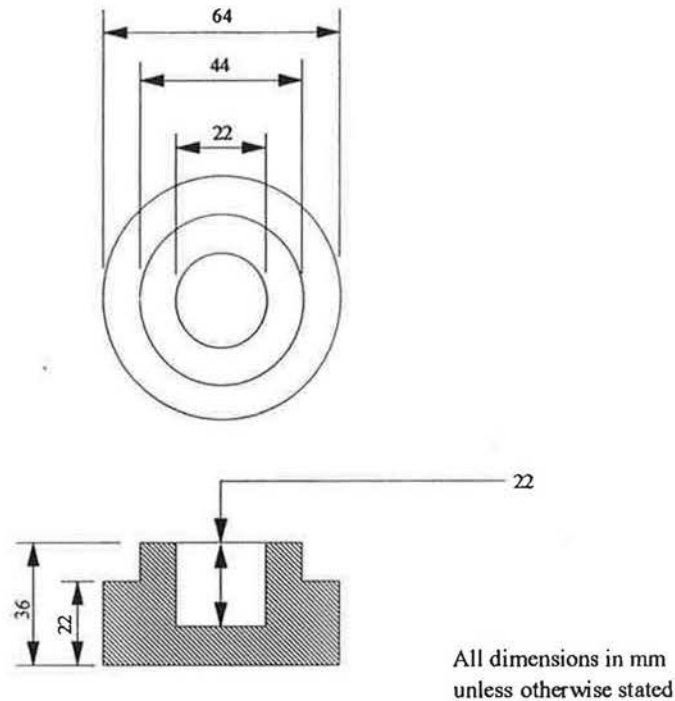


Figure 51 Heating block

Figure 52 shows the circuit diagram of the heating block and control box. The heating of the block was provided by a soldering iron element, type Antex CS24E and temperature control of this element was achieved using a thermistor, type Philips NTC 2322 460 63222. Both the heating element and thermistor were controlled by the control box via a signal cable. Temperature setting of the heating element was carried out by adjusting the screw in the control box which will varied the resistance of the resistor, R3 as shown in Figure 84. The thermistor denotes as Th1 in the circuit diagram is a temperature sensor. Once the thermistor sensed the heating block had reached the preset temperature, the LED light on the front panel of the control box was turned off.

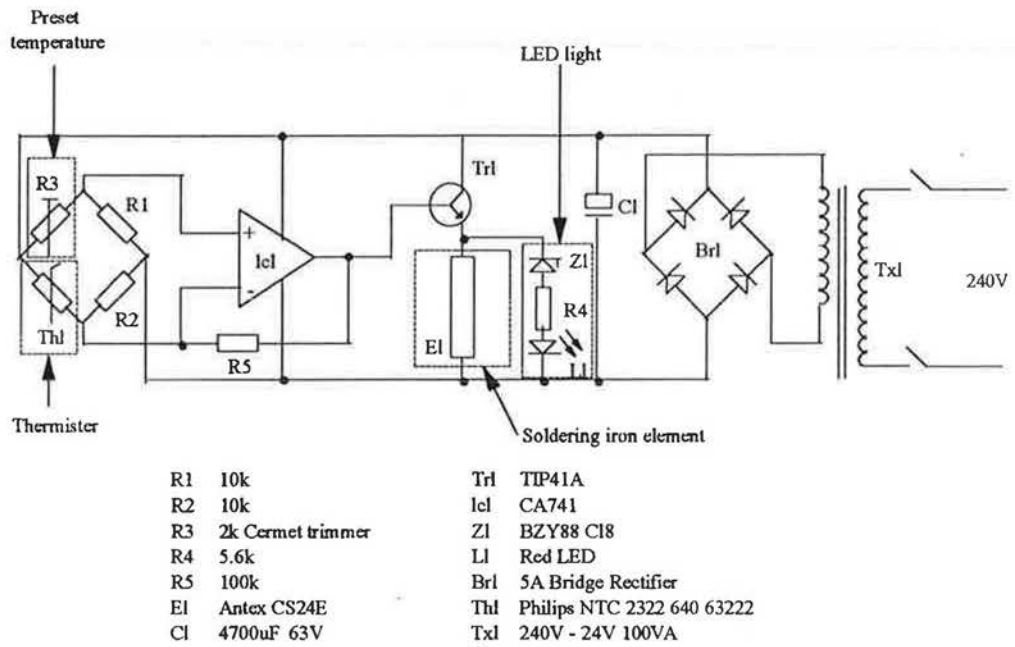


Figure 52 Circuit diagram of the tracer injection unit

This control box was capable of controlling three heating blocks simultaneously. The new prototype injection system consisted of the control box and the heating block are light and compact. This enabled it to perform tracer-gas injection even in very small and awkward parts of the duct network.

5.2 Development of the prototype sampling system [39]

Following the injection of tracer gas at the upstream end of the duct, the monitoring of air samples was carried out at the downstreamed. The concentration of the gas was analysed and the airflow rate evaluated. The analysis could be carried out in a real time or non-real time. In the event of non-uniform mixing, the direct sampling and real-time analysis of the air samples would show fluctuations of the tracer gas concentration and so non-

real time analysis would be preferred.

Non-real time analysis requires a sampling system to take air samples from the duct. This sampling system should have the following features:

- i. Able to collect air samples simultaneously over a period of time
- ii. Versatility, i.e., also able to measure air change rate in buildings
- iii. High sampling frequency of up to once every 5 seconds
- iv. Samples can be collected in bags or tubes
- v. Compact and portable
- vi. Simple and user-friendly
- vii. Economical to run
- viii. Low maintenance cost
- ix. Moderate production cost
- x. Robust

From these design criteria, the essential features of the sampling system could be defined.

5.2.1 The prototype sampling system design

Figure 53 shows the prototype sampling system. It consists of solenoid valves, adsorber tubes, a manifold, a pump, a flow meter and a programmable logic controller.

5.2.1.1 Choice of components

In this section all the components making up to the prototype sampling system are described in a logical sequence from the inlet of the pump to the solenoid valves at the end of the adsorber tubes.

i. The pump

An oil-free gas-tight diaphragm pump, type DA7 SE was supplied by Charles Austen Pumps Limited, UK. The maximum flow rate supplied by this pump is 14 L/min. This flow rate is sufficient to overcome the large resistance to flow presented by the manifold and the packed adsorber tubes during the sampling process.

ii. Flow meter

A flow meter, type GPV was supplied by Platon Limited, UK. The float and needle valves in the flow meter were made from stainless steel. It had a maximum flow capability of 5 L/min and an accuracy of $\pm 5\%$.

iii. Manifold

The sampling unit manifold (Figure 54) was made from a 2500 x 145 x 18 mm thick aluminium plate. The manifold was designed with a minimum "dead" volume and as the tracer gas in the manifold was purged between samples, the effect of this volume was negligible. A 9 mm hole was drilled across the length of the plate with both ends of it tapped and threaded at 1/8" bsp to a depth of 20 mm. One 1/4" union fittings were fitted on each side of the end plate. On the other two longer sides, five 1/8" bsp threaded

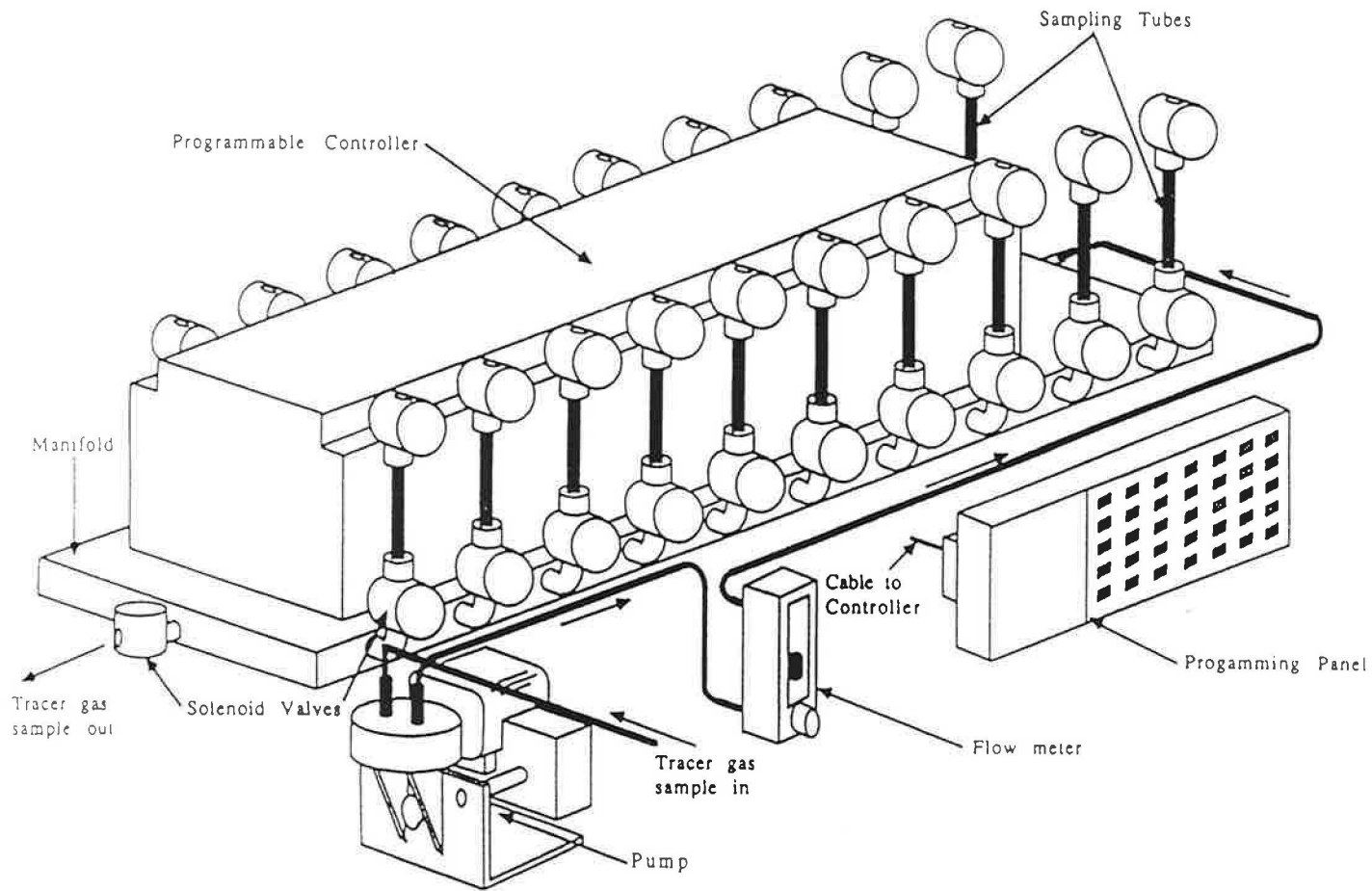
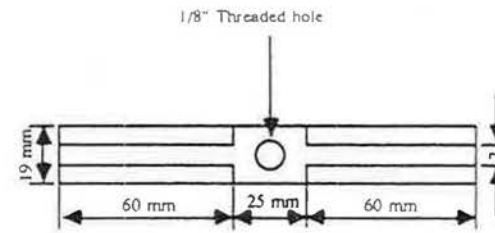
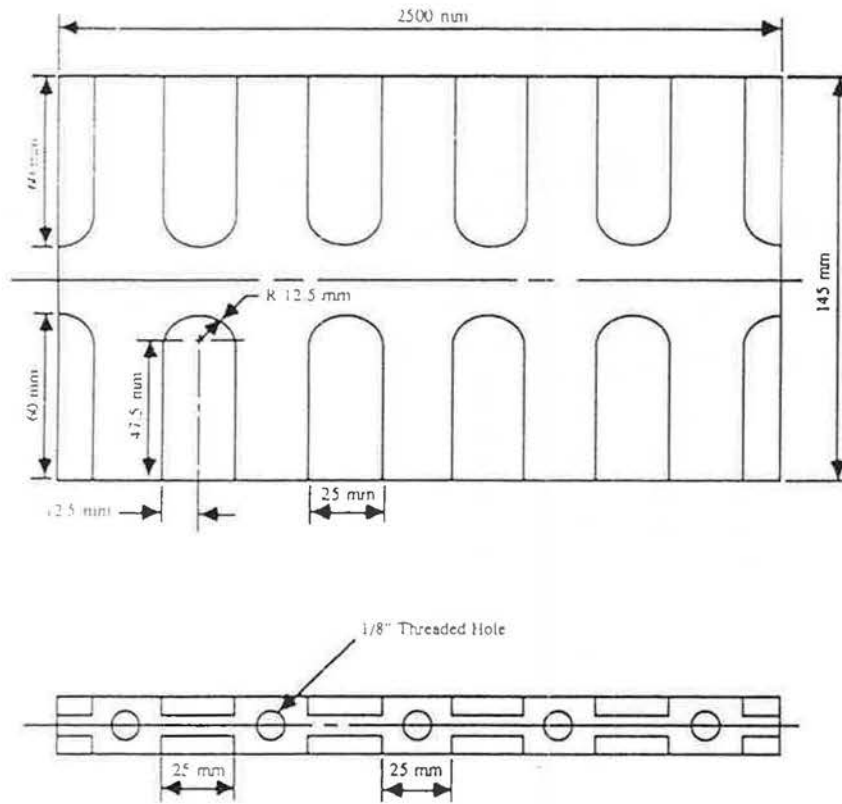


Figure 53 The prototype sampling system



Scale 1 : 2

Figure 54 Details of the sampling unit manifold

holes were made at an interval of 50 mm on each side. 1/4" elbow union fittings were fitted to these threaded holes to receive solenoid valves.

iv. Solenoid valves

Ten solenoid valves were supplied by Western Automation Ltd. at the following specifications: brass body; 24 volts DC; 1/8" orifice; Rc pipe fittings and urethane seat (to minimise absorption of perfluorocarbons). The valves were normally closed; open when energised.

v. Adsorber tubes

Adsorber tubes designed to be compatible with the B&K Thermal desorber, type SBK 1355 (Section 5.4.1), were obtained from Perkin Elmer Ltd.. Each tube assembly consisted of an empty tube with a retaining gauze at the front end, a separate gauze for placing behind the packing material and two blank end caps for sealing when not in use (see Figure 55). The packing method is described in section 5.4.2.2. The packing material used in this work was Chromosorb 102, 60-80 mesh, supplied by Chrompack Ltd., UK.

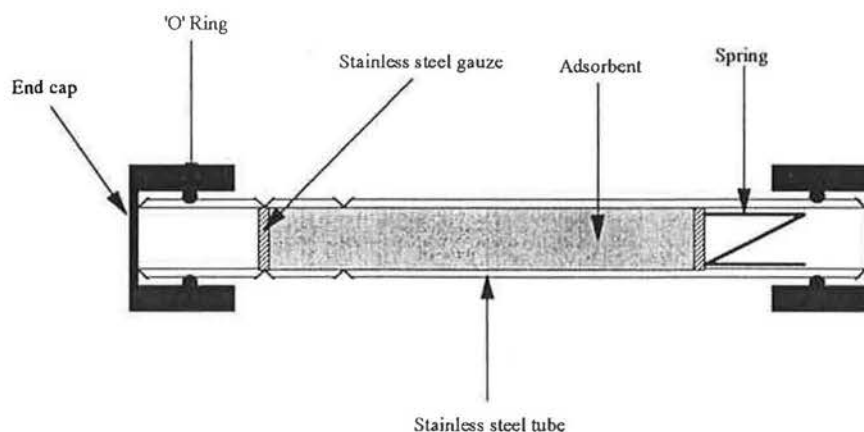


Figure 55 A single adsorbent tube with end cap

vi. Adsorber tube holders

The adsorber tube holder was designed for connection of the adsorber tubes to the solenoid valves and repeatable and high quality sealing of the tube. At the same time, it had to allow for speedy installation and recovery required during tracer gas tests. The design involved the use of push-fit connectors working on the same principle as the blank sealing caps used during storage. These sealing caps form a push fit over the adsorber tubes and are sealed by an 'O' ring contained in the groove near the edge of the cap. Figure 56 shows the details of a adsorber tube holder. A groove was cut in each connecting piece to take an 'O' ring the same size as those used in storage. A set of analytical cap 'O' rings was from Perkin Elmer Ltd. and these were placed in the new connectors.

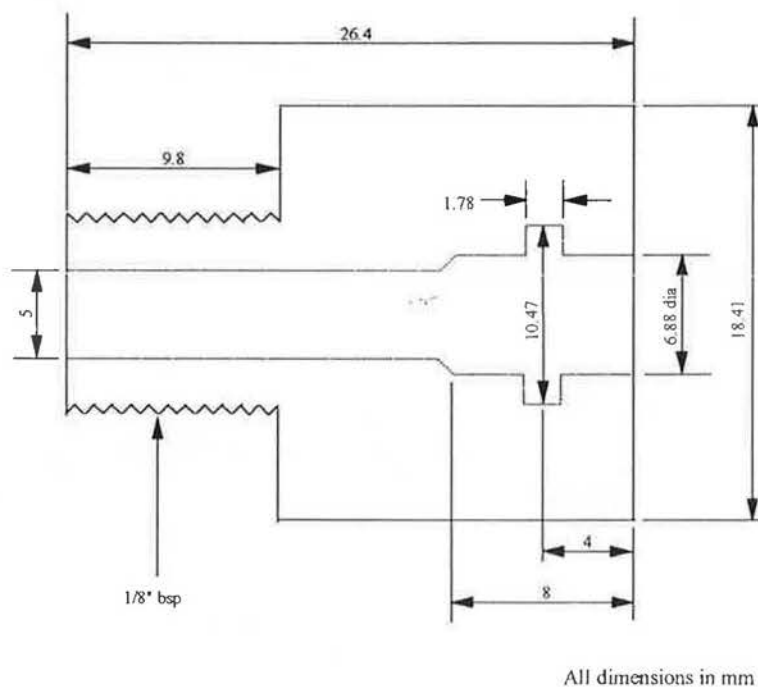


Figure 56 Adsorber tube holder

The adsorber tubes are reliably sealed into the rest of the system so that all the air drawn by the pump comes in at the solenoid valve and passes inside the adsorber tube and out through another solenoid valve (see Figure 57).

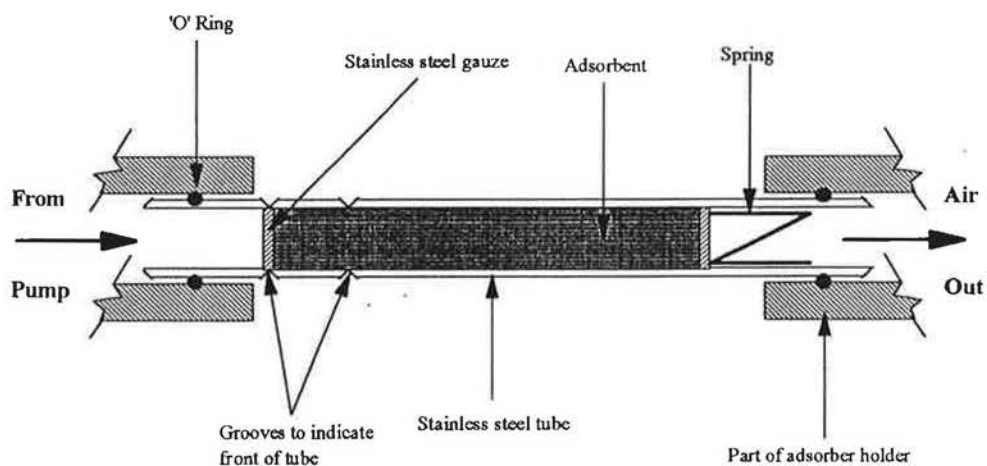


Figure 57 Schematic of connection at adsorber tube holder

vii. Nylon tubing and connectors

All the flexible connections between adsorber tubes, manifolds, the pump and the flow meter were made from nylon tubing 8 mm O.D. and 5 mm I.D.. There was some concern over choosing a suitable flexible material because many, such as conventional rubber hose and silicone rubber have a high adsorption affinity for perfluorocarbons. It is important that none of the perfluorocarbon tracers should be removed from the sampling point by any means other than air movement. In this instance, it is safe as both ends of the sample tube are isolated by solenoid valves.

An Enots brass connector, manufactured by IMI Enots Ltd., is a push-in tube fitting suitable for use with nylon tubings. The tubing is pushed into the brass collet where it is tightly held, sealing being achieved by a nitrile 'O' ring. These connectors have been designed for working at high pressures.

viii. The programmable logic controller

Operation of each pair of solenoid valves was controlled automatically by the programmable logic controller. This controller MELSEC F1 series Type F1-30MR-ES was supplied by Mitsubishi. The controller has been designed to simulate the action of a relay-based system which is most suitable for controlling the duration of the tube's exposure to the gas samples at a pre-determined time interval and sequence. This controller is capable of controlling the duration of exposure for intervals as short as 0.01 seconds to as long as 99.9 seconds. The program used to operate the system was written in Step Ladder. Input of the program to the controller was carried out via the programming panel, MELSEC Type F2-20P-E supplied by Mitsubishi. This could either be mounted directly onto the base unit (programmable) or mounted remotely using the remote cable, Type F-20P-CAB.

ix. The fixed voltage power supply

The fixed voltage power supply was supplied by RS Component Ltd.. It was used to step down the voltage from 240V AC to 24V DC in order to operate the solenoid valves.

5.2.2 Building the sampling system

The assembly of the sampling system was carried out piece by piece from the pump as a starting point with systematic leak checks at each connection until the sampling system was reached.

Nylon tubes, 6 mm bore and 1.5 mm thick wall, were used for the connection between the pump outlet and the inlet of flow meter. A reduction in tube size from the 6 mm bore nylon tubes to nylon tubes of 23 mm bore with 1 mm thick wall were made in the line between the outlet of the flow meter to the manifold. This 25 mm nylon tube was connected to one end of the manifold via a 1/4" union brass tube fitting with 1/8" bsp

thread. The five 1/8" bsp threaded holes on each side of the plate were to receive 1/4" elbow union brass tube fittings which in turn connected to the inlet port of the solenoid valves. The remaining 1/8" bsp threaded hole was fitted to the inlet port of the solenoid valve via a 1/4" union brass tube fitting. Each pair of solenoid valves was connected by an adsorber tube via push-fit connectors (see Figure 58) except the one at the end which was used to control the exhaust air. The Enots brass connectors were connected to the outlet port of each solenoid valve to receive the 3/8" OD nylon tubes for exhaust purposes. All these solenoid valves were connected to the programmable logic controller via electrical cables. The program which governs the duration and sequence of operation for each set of solenoid valves was input into the logic controller via the programming panel.

The manifold was designed to support the programmable logic controller. This reduced the overall size of the sampling unit.

5.2.3 Detailed construction of the case for the sampling system

A case was designed to protect and allow the sampling system to be portable. The construction details of the case are illustrated in Figure 59. The size of the case was 350 mm x 520 mm x 200 mm. The openings in the front panel are designed to receive the programming panel, flow meter, on/off switch and inlet port.

5.3 General instructions for the sampling system

The stepwise procedure for setting up the instrumentation for an experiment using a PFT as the tracer gas is as follows:

- i. Preset the programmable logic controller to the required settings, i.e., the desired sequence and duration of sampling and purging between each sample.

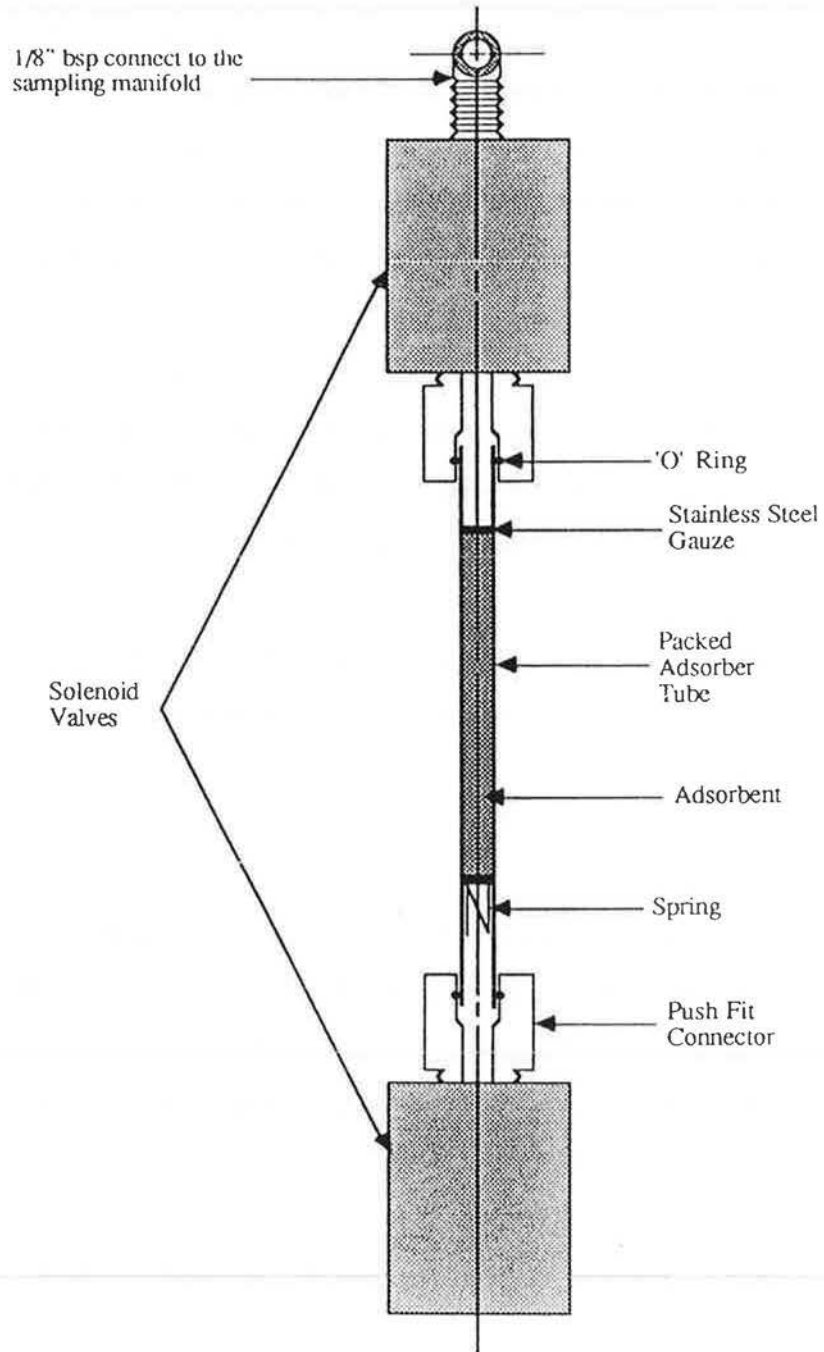


Figure 58 Details of connection

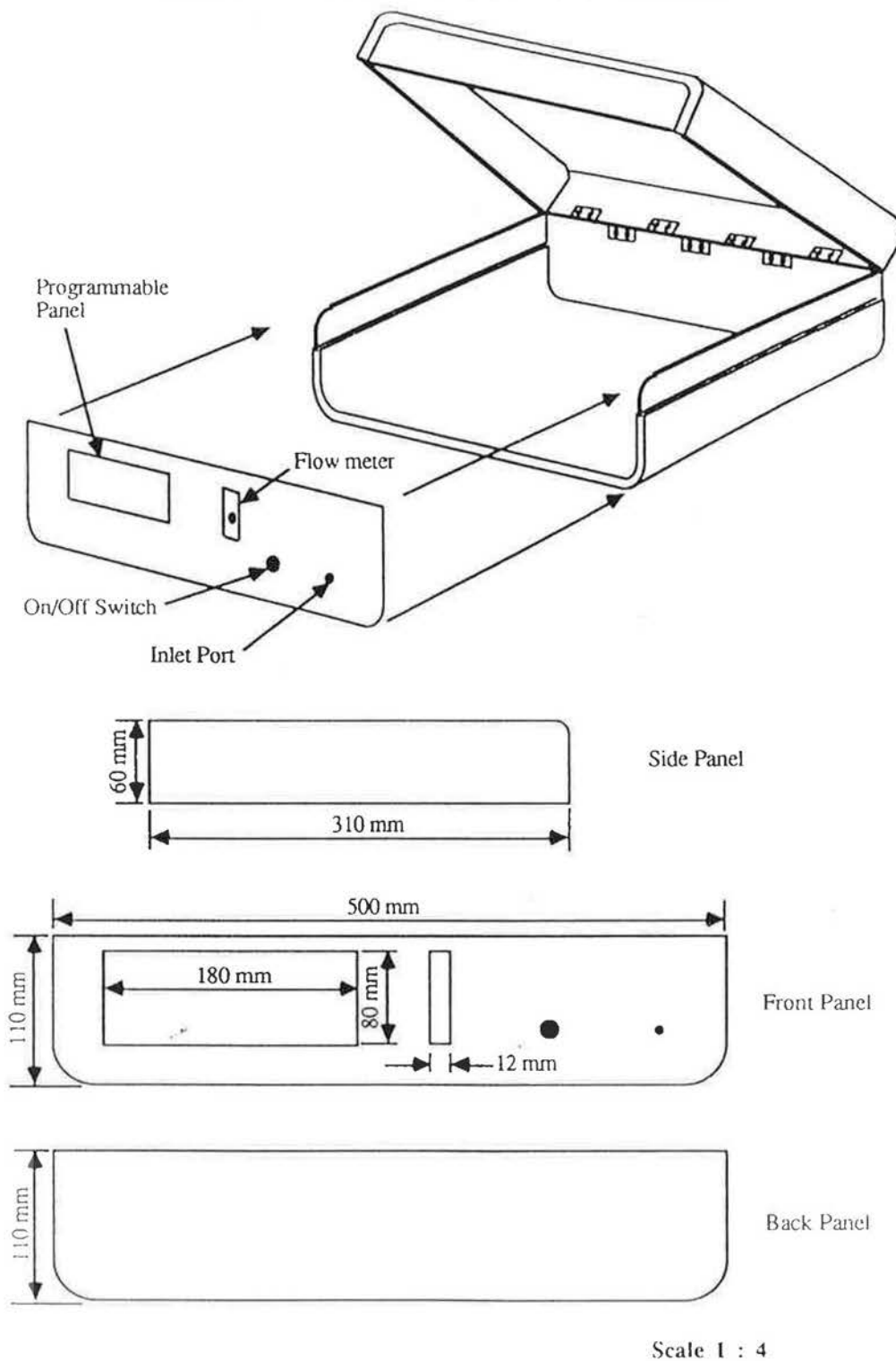


Figure 59 High frequency sampling system's case

- ii. Set the flow meter to the desired flow rate.
- iii. Check that the controller and all solenoid valves are working correctly by performing a test run.
- iv. Connect fresh adsorber tubes to the sampling system and note their positions with respect to the solenoid valves which are identified by numbers.
- v. Insert the sampling tubes into the inlet port of the pump via the manifold.
- vi. Take the exhaust tube of each pair of solenoid valves to a place distant from the duct section to prevent recirculation of tracer gas.
- vii. Set up the injection section.

The instrumentation set-up and testing procedure are complete. The next set of instructions describe how to carry out a complete airflow measurement using the prototype sampling system:

- i. Switch on the fan of the duct.
- ii. Start the injection of PFT into the duct using the injection unit.
- iii. Switch on the sampling system after allowing time for injection of tracer gas to stabilize.
- iv. At the end of the measurement, remove the adsorber tubes from their holder and replace end caps.

5.4 Sample analysis

The analysis of these sampling tubes has three main features, desorption of the gases from the adsorber tube, separation into components and quantitative analysis. These tasks can be performed using either a Perkin Elmer ATD50 automatic thermal desorber and a Perkin Elmer Sigma 3B gas chromatography or a B&K Thermal Desorption System with a B&K Multi-Gas monitor. The analysis of samples using the former set of instruments was found to be too costly, time-consuming and had the disadvantage that only specifically-trained personnel could carry out the analysis. The latter instruments are less costly and no special operator skills are required. The only disadvantage of these instruments is that they have to be operated manually. The B&K thermal desorption system and a multi-gas analyser were used for this work.

The thermal desorption system, type SBK 1355, was used to desorb the gases from the adsorber tubes while the multi-gas monitor, type 1302, was used to separate and analyse the tracer gases in the adsorbent. Both instruments were supplied by Bruel and Kjaer, Denmark. The type SBK 1355 thermal desorber system is specifically designed as an accessory for the type 1302 multi-gas monitor which has an accuracy of $\pm 1\%$. The type SBK 1355 extends the detection limits of the Type 1302 from parts per billion (ppb) to parts per trillion (ppt), and allows an area survey to be carried out for volatile organics and some permanent gases. In general, the adsorbent packed in the sampling tubes has a high affinity for the compound interest at low temperature but a low affinity at high temperature. The criteria in choosing an acceptable adsorbent are illustrated in section 5.4.4.

Each instrument is described here with reasons why it is chosen, its working principle and how it was calibrated.

5.4.1 The thermal desorption unit

The function of the thermal desorption unit is to desorb gases which are adsorbed by the solids by heating the solid in the presence of a flowing, inert gas such as nitrogen. This is the safest and most efficient way of desorbing gases and is carried out by heating the whole tube containing the adsorbent.

Once the tube has been packed with adsorbent, it can be used many times. Each time it is desorbed for analysis, it becomes conditioned for a new test.

5.4.1.1 Description and functions

This type SBK 1355 thermal desorber system (see Figure 60) consists of three main units:

- i. The computer control unit
The unit is operated via a keypad and LCD display mounted on the front panel of the instrument. The front panel also contains a number of LED which show the current status of the instrument (ready, purging, sampling and analysing). The computer unit allows control of:
 - a. Oven temperature up to 250°C
 - b. Number of flushes.
 - c. Sample tube flush time.
 - d. Run start.
 - e. Run stop.

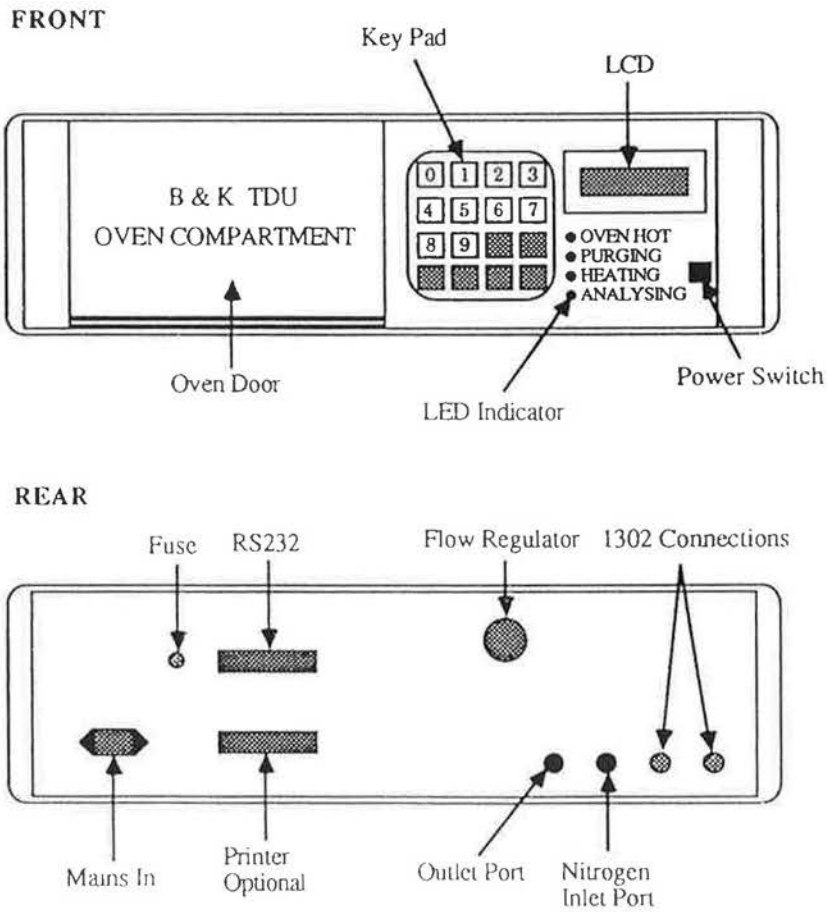
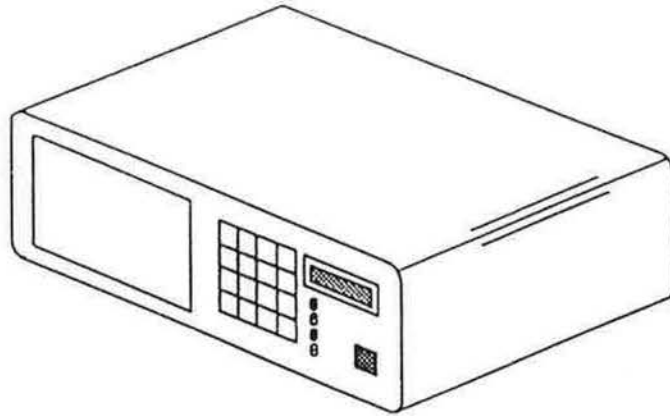


Figure 60 Type SBK 1355 thermal desorber

ii. Oven

The oven is controlled by the computer system and can be programmed to a maximum of 250°C. The actual temperature for desorption will depend upon the adsorbent used. Typically this is 250°C.

iii. Pumping and storage

The SBK 1355 uses a series of valves, a vacuum pump and a nitrogen cylinder to perform a series of operations:

- a. Flushing of the tube prior to heating (this is important to prevent the adsorbent oxidising),
- b. Evacuation of the analytical loop (50 ml),
- c. Filling the analytical loop with a sample in nitrogen,
- d. Flushing the analytical loop after analysis,
- e. Maintaining an open loop for the multi-gas monitor at all times.

5.4.1.2 System use

The thermal desorption system has four basic operating modes:

- i. Tube clean mode
- ii. Manual purge mode
- iii. Calibration mode
- iv. Analytical mode

Typically a tube would be placed in the thermal desorption unit. Thermal desorption is completed in one stage (Figure 61). However, before desorbing and analysing the tube, the pneumatics of the system should be flushed with nitrogen to ensure no memory effect. The sample tube should also be flushed to remove any oxygen. The oven heats to pre-set

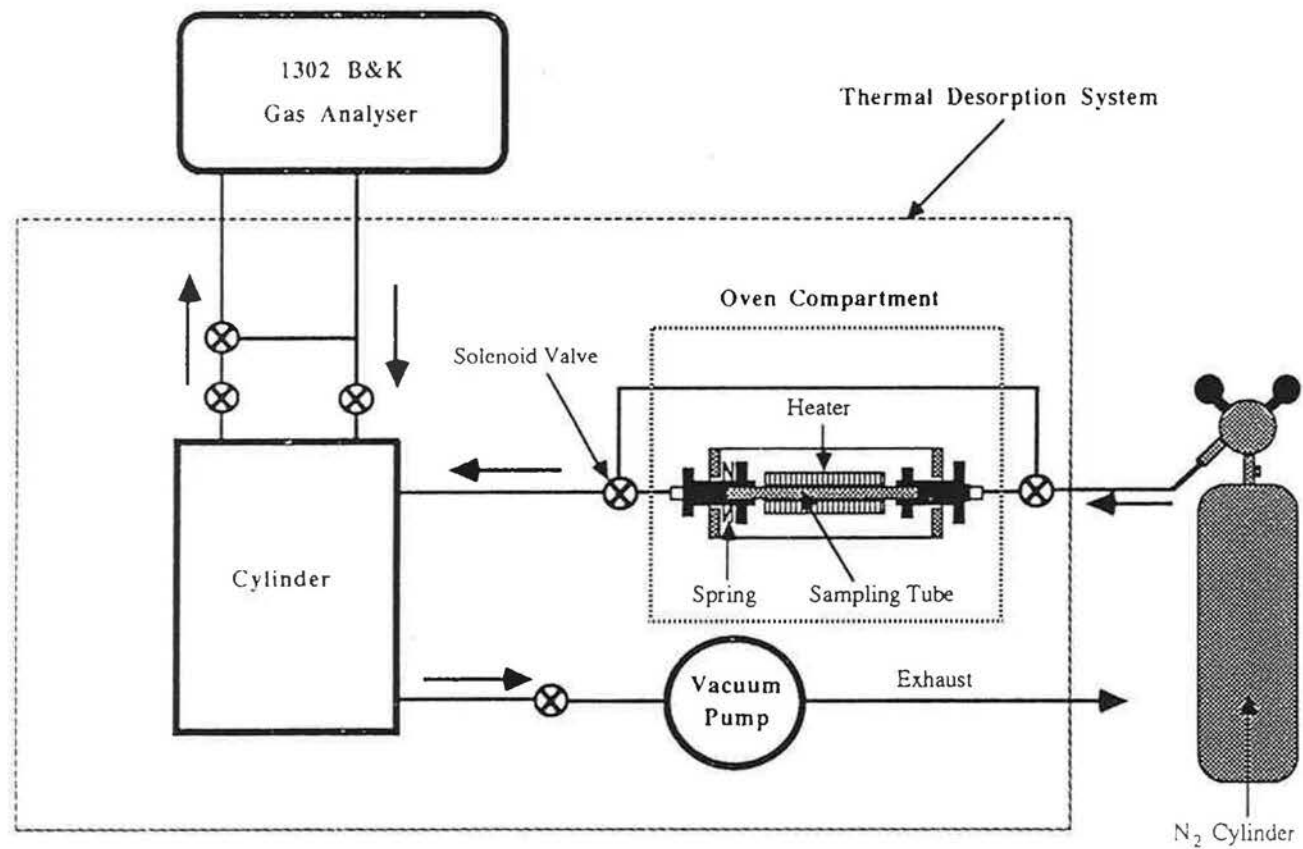


Figure 61 Schematic of the thermal desorber/gas analysis system

temperature, while the sample loop is evacuated by the vacuum pump. After the temperature has stabilised the sample is passed from the tube into the sample loop by a flow of nitrogen. When the loop has reached atmospheric pressure the nitrogen flow shuts off and the sample loop connects to the multi-gas monitor. The oven cools and the multi-gas monitor would then analyse the loop and the result is shown. The loop is then flushed and disconnected from the multi-gas analyser ready for the next analysis.

5.4.1.3 Analysis of results from the multi-gas monitor

The results displayed on the screen of the multi-gas monitor are not the true concentration of tracer gas collected in the adsorber tube. These results have to be interpreted depending upon the calibration mode used. There are several ways of calibrating the thermal desorption system with the multi-gas monitor; the method chosen will depend on the accuracy of the measurement required.

The most accurate way of calibrating the system is described below with reference to an example.

5.4.1.3.1 Calibration method

It uses the type SBK1355, factors from the electronic database (WT9336) and the compound of interest. The procedure is as follows:

- a. The WT9336 Electronic database is used to send the appropriate filter details to the type 1302 monitor. For example, if perfluoro-n-hexane (PP1) was being measured using UA0696, the calibration TD0696 would be sent to the type 1302. TD0696 contains zero and humidity compensation data for the filter UA0696.

- b. A tube containing the adsorbent to be used (in these case chromosorb 102) would be cleaned using the tube clean routine on the type SBK1355.
- c. The tube would be analysed on the type SBK1355 and the result shown on the screen display of the type 1302 monitor as 0.05 mg/m^3 . Plot the point (0, 0.1) on the graph paper and ignore the units (mg/m^3). Figure 62 shows the point (0, 0.1) on the graph.

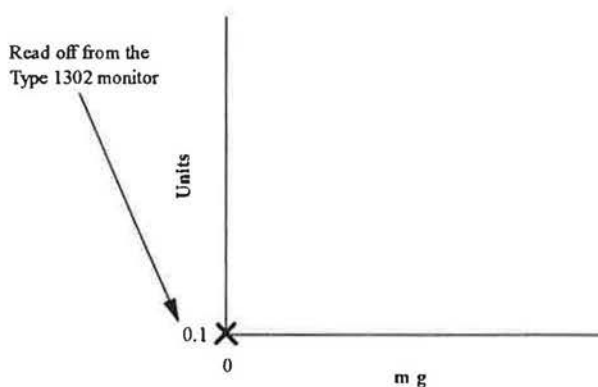


Figure 62 First point plotted on the calibration graph

- d. A known amount of perfluoro-n-hexane (0.124 mg) would be drawn into a SGE (Scientific Glass Engineering) 0.5 μl capacity syringe, type 0.5B-7, supplied by Phase Separations Ltd., UK. and injected into the chromosorb 102 in the tube.
- e. The tube is analysed and again the result is shown on the display of the type 1320 monitor as 121 mg/m^3 . Ignore the units and plot the point (121, 0.124) onto the graph shown in Figure 62.

- f. Draw a line between the two points and Figure 63 shows the calibration graph for the adsorber tube with ≈ 0.435 mg of chromosorb 102.

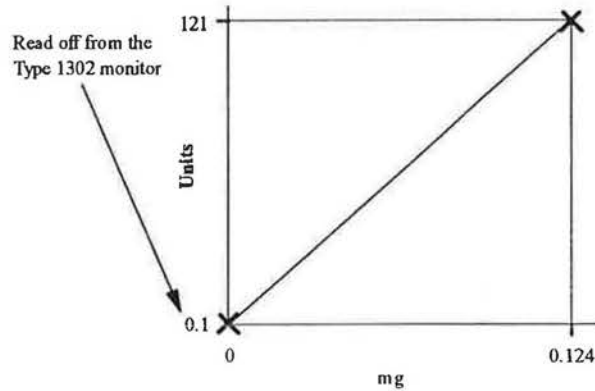


Figure 63 The calibration graph

- g. The results obtain from the type 1302 monitor can be plotted onto the y-axis of this calibration graph and the amount of tracer gas (mg) in the adsorbent of the tube can be read off from the x-axis. With the knowledge of the volumetric flow rate (m^3) of the sample through the tube, the concentration (mg/m^3) in the tube can be evaluated.

This method of calibration is not restricted to one point calibration. Multi-point calibration can be carried out by injecting different amounts of tracer into the tube to produce a few more points on the calibration graph. This will help to determine the accuracy of the calibration graph.

5.4.2 Packing and conditioning the adsorber tubes

5.4.2.1 The adsorber tube

The adsorber tube (see Figure 55) consists of a small stainless steel tube which has two rings at one end. This is the top of the tube. The second of these rings holds a stainless steel gauze against which the adsorbent sits. The adsorbent is held by a second gauze and a spring. In storage both ends of the tubes are covered with storage end caps. During measurement, both the end caps are removed and the tube is fitted to the push-fit connectors with the air flow from the pump entering the top of the tube.

5.4.2.2 Packing the tube

The procedure of packing the tube is as follows (see Figure 64):

- i. Label each adsorber tube and weigh with its two storage end caps, the two stainless steel retaining gauzes and retaining spring.
- ii. The first gauze is placed in the tube and pushed into its slot. This is easily done using a suitably sized hexagonal key.
- iii. As a rule of thumb, fill two-thirds of the tube with adsorbent (the amount will depend upon the adsorbent being used).
- iv. Tap slightly to ensure that the adsorbent has settled.
- v. Using the hexagonal key, the second gauze is pushed into place, and the retaining spring pushed into position.
- vi. Replace the two storage end caps and weigh the tube to determine the mass of adsorbent in tube.

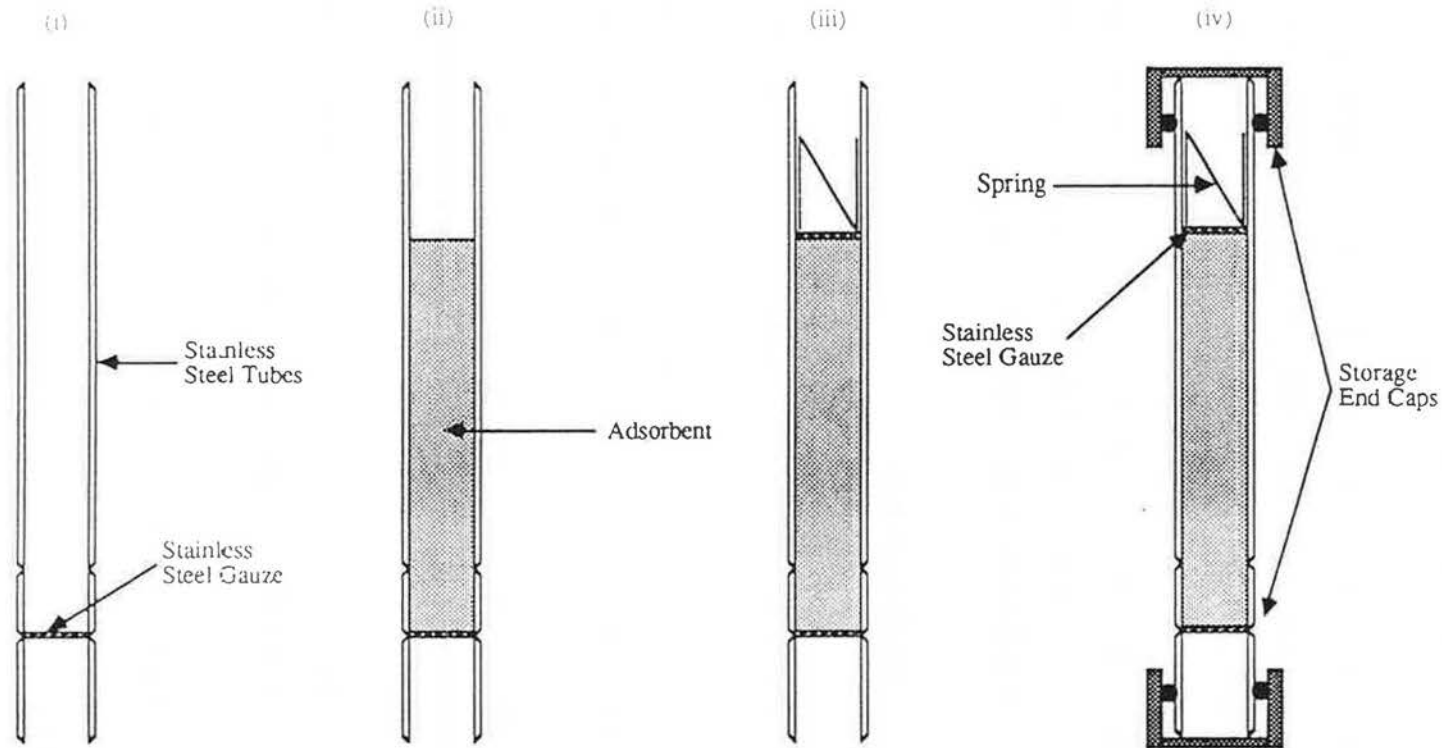


Figure 64 Procedure of packing the tube

- vii. Carefully check the adsorbent is not leaking from the tube as this could cause a blockage in the system.

5.4.2.3 Conditioning the packed adsorbent tube

The packed adsorber tubes were conditioned before used in the field to remove spurious compound from the packing material. This was done using the clean mode on the thermal desorber.

5.4.3 Choice of perfluorocarbon tracers

Table 16 shows a list of perfluorocarbon tracers. The criteria for choosing the most suitable perfluorocarbon tracer were based on boiling point, density and cost. The tracer is required to have a low boiling point so that the time taken for the heating element to heat up the bottle of tracer to its boiling point will be short. It is also required to have a density close to the density of air so as to prevent condensation and stratification. Low cost is also important.

From the information gathered in Table 11, perfluoro-n-hexane (PP1) was chosen as the tracer for airflow measurements in the HVAC system.

5.4.4 Choice of adsorbent

The technique of concentrating small amounts of organic vapour in the atmosphere either cryogenically or on solid adsorbents was initially developed by workers interested in identifying and measuring low levels of hazardous organic vapour in the atmosphere and depends primarily on the chemical properties of the gases being collected [40]. Different adsorbents have different affinities for various organic vapours. They also differ in thermal stability and in the extent to which their performance is inhibited by the presence of water vapour. In general, the choice of an adsorbent for a

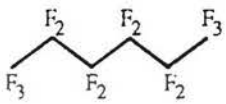
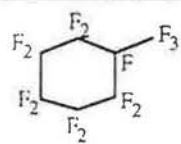
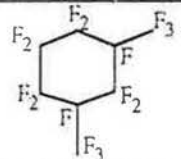
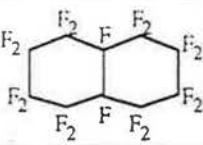
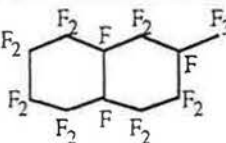
| Trade Name | Chemical Name | Formula | Molecular Weight | Boiling Range | Density (20°C) g/ml | Cost (£/100g) |
|------------|------------------------------|--|------------------|---------------|---------------------|---------------|
| PP1 | Perfluoro-n-hexane |  | 338 | 54 - 60 | 1.68 | 19.80 |
| PP2 | Perfluoromethylcyclohexane |  | 350 | 73 - 78 | 1.79 | 22.80 |
| PP3 | Perfluorodimethylcyclohexane |  | 400 | 92 - 104 | 1.85 | 19.80 |
| PP5 | Perfluorodecalin |  | 462 | 135 - 143 | 1.93 | 23.80 |
| PP9 | Perfluoromethyldecalin |  | 512 | 151 - 165 | 1.96 | 21.40 |

Table 11 List of perfluorocarbon tracers

particular task should be made according to the following criteria:

- i. The adsorbent should show high efficiency for both collection and recovery of adsorbed gases.
- ii. The adsorbent should have little or no affinity for water vapour.
- iii. The adsorbent should not undergo any structural or chemical change at the temperature necessary for desorption.

The thermal desorption system uses industrial standard tubes allowing a wide range of published material on all aspects of thermal desorption, including adsorbent selection and diffusive uptake rates (full details have been incorporated on EH40 database. Available from HMSO ISBN 88560-5). Table 12 shows a list of adsorbents with their corresponding compounds.

| Boiling Points (°C) | Adsorbent | Compounds |
|---------------------|--------------------|-------------------------------------|
| < -30 | Molecular Sieve 5A | CO N ₂ O CH ₄ |
| -30 to 30 | Spherocarb | ethylene oxide |
| 30 - 100 | Chromosorb 106 | methanol acetone |
| > 100 | Tenax GC or TA | benzene |

Table 12 List of adsorbents

According to the advice given by Perkin-Elmer Ltd., on the collection of compounds such as, PP1 and PP2, the most suitable adsorbent is the styrene divinyl benzene co-polymer Chromosorb 102 of Chrompack (UK) Ltd..

5.4.5 Optimum sampling volumes

When measuring of airflow in a duct using adsorber tubes, it is important to ensure that all the tracer gas in the air sample drawn through each tube is deposited on the adsorbent and that none break through to the other end of the tube [41]. The optimum sampling volume of an adsorber tube is the maximum volume of air containing a given mixture of tracer gases which may be sampled over a variety of conditions such as humidity, temperature and sampling flow rate without significant breakthrough.

The breakthrough volume of an adsorber tube is the volume of air which when drawn through a tube laden with some tracer gas produces the smallest detectable amount of the tracer gas in the tube effluent.

Breakthrough volume is strongly dependent on temperature and sampling flow rate, so that optimum sampling volume must have a safety margin to allow for changes in these parameters.

Breakthrough volumes can be measured directly [40] or indirectly [41]. Pellizzari [40] created a gas mixture of known concentration in a flask connected on one side to a helium gas supply and on the other side to a packed adsorber tube. The effluent was monitored by a flame ionisation detector. The experiment was repeated for different adsorbents, gases and purging rates. The effluent from the packed adsorber tube was monitored closely in conjunction with part of the same gas mixture diverted through an empty adsorber tube. The percentage collection efficiency for each adsorbent and mixture of gases was estimated by comparing amounts of tracer gases seen in the tube effluent of the packed and empty adsorber tubes.

Brown and Purnell [41] used a similar method to measure breakthrough volumes, the only difference was that they used a continuous atmosphere of constant concentration. Experiments were all carried out on the adsorbent

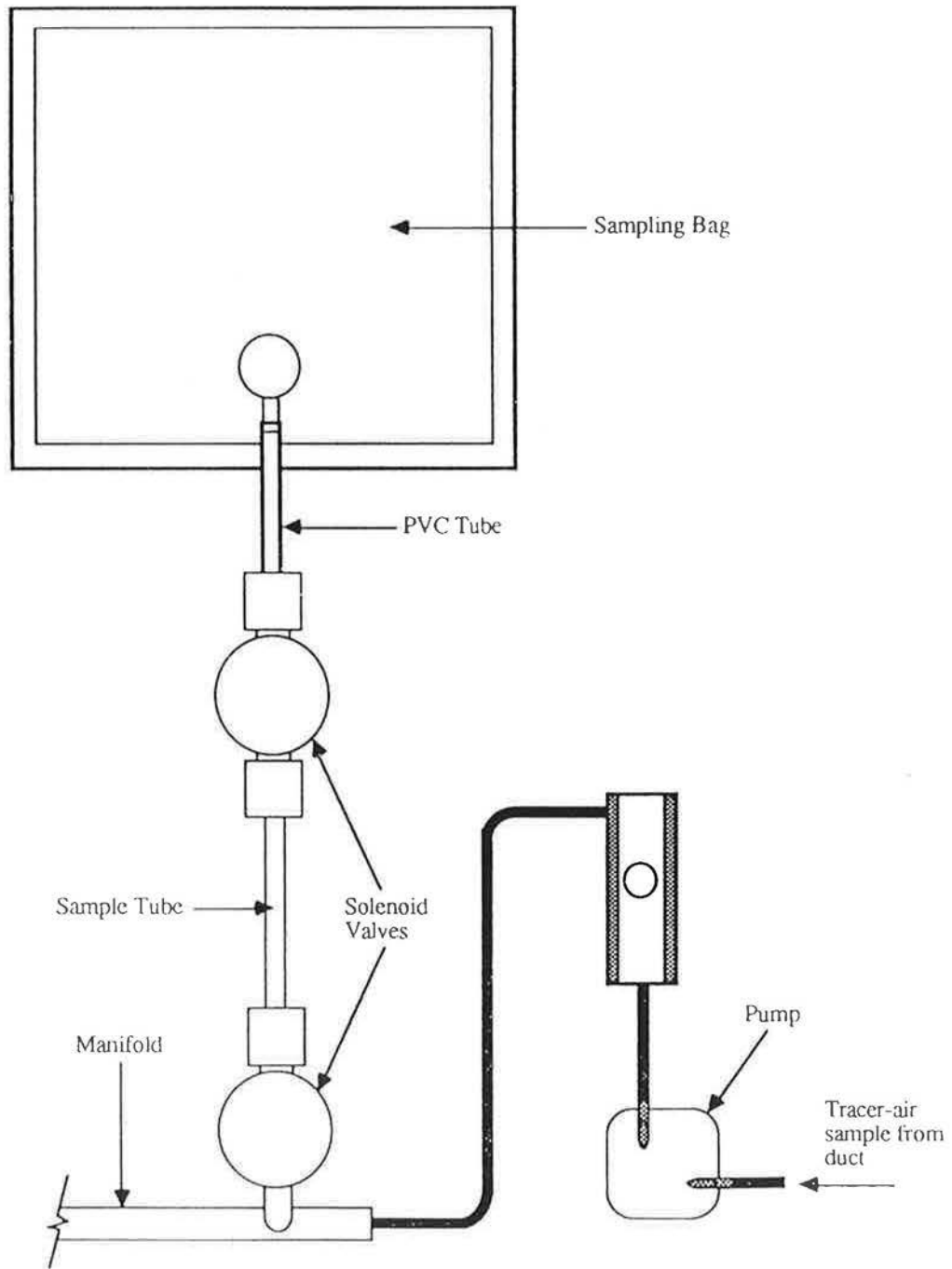


Figure 65 Instrumentation for determining the optimum sample volumes or breakthrough volumes

Tenax GC for different gases and sampling conditions. Because this technique is difficult and time-consuming to employ, Brown and Purnell developed an indirect technique for breakthrough volume measurement and used the direct method to confirm its validity.

5.4.5.1 Determine the optimum sampling volumes

In the present work, the multi-gas monitor and a thermal desorption system were used to determine the concentration of tracer gas in the adsorbent of the tube instead of using gas chromatography. It gives a direct read-off in either ppm or mg/m³. In this context, the technique to determine the optimum sampling volume is similar that used by Brown and Purnell.

Figure 65 shows the instrumentation for determination of optimum sampling volumes of tubes packed with Chromosorb 102. In addition to the original set-up of the prototype sampling system, sampling bags were connected to the outlet of each solenoid valve to collect the effluent from the adsorber tube. A series of tests were carried out by adjusting the flow meter to provide a range of airflow rates from 2.0 to 3.5 L/min through the adsorber tubes. The duration of sampling for each tube was set to 60 seconds (i.e., the sampling volumes vary over a range of 2.6 and 2.9 litres).

In the ideal case, the concentration of tracer gas in the bag should be close to zero if the optimum sampling volume for the Chromosorb 102 packed tube is to be achieved. Table 13 shows the result of 3 tests for determining the optimum sampling volume of adsorbent tube packed with approximately 0.435g Chromosorb 102.

| No. | Sampling Rate (L/min) | Concentration, (mg/m ³) | |
|-----|-----------------------|-------------------------------------|-------|
| | | Bag | Tube |
| 1 | 2.6 | 0.0005 | 15.55 |
| 2 | 2.8 | 0.00128 | 29.9 |
| 3 | 3.0 | 25.78 | 4.55 |

Table 13 Results of the optimum sampling volumes

The sampling volume of tube number 2 is the optimum one as the result shows that most of the tracer gas was adsorbed by the Chromosorb 102 in the tube and only a small amount of it broke through and collected in the bag. However, the sampling volumes for tubes number 1 and 3 were below and above the optimum sampling volume, respectively. In both cases, there were not much tracer gas adsorbed in the tube. These tests show that the optimum sampling volume for these tubes packed with approximately 0.435 g of Chromosorb is 2.8 litre.

5.5 Advantages and disadvantages of the new PFT system

The PFT system has several advantages over the conventional method. A small-injection system is required instead of a large gas cylinder and the PFT system could be used for long-term monitoring of airflow. PFTs exist only at very low concentrations in the ambient and are easily detected (parts per billion range or less) and so this minimises the amount of tracer gas required to carry out airflow measurements. Several perfluorocarbons such as perfluoro-n-hexane, perfluoro-methyl-cyclohexane, perfluoro-decalin are available for airflow measurements and these could be stored at room temperature in small containers. The main disadvantage of the PFT system is the relatively high capital cost of the thermal desorber and gas monitor.

5.6 Laboratory tests of the new PFT technique for measuring airflow in ducts

Experiments were carried out using the modified prototype injection and sampling system to evaluate the accuracy of the new PFT technique [36]. The PFT system was used for different airflow rates and results were compared with measurements made by the pitot-static traverse method. Additional experiments involved injection of sulphur hexafluoride (SF_6) as the tracer gas and collection of samples in bags using the sampling system.

5.6.1 Experimental work

The experimental work was carried out using the duct system and instrument as shown in Figure 66. The duct system was constructed using a galvanised mild steel duct 6 m long with a cross-section of 300 mm x 300 mm. The downstream end was connected to an axial fan by means of a diffuser. The flow rate through the duct was varied using a speed controller made by ABB Stromberg Drives, Finland. The fan was driven by an AC motor of 4 kW and with a maximum speed of 2880 rpm. The fan was manufactured by Elta Fan Ltd., UK.

Background contaminants in the adsorbent tubes can give rise to interference and inaccuracies in airflow measurements. To prevent this, all sampling tubes were cleaned before and after each use. The thermal desorption system is set to cleaning mode to remove contaminants contained in the adsorbent.

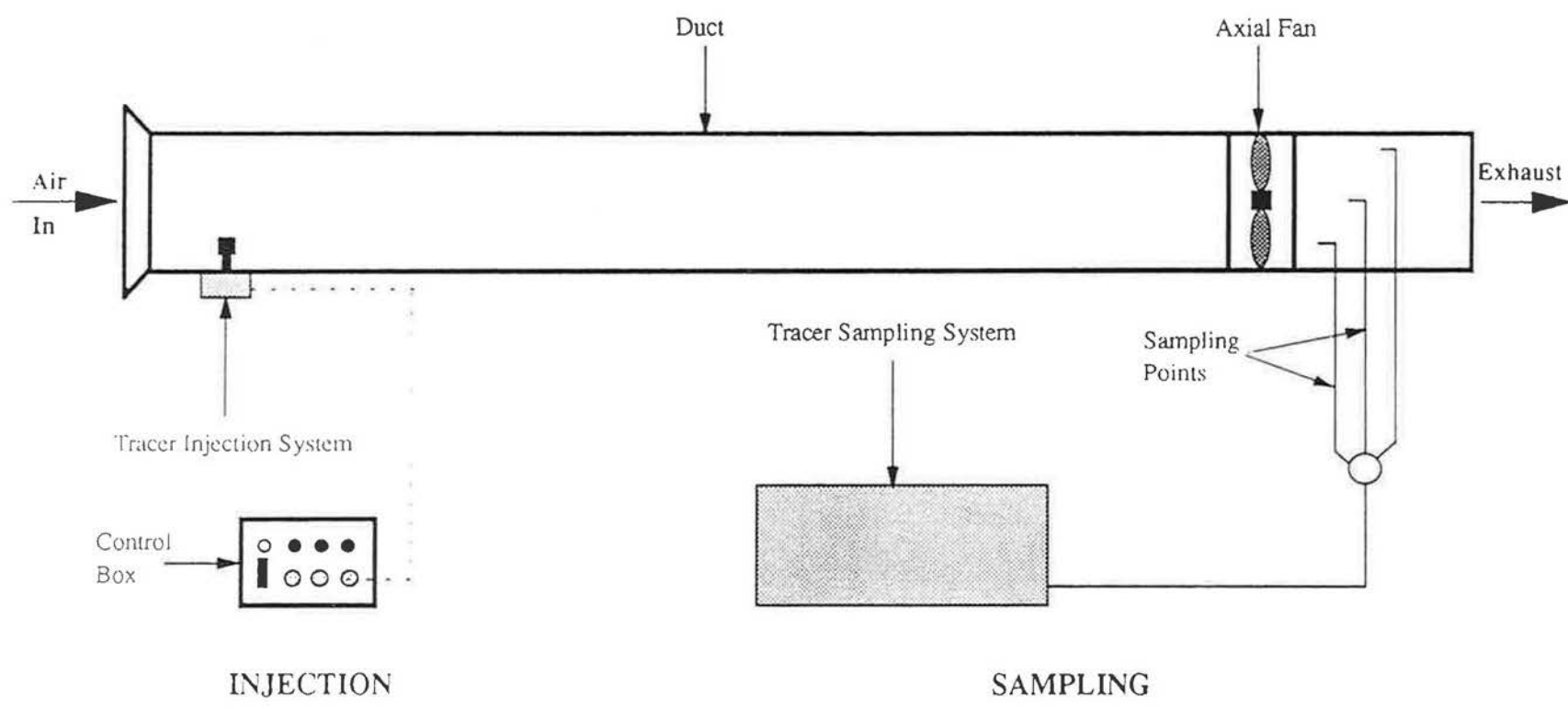


Figure 66 Instrumentation for PFT technique

Airflow measurements commenced by filling the vessel with perfluoro-n-hexane (PP1) and then weighing it. Tracer gas was injected into the duct by placing the tracer-injection system at a point downstream of the duct system. Samples were collected in clean tubes fitted onto the sampling system via the sampling probes inserted into the duct downstream of the injection point. After 6 minutes, the injection and sampling process were stopped and the vessel was reweighed. The difference in weight of the vessel and dividing by the duration of injection (i.e., 6 minutes). Analysis of the sampling tubes were performed by setting the thermal desorption system to analytical mode. A calibration graph (see section 5.4.1.3.1 for calibration method) [units against the amount of tracer gas in terms of weight (mg)] was required to determine the actual concentration of tracer-gas in tubes as the direct readout values from the type 1302 multi-gas monitor required a factor adjustment. Once the injection rate, q , (mg/s) and concentration of tracer-gas in the sampling tube, C , (mg/m^3) are known, the airflow rate, F , (m^3/s) in the duct can be evaluated using the constant-injection expression (see Section 2.2.1.1.).

Additional airflow measurements were obtained by collecting samples in sampling bags via the sampling system. Figure 67 shows the connection of bags at the sampling system. Sampling bags were connected to the solenoid valves via empty adsorber tubes. The process of collecting gas sample in the sampling bag is stopped once the programmable logic controller send a voltage signal to de-energise the normally-closed solenoid valve at the end of preset duration. Analysis of the gas samples in these bags were carried out by using the type 1302 multi-gas analyser. The pitot-static traverse method was employed in the same experiment to provide a comparison between the airflow measurements made using different techniques.

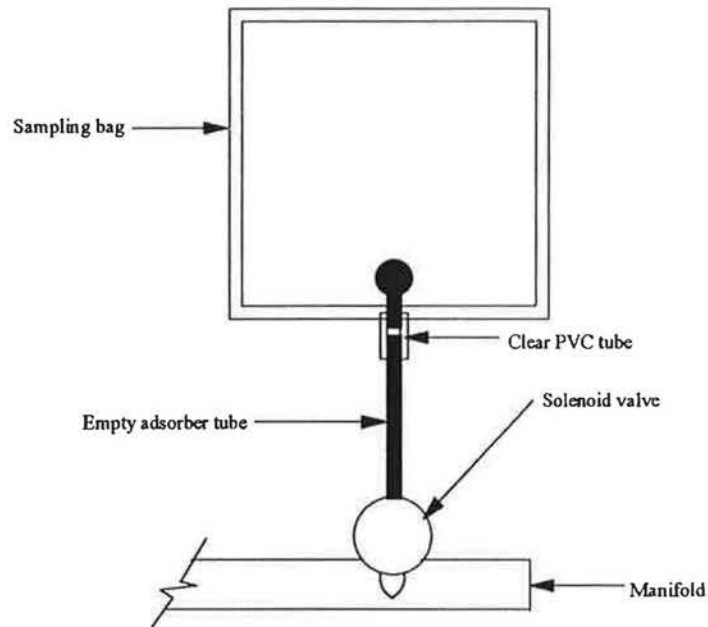


Figure 67 Connection between bag and sampling system

In addition, airflow measurements in the ducts were carried out by injecting sulphur hexafluoride (SF_6) tracer gas at a constant rate or pulse into the duct and collecting samples in bags via the sampling systems. These measurements were carried out over a range of flow rates to show that the system can be used with other type of tracer gas besides perfluorocarbon tracers.

5.6.2 Results and discussion

Table 14 and 15 compare measurements of airflow rate made with a pitot tube and the PFT technique using sampling tubes and bags.

| No. | Airflow Rates, (m ³ /s) | | Percentage Difference (F _{st} - F _p)/F _p |
|-----|------------------------------------|------------------------------------|---|
| | Pitot-Tube, (F _p) | Sampling Tubes, (F _{st}) | |
| 1 | 0.495 | 0.530 | 7.1 |
| 2 | 1.038 | 1.070 | 3.1 |
| 3 | 1.455 | 1.394 | -4.2 |

Table 14 Comparison of airflow measurements in a duct using a pitot tube and PFT technique, sampling tubes

| No. | Airflow Rates, (m ³ /s) | | Percentage Difference (F _{sb} - F _p)/F _p |
|-----|------------------------------------|-----------------------------------|---|
| | Pitot-Tube, (F _p) | Sampling Bags, (F _{sb}) | |
| 1 | 0.453 | 0.432 | -4.6 |
| 2 | 0.750 | 0.734 | -2.1 |
| 3 | 1.206 | 1.191 | -1.2 |

Table 15 Comparison of airflow measurements in a duct using a pitot tube and PFT technique, sampling bags

Measurement of airflow rate obtained using the pitot-static traverse method and PFT technique using sampling tubes and bags were in close agreement. The difference between airflow rates estimating using the PFT technique (using tubes) and measurements made using a pitot-tube was in the range -4.2 to 7.1%. In the case of airflow rate measurements made using the PFT technique (i.e., using bags) and pitot-static traverse method, the difference was in the range -4.6 to -1.2%.

Table 16 shows the measurement of airflow rate made with a pitot-tube and tracer-gas techniques (using SF₆ tracer gas, sampling system and bags).

| No. | Airflow Rates, (m ³ /s) | | | Difference, (%) | |
|-----|------------------------------------|--------------------|-----------------|--|--|
| | Pitot Tube | Constant Injection | Pulse Injection | (F _{ci} - F _p)/F _p | (F _{pu} - F _p)/F _p |
| 1 | 0.372 | 0.367 | 0.333 | -1.344 | -10.484 |
| 2 | 0.528 | 0.495 | 0.481 | -6.250 | -8.940 |
| 3 | 0.720 | 0.656 | 0.682 | -8.889 | -5.278 |
| 4 | 0.753 | 0.753 | 0.698 | 0.040 | -7.291 |
| 5 | 0.953 | 0.880 | 0.860 | -7.660 | -9.759 |
| 6 | 1.164 | 0.999 | 1.055 | -14.175 | -9.364 |
| 7 | 1.245 | 1.054 | 1.042 | -15.341 | -16.305 |
| 8 | 1.337 | 1.212 | 1.254 | -9.349 | -6.208 |
| 9 | 1.785 | 1.515 | 1.657 | -15.126 | -7.171 |

Table 16 Comparison of airflow measurements in a duct using a pitot tube and tracer-gas techniques

The above results indicate that the airflow measurements obtained from the pitot-static traverse method and tracer-gas techniques were in closed agreement. The difference between airflow rate estimated using constant-injection technique measurements and measurements made using a pitot tube was in the range -15.1 to 0.1%. In the case of airflow rate measurements made using the pulse-injection technique and pitot-static traverse method, the difference was in the range -16.3 to -5.3%.

6. FIELD TESTING [36]

Tracer-gas techniques were applied to measurements of airflow in full-scale HVAC systems in an office building. The office building is located at the Midlands. It was constructed in 1990 to an energy-efficient design and was first occupied in 1991. It is a two-storey building and measurements were carried out in the general office located on the ground floor. The office has an open-plan design and has a floor area of 126 m².

Air conditioning of the office is provided by a heat pump system through an air-handling unit. Figure 68 shows the schematic of the air distribution system. The ventilation air from the air handling unit is delivered to the office through three air diffusers at the suspended ceiling. The air extracted from the office via two grilles is completely purged to the outside.

6.1 Description of measurements

6.1.1 Measurement of airflow in air handling unit and exhaust system

Measurements of airflow were carried out in the air handling unit and exhaust system by using the pitot-static traverse method, tracer-gas techniques such as constant-injection and pulse-injection, and PFT technique using sampling tubes.

Velocity pressure and tracer gas tapings were positioned along the ducts at the air handling units. The velocity tapings allowed insertion of a pitot tube which could be traversed across the duct cross-section in order to measure velocity at various distances from the duct wall. Velocity pressures were measured using an EMD 2500 micromanometer made by Airflow Development, UK.

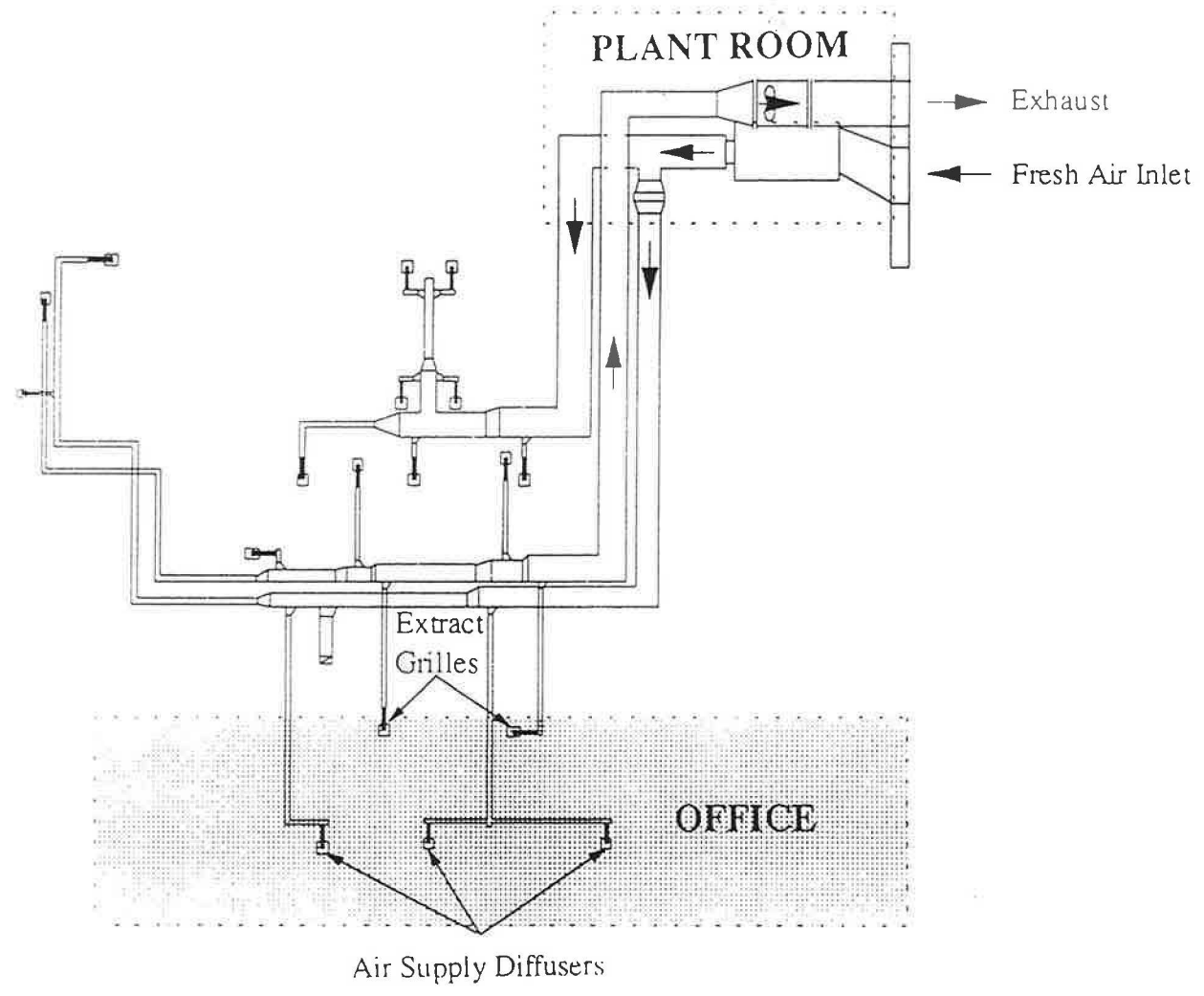


Figure 68 Schematic of the air distribution system

For the constant-injection technique, SF₆ tracer gas was supplied at a constant rate into the fresh air inlet of the duct using a mass flow controller, type F100/200, made by Bronkhorst High-Tech BV, Ruurlo, Holland. The controller had a maximum flow capability of 5 L/min and a measurement accuracy of ±1%. The flow rate was controlled using a variable power supply and the rate of tracer-gas injection was displayed on a digital unit.

For the pulse-injection technique, tracer gas was injected into the fresh air inlet of the duct using a syringe. Multi-point injection was necessary for the approximation of a uniform concentration across the cross-section of the duct at the measurement point. It was necessary to measure the concentration of the tracer gas at the downstream point to determine the integral of the concentration. This was achieved by filling an air sample bag by means of a small pump. Sampling was begun 10 seconds before the pulse was injected, and continued until the pulse was completely purged from the duct.

The PFT technique involved the constant-injection of perfluoro-n-hexane (PP1). Figure 69 shows the instrumentation set-up for airflow measurements at the air handling unit. The tracer-injection system was inserted into the duct close to the fresh air inlet and sampling was carried out downstream of the air handling unit. Samples were collected in sampling tubes at the sampling system. Additional airflow measurements were conducted at the exhaust duct system (not shown in Figure 69).

The concentration of SF₆ tracer gas was measured using an infra-red gas analyser, type BINOS 1000, made by Rosemount GmbH, Hanau, Germany. The accuracy of the analyser was estimated to be within ±2%. However, the concentration of samples in the bag was analysed using a Multi-gas monitor, Type 1302 while the separation and analysis of the concentration of samples collected in the adsorber tube is carried out by the Thermal Desorption System, Type SBK1355 and Multi-Gas Monitor, Type 1302,

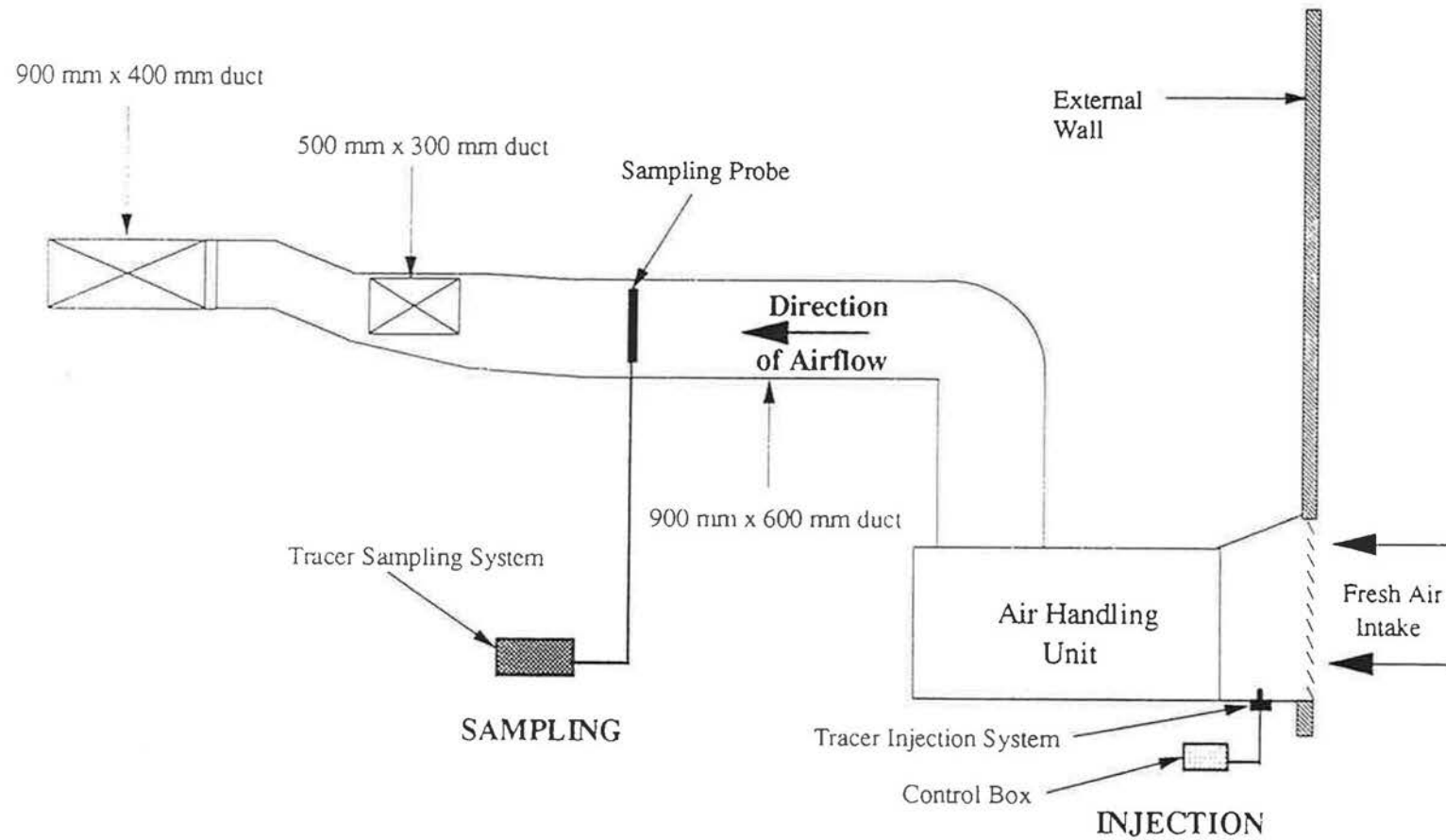


Figure 69 Instrumentation for airflow measurements at the air handling unit

respectively. The accuracy of this gas monitor is $\pm 1\%$.

6.1.2 Results and discussion

Airflow rates in the air handling unit and exhaust system were measured with the pitot tube, constant-injection technique, pulse-injection technique and PFT technique using both sampling tubes and bags. Table 17 compares the measurements of airflow rate made with pitot tube (P), PFT technique with sampling tubes (PFT), constant-injection (CI) and pulse-injection (PU) techniques at the air handling unit (AHU) and exhaust duct system (EDS).

| Type | Airflow Rates, (m^3/s) | | | | Percentage Difference | | |
|------|--|----------------|--------------------|--------------------|-----------------------|----------------------|----------------------|
| | P (F_p) | PFT (F) | CI (F_{ci}) | PU (F_{pu}) | $(F_t - F_p)/F_p$ | $(F_{ci} - F_p)/F_p$ | $(F_{pu} - F_p)/F_p$ |
| AHU | 1.49 | 1.57 | 1.48 | 1.55 | 5.37 | -0.67 | 4.03 |
| EDS | 1.50 | 1.35 | 1.45 | 1.54 | -10.0 | -3.33 | 2.67 |

Table 17 Measurement of airflow rate in the air handling unit and exhaust duct system

Measurements of airflow rate obtained from the pitot-static traverse method, PFT technique and tracer-gas techniques (i.e., constant and pulse-injection techniques) were in close agreement. The difference between airflow rate estimated using the PFT technique and measurements made using a pitot tube at the air handling unit and exhaust duct system were 5.37% and -10.0%, respectively. In the case of airflow rate measurements at the air handling unit and exhaust duct system using a pitot tube and constant-injection technique, the differences were -0.67% and -3.33%, respectively. Lastly, the difference in airflow measurement at the air handling unit and exhaust duct system using the pitot tube and pulse-injection technique were 4.03% and 2.67%, respectively.

7. DETERMINATION OF THE AIR-TIGHTNESS OF DUCT SYSTEM USING TRACER-GAS TECHNIQUES

Tracer-gas techniques such as constant-injection and pulse-injection, have been successfully employed for the measurement of airflow in an HVAC system. In addition, it can be used to determine the air-tightness of ducts in a HVAC system [42]. The air-tightness of ducts in buildings is important as leakages would cause the actual flow to be more or less than the design flow in an extract and air supply duct, respectively. The importance of air-tightness of ducts is further illustrated by application in the petrol-chemical industry where natural gas transportation is carried out in huge ducts. Any leakage in the pipelines would be costly and detrimental.

7.1 Review of techniques

The concentration-decay and constant-injection technique can be used in the measurement of air-tightness of ducts.

7.1.1 Concentration-decay technique

In this technique (see section 2.2.1.3.1 for theory), the air-tightness of the duct are determined by injecting tracer gas into that particular section of the duct under test and then sealing both ends of the section. Time is allowed for the injected tracer gas to mix with the air in the duct and form a uniform concentration throughout the duct section under test. Holes are drilled along the duct for insertion of sampling tubes. The decay of the tracer-gas concentration is monitored over a period of time. The slope of the graph for natural log of tracer-gas decay against time is the air-tightness of the duct.

7.1.2 Constant-injection technique

This technique (see section 2.2.1.1 for theory) is used to check the air-tightness of the duct, before and after access holes or measuring devices have been installed. The duct system used for the air-tightness testing has a number of holes sealed by rubber bungs. These holes are to simulate leakage after the access holes or devices have been installed. There are two ways of evaluating the air-tightness of ducts.

The first method is employed when the position of the leak is known. The injection points are fixed and the sampling points are inserted into the duct before and after the leaky section. The difference in the flow rate before and after this leaky section of the duct will be the leakage rate. This technique is called the Stationary Technique as it is related to the fixing of injection points. The second method is used to locate the leaky section and determine the leakage rate. This method is called the Mobile Technique because both the injection and sampling points are moved along the ductwork. Any difference in airflow between the two sections of the duct is the leakage rate. The second method is used more frequently because the location of leaks in ductwork are not usually known.

7.2 Methodology

The advantages of using the constant-injection tracer-gas technique for studies of air-tightness outweigh those of the concentration-decay technique. The method of determining the air-tightness of ducts has therefore been developed using the constant-injection technique.

7.2.1 Stationary technique

Figure 70 shows the instrumentation for the stationary technique. Holes of 10 mm in diameter were drilled on the top of a 300 mm x 300 mm square duct to simulate a leak. Tracer gas was injected into the duct at a constant rate using a mass flow controller. Sampling probes were inserted into the duct at points 1 and 2 (i.e., before and after the leak, respectively). The concentrations of these tracer-air samples were measured using a BINOS 1000 infra-red gas analyser. The airflow rate was evaluated using the constant-injection expression as shown in section 2.2.1.1. The difference in airflow rates before and after the leak was the leakage rate of the duct. Static pressures were also monitored over these leaks. This experiment was repeated at various flow rates.

7.2.2 Mobile technique

In the mobile technique, the instrumentation is set-out as shown in Figure 71. Initially, the holes in the duct are sealed by rubber bungs. The injection and sampling points were placed at point I1 and S1, respectively. The airflow in the duct was measured using the constant-injection tracer-gas technique. Some rubber bungs were removed between I1 and S1 to simulate leaks in the duct. The airflow in the duct was once again measured using the constant-injection technique. The difference between the measured airflow rates was the leakage rate through these holes. The injection and sampling points were moved along the duct to position I2 and S2, respectively leaving the earlier holes open to determine the total leakage rate due to the holes between point I1 and S2 on the duct. Static pressures were monitored along these holes. This experiment was repeated at various flow rates.

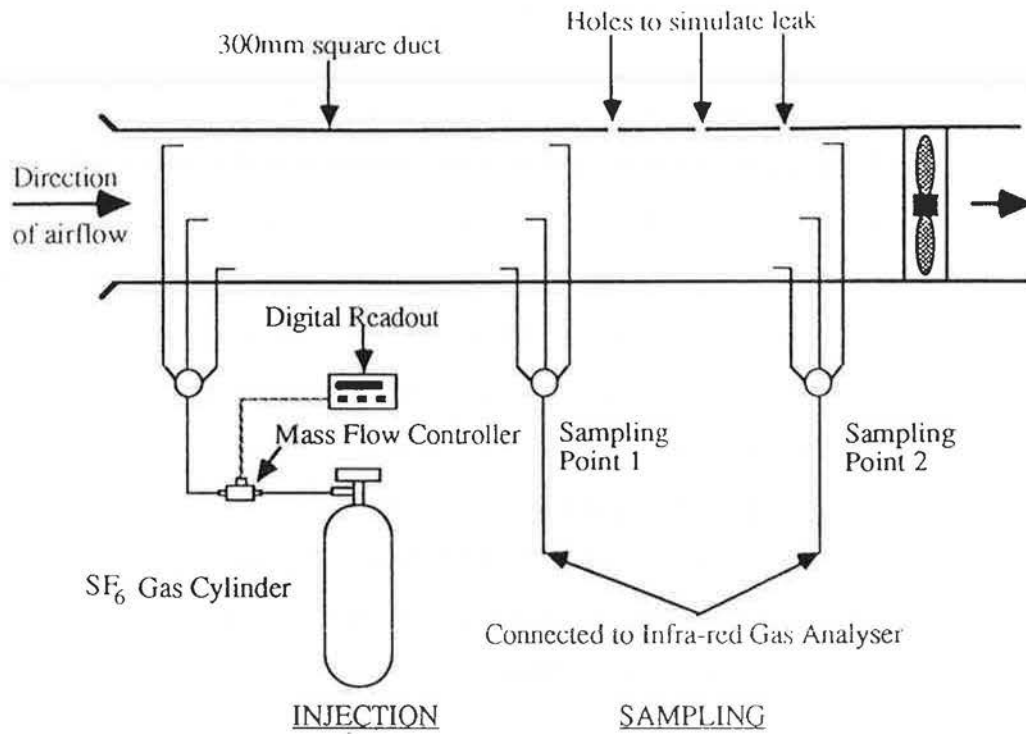


Figure 70 Instrumentation for determining air-tightness of duct system, stationary technique

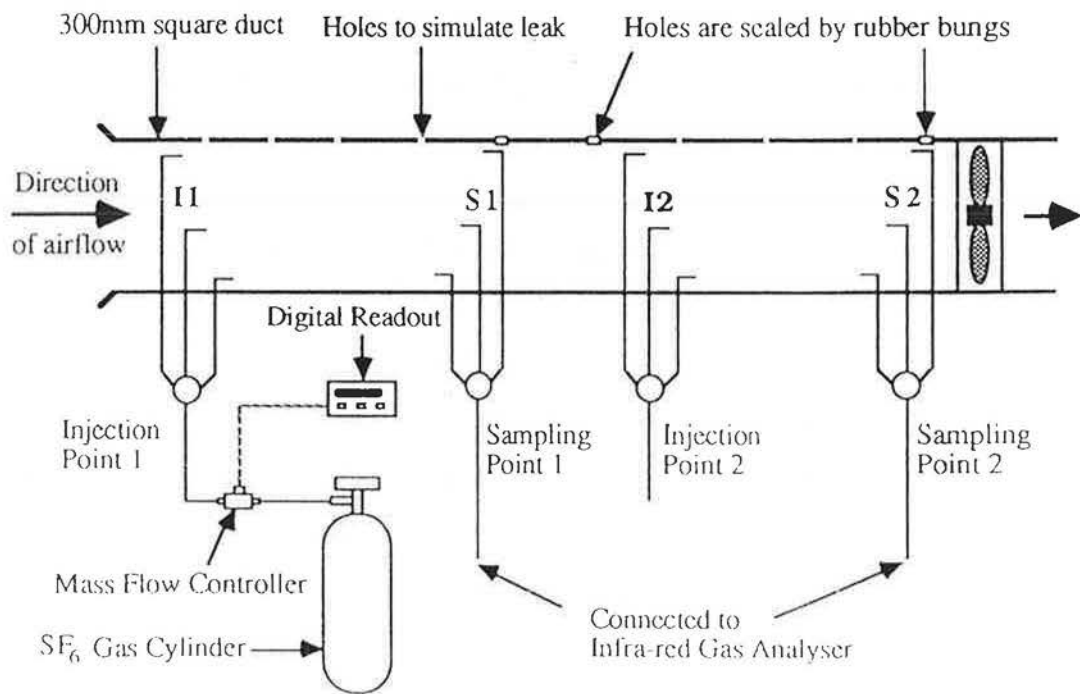


Figure 71 Instrumentation for determining air-tightness of duct system, mobile technique

7.3 Results and discussion

Air-tightness tests were conducted in the duct using these two techniques and the results are analysed in this section.

7.3.1 Stationary technique

Table 18 shows the leakage rates of the duct at various air flow rates. The leakage rate increases with the airflow rate in the duct.

| Flow Rate (m ³ /s) | Leakage Rate (m ³ /s) |
|----------------------------------|-------------------------------------|
| 0.795 | 0.039 |
| 0.85 | 0.048 |
| 0.98 | 0.062 |
| 1.038 | 0.072 |

Table 18 Airflow rate with respect to leakage rate in 300 mm x 300 mm square duct, stationary technique

A relationship of the leakage rate and airflow rate (see Figure 72 for the graph) was developed for the 300 mm x 300 mm square duct as shown in Equation (32).

$$L = 0.0644 F_{ci}^{2.04} \quad (32)$$

The relationship of leakage rate and pressure drop (see Figure 73 for the graph) across the leaks was also established as shown in Equation (33) below:

$$L = 0.006 \Delta P_L^{0.85} \quad (33)$$

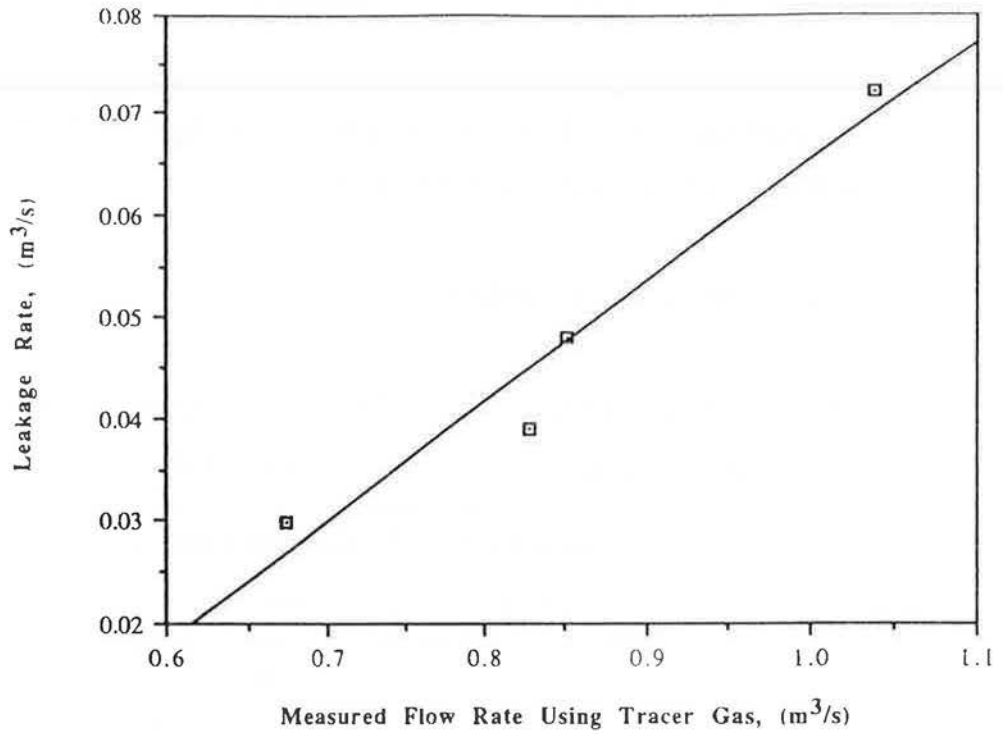


Figure 72 Variation of air leakage rate with airflow rate in duct system

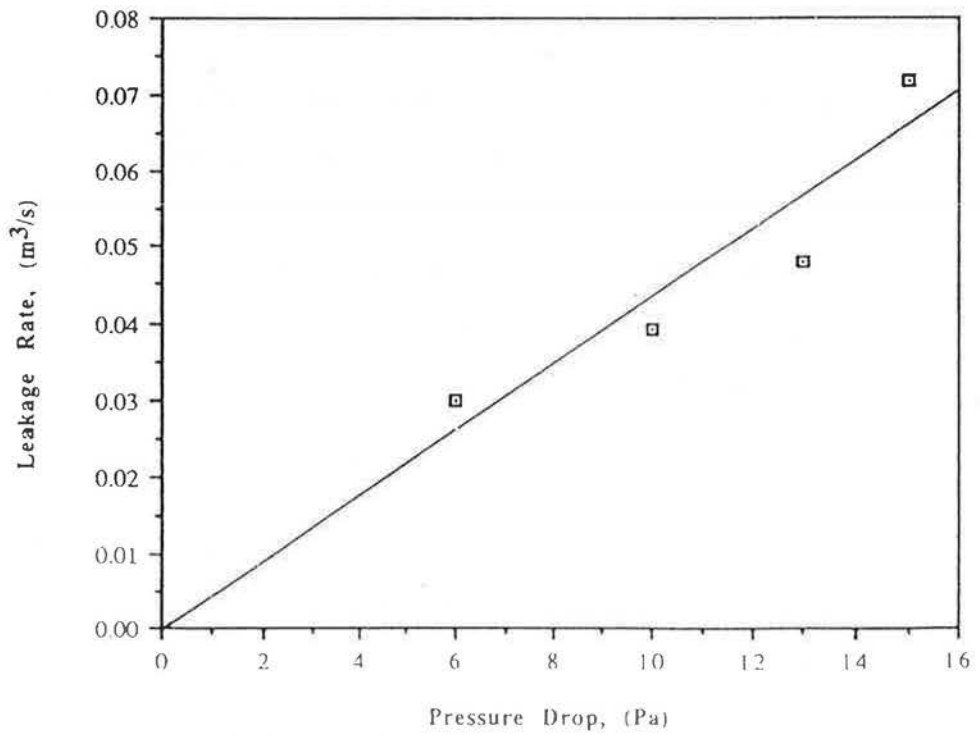


Figure 73 Variation of air leakage rate with pressure drop in duct system

7.3.2 Mobile technique

Table 19 shows that the increasing leakage rate is due to the removal of rubber bungs on the duct and the increasing airflow rate in the duct. A relationship is established between the leakage rate and airflow rate for this 300 mm x 300 mm square duct (see Table 20).

| Flow Rate, (m ³ /s) | Leakage Rate, (m ³ /s) | | | |
|-----------------------------------|-----------------------------------|-----------------|-----------------|-----------------|
| | 9 Bungs Off | 18 Bungs Off | 27 Bungs Off | 36 Bungs Off |
| 0.975 | 0.0116 | 0.0242 | 0.0376 | 0.0549 |
| 0.999 | 0.0124 | 0.0282 | 0.0443 | 0.0625 |
| 1.093 | 0.0159 | 0.0349 | 0.0580 | 0.0871 |
| 1.128 | 0.0163 | 0.0374 | 0.0614 | 0.0922 |
| 1.291 | 0.0205 | 0.0606 | 0.1061 | 0.1593 |

Table 19 Airflow rate with respect to leakage rate in a 300 mm x 300 mm square duct, mobile technique

| No. of Rubber Bungs Off | Leakage Rate (L) |
|-------------------------|-------------------|
| 9 | 0.0126 $F^{2.03}$ |
| 18 | 0.0268 $F^{3.11}$ |
| 27 | 0.0422 $F^{3.53}$ |
| 36 | 0.0612 $F^{3.71}$ |

Table 20 Relationships of leakage rate and airflow rate in 300 mm x 300 mm square duct

The relationship of leakage rates and pressure drop across these holes were also established (see Table 21).

| No. of Rubber Bungs Off | Leakage Rate (L) |
|-------------------------|---------------------------|
| 9 | 0.0019 $\Delta P^{0.7}$ |
| 18 | 0.0007 $\Delta P^{1.39}$ |
| 27 | 0.0002 $\Delta P^{1.64}$ |
| 36 | 0.00008 $\Delta P^{1.78}$ |

Table 21 Relationships of leakage rate and pressure drop across the leak in 300 mm x 300 mm square duct

REFERENCES

1. P.R. Morey and D.E. Shattuck, "Role of ventilation in the causation of building-associated illnesses", *Occupational Medicine: State of the Art Review*, Vol. 4, No. 4, p. 625-642, Philadelphia, Hanley & Belfus, Inc., 1989.
2. K.J. Helsing, C.E. Billings, J. Conde and R. Griffin, "Cure of a sick building: A case study", *Environmental International*, Vol. 15, p. 107-114, 1989.
3. J.B. Dick, "Measurement of ventilation using tracer gases", *Heat. Pip. Air Condit.*, Chp 22, p. 131-137, 1950.
4. S.J. I'Anson, C. Irwin and A.T. Howarth, "A multiple tracer gas technique for measuring air-flow in houses", *Building Environment*, Vol. 17, p. 245-252, 1982.
5. D.T. Harrje, G.S. Dutt and D.L. Bohac, "Documenting air movements and infiltration in multicell buildings using various tracer gas techniques", *Preprint ASHRAE Trans.* 91, HI-85-40, No. 3, 1985.
6. R. Niemela, E. Toppila and A. Tossavainen, "A multiple tracer gas technique for the measurement of airflow patterns in large industrial premises", *Building and Environment*, Vol. 22, No. 1, p. 61-66, 1987.
7. M.H. Sherman, "On the estimation of multizone ventilation rates from tracer gas measurements", *Building and Environment*, Vol. 24, No. 4, p. 355-362, 1989.

8. A. Persily and J. Axley, "Measuring of flow rates with pulse injection techniques", American Society for Testing and Materials, Philadelphia, 1989.
9. S.B. Riffat and S.F. Lee, "Turbulent flow in duct: Measurement by a tracer gas technique", Building Services Engineering Research and Technology, Vol. 11, No. 1, p. 21-26, 1990.
10. J. Sateri, "PFT measurement in ventilation ducts", Proceedings 12th AIVC Conference, Canada, Vol. 1, p. 375-386, 1991.
11. British Standard, "Measurement of fluid flow in closed conduits", BS 1042, Part 2, Section 2.2, 1983.
12. L.F.G. Simmons, "A shielded hot wire anemometer", J. Scient. Instrum., Vol 26, p. 1407, 1949.
13. J.O. Sateri, "The development of the PFT-method in the nordic countries", NBS-I 1991. Document D9:1991, Swedish Council for Building Research (Distribution: Svensk Byggtjanst, S-17188 Solna, Sweden).
14. R.N. Dietz and E.A. Cote, "Air infiltration measurements in a home using a convenient perfluorocarbon tracer technique", Environment International, Vol. 8, No. 1 6, p. 419-433, 1982.
15. B.P. Leaderer, L. Schaap and R.N. Dietz, "Evaluation of the perfluorocarbon tracer technique for determining infiltration rates in residences", Environmental Science and Technology, Vol. 19, p. 1225-1232, 1985.

16. R. Walker and M. Smith, "A passive solution", *The Chartered Institute of Building Services Engineer Journal*, Vol. 15, No. 10, p. 57, 1993.
17. L. Shao, S. Sharples and I.C. Ward, "Tracer gas mixing with air", *Building Services Engineering Research and Technology*, Vol. 14, No. 2, p. 43-50, 1993.
18. N. Dupoux and J.C. Laborde, "New injection system for a short mixing of test aerosols and gas tracers inside ventilation ducts", 3rd International Symposium on Ventilation for Contaminant Control, Ohio, USA, 1991.
19. D.C. Cornish, G. Jepson and M.J. Smurthwaite, "Sampling of gases and liquids", *Sampling Systems for Process Analysers*, Chp. 3, p. 25-95, 1981.
20. A. Svensson, "Methods for measurement of airflow rates in ventilation systems", *The Nordic Ventilation Group, National Swedish Institute for Building Research*, 1982.
21. S.B. Riffat and M. Holmes, "Measurement of airflow in HVAC systems using tracer-gas techniques", *Proceedings 11th AIVC Conference, Italy*, Vol. 1, Sept. 1990.
22. S.B. Riffat, K.W. Cheong and M. Holmes, "Measurement of entrance length and friction-factor of ducts using tracer-gas techniques", *Proceedings 12th AIVC Conference, Canada*, Vol. 2, p. 321-334, 1991.
23. S.B. Riffat and K.W. Cheong, "Measurement of air flow through porous medium", *Applied Energy*, Vol. 40, p. 21-29, 1991.

24. K. Vafai and M. Sozen, "Analysis of energy and momentum transport for fluid flow through porous bed", Transactions ASME, Vol. 112, p. 690-699, 1990.
25. K. Vafai and C. Tien, "Boundary and inertia effects on flow and heat transfer in porous media", Journal of Heat and Mass Transfer, Vol. 24, p. 195-203, 1981.
26. R.M. Fand and R. Thinakaran, "The influence of the wall on flow through pipes packed with spheres", Transactions ASME, Vol. 112, p. 84-88, 1990.
27. B.A. Masha, G.S. Beavers and E.M. Sparrows, "Experiments on the resistance for non-Darcy compressible gas flows in porous media", Journal of Fluids Engineering, Transactions ASME, Vol. 96, p. 353-357, 1974.
28. J.C. Koh, J.L Dutton, B.A. Benson and A. Fortini, "Friction factor for isothermal and non-isothermal flow through porous media", Journal of Heat Transfer, Vol. 99, p. 367-373, 1977.
29. B.J. Huang, "Entrance effect of fluid flow into porous media in an impermeable channel", Journal of Chinese Institute of Engineering, Vol 13, No. 1, p. 1-10, 1990.
30. P.H. Baker, S. Sharples and I.C. Ward, "Air flow through cracks", Building and Environment, Vol. 22, No. 4, p. 293-304, 1987.
31. K.W. Cheong and S.B. Riffat, "Performance testing of HVAC systems using tracer gas techniques", Ventilation '91 Conference, USA, 1991.

32. S.B. Riffat and K.W. Cheong, "Tracer-gas techniques for design and commissioning of HVAC system", 1st International Conference On Environmental Engineering, Leicester, England, 1993.
33. K.W. Cheong and S.B. Riffat, "A new method for determination of velocity pressure loss-factors for HVAC system components", Proceedings 13th AIVC Conference, p. 549-561, France, 1992.
34. CIBSE Commissioning Code, Series A, "Air distribution systems, high and low velocity", The Chartered Institution of Building Services Engineers, London, United Kingdom, 1971.
35. R.N. Dietz, R.W. Goodrich, E.A. Cote and R.F. Wieser, "Detailed description and performance of a passive perfluorocarbon tracer system for building ventilation and air exchange measurements", ASTM STP 904, Philadelphia, p. 203-264, 1985.
36. K.W. Cheong and S.B. Riffat, "Perfluorocarbon tracer (PFT) for measurement of airflow in ducts", Building Services Engineering and Research Technology, Vol. 15, No. 1, 1994.
37. Analytical Instrument Development, Inc, "Developing TLV Level Standards - Diffusion Tubes", Analytical Instrument Development, Inc. Rt. 41 & Newark Rd., Avondale, PA. 19311, USA, Paper AN 204A.
38. Analytical Instrument Development, Inc, "OSHA Standards Table", Analytical Instrument Development, Inc. Rt. 41 & Newark Rd., Avondale, PA. 19311, USA, Paper AN 208A.

39. K.W. Cheong and S.B. Riffat, "Development of a new tracer-gas sampling system", Proceedings 14th AIVC Conference, p. 407-420, Copenhagen, Denmark, 1993.
40. E.D. Pellizzari, J.E. Bunch, B.H. Carpenter and E. Sawicki, "Collection and analysis of trace organic vapour pollutants in ambient atmospheres: Technique for evaluating concentration of vapours by sorbent media" Environmental Science and Technology, Vol. 9, p. 552-555, 1975.
41. R.H. Brown and C.J. Purnell, "Collection and analysis of tracer organic vapour vapour pollutants in ambient atmospheres: The performance of a Tenax GC adsorbent tube", Journal of Chromatography, Vol. 178, p. 78-90, 1979.
42. K.W. Cheong, "The application of tracer-gas techniques for measuring airflow in HVAC systems", PhD Thesis, School of Architecture, University of Nottingham, 1994.